THE UNIVERSITY OF MANITOBA

ELASTIC ECHOES FROM POWDER MATERIALS

by

S. Kupca

A THESIS
SUBMITTED TO THE FACULTY OF GRADUATE STUDIES
IN PARTIAL FULFILMENT OF THE REQUIREMENTS FOR THE DEGREE
OF DOCTOR OF PHILOSOPHY

DEPARTMENT OF PHYSICS

WINNIPEG, MANITOBA

September 1975

"ELASTIC ECHOES FROM POWDER MATERIALS"

by

S. KUPCA

A dissertation submitted to the Faculty of Graduate Studies of the University of Manitoba in partial fulfillment of the requirements of the degree of

DOCTOR OF PHILOSOPHY

ABSTRACT

An echo of elastic origin in the MHz frequency range of 10-100 MHz was observed from powders of various materials. The echo originates from the nonlinear response of the vibrating particles to RF driving pulses.

This echo is observed in a wide and continuous frequency range and is formed by the excitation and refocusing of single particle resonance modes. The echo amplitude depends strongly on the intensity of the biasing magnetic field H, for normal metals it increases steadily with magnetic field (0 - 50 KOe) and for ferromagnetic metals it passes through a maximum. The excitation process is different for normal and ferromagnetic metals, being "direct" (the electronic and ionic motion are directly coupled to the RF-field in the presence of a static magnetic field) for the former, and "magnetostrictive" for the latter.

This kind of echo can also be excited in piezoelectric powders. Echoes from Rochelle salt are reported, in both the piezoelectric and the ferroelectric region.

Apart from the differences originating in the excitation process, the echo from all powders behaves similarly.

The relaxation of the echo is determined by the elastic energy losses of the particles. For normal metal powders the losses are dominated, in most of the cases, by surface

energy losses while for ferromagnetic metals the microeddy current losses are usually dominant.

The echo formation depends strongly on temperature, sample purity, and mechanical or magnetic (ferromagnets) history. For most of the normal metal samples the variation of the echo amplitude follows the variation of the electrical resistivity. For ferromagnetic metals the echo amplitude is related to domain structure and domain wall mobility.

The echo, following two RF pulses (at time $t = o, \tau$) of intensities h_1 and h_2, varies approximately as $h_1 h_2^2$ ($h_1 h_2^2 H^4$ for normal metals). Typically, more echoes (at $t = 2\tau, 3\tau \ldots$) with different relaxation times $T_1, T_2 \ldots$ follow a two pulse excitation. The relations $T_2 \simeq 3/4\ T_1$ and $T_s = \frac{1}{2} T_1$, for a stimulated echo following a 3-pulse excitation (a third pulse at time T leads to a stimulated echo at $t = T + \tau$), which follow from a simple model are approximately satisfied for all the samples.

Qualitatively the echo formation can be understood on the basis of a model, where individual particles of the sample represent oscillators with their own resonance frequencies. Parametric interaction between the RF field and the amplitudes of the oscillators leads to components in the oscillator amplitudes which can refocuse at times $t = nT \pm m\tau$, n,m

integers, independent of the oscillators frequencies, and lead to echoes. The echo properties and possible origins of the nonlinearities leading to the parametric mixing are discussed for different materials. The observed echo pattern for a 3-pulse excitation requires a 7-th order mixing process to be present.

This echo, in many aspects, is similar to elastic echoes observed from bulk solids, and experimentally it is verified that the echo from bulk solids and powders behave similarly.

The mechanical quality factor of the powders depends on the size and the shape of the particles, but it can be of the order of 10^4 which makes the relaxation time of the echo sensitive to the intrinsic anelastic losses in powders. This makes the echo technique a convenient method for the study of powdered materials.

ACKNOWLEDGMENT

I am grateful to my supervisor, Dr. C. W. Searle, for guidence and supervision of the research project and the thesis as well as for the financial support.

I am also thankful to Dr's. I. Maartense and G. Williams for many stimulating discussions and helpful hints.

I must acknowledge my friends and fellows graduate students for discussions and help in various parts of the project. Excellent typing was done by my friend V. Beyak.

My wife's patience if not encouragement made this thesis possible.

TABLE OF CONTENTS

		Page
CHAPTER I.	Introduction	1
CHAPTER II.	Echo Formation Processes	7
2.1.	Classical echo process	7
2.2.	Echo due to parametric mixing	15
2.3.	The Relaxation Time	25
2.4.	Relaxation Time of the Echoes	26
2.5.	Echo Pattern Produced by Parametric Coupling.	28
2.6.	Other Echo Descriptions	30
2.7.	Phase Relationship Between RF Pulses and Echoes	32
2.8.	Consequencies of the Various Echo Mechanisms.	32
2.9.	Echo from a Real System	33
2.10.	Nonresonant Excitation	39
2.11.	Elastic Properties of the Particle	41
2.12.	Various Echo Mechanism in Powders	44
2.13.	Origin of the Loss	46
2.14.	Driving Force	47
CHAPTER III.	Apparatus	58
3.1.	Electronics	58
3.2.	Magnetic Field Calibrations	60
3.3.	Measuring of Echo Spectrum	60
3.4.	Cryogenic System	61
3.5.	Miscellaneous	63

		Page
	3.6. Sample Preparation	63
	3.7. Echo Detection	69
	3.8. Effect of Repetition Rate	69
CHAPTER IV	Experimental Results and Discussion	72
	4.1. Introduction	72
	4.2. Experimental Results	74
	A. Common Properties of Echo from Powders .	74
	B. Echoes From Normal Metals	94
	C. The Echo from Ferromagnetic Powders . .	107
	D. The Echo from Piezoelectric Powder . .	126
	E. Determination of the Elastic Modes . .	126
	4.3. Discussion of the Experimental Results . .	128
	A. Common Properties of the Powders	131
	B. Echo from Normal Metals	140
	C. Echo from Ferromagnetic Materials . . .	157
	D. Echo from Piezoelectric Powders	181
	E. Character of the Elastic Modes	183
	4.4. Conclusions	183
CHAPTER V	Conclusions and Suggestions for Further Study . . .	191
APPENDIX I	Normal Modes Formulation	199
APPENDIX II	Quantum Mechanical Formulation	202
APPENDIX III	Permanently Stored Echoes in Power Materials . . .	206
REFERENCES		212

LIST OF FIGURES

Figure		Page
2.1	Gould's Model of Echo Formation	11
2.2	Echo Pattern Following 3 Pulse Excitation	24
2.3	Direct Excitation Process by Eddy Currents a) Longitudinal b) Transversal	51
3.1	Block Diagram of the Pulse Spectrometer	58
3.2	Example of the Powder Samples	62
3.3	Echo Amplitude as a Function of Time for Different Repetition Rate (Cu, 4.2°K)	71
4.1	Echo Envelope	76
4.2	Echo Envelope for Loose and Compressed Powder	78
4.3	Echo Envelope for Different Gas Pressures in the Sample Tube	78
4.4	Relaxation Time of a Function of Frequency for (a) Al Powder of Different Sizes and (b) Different Materials .	80
4.5	Box Car Trace of the Echo Pattern from Ni Powder . . .	81
4.6	Echo Pattern Following a 3 Pulse Excitation	81
4.7	Relaxation Time of the Echo from Rochelle Salt.	84
4.8	Complex Echo Shape Following the Excitation by 2 RF-Pulses of Different Width	84
4.9	Position of the Echo Following 1 Pulse as a Function of Pulse Width	86
4.10	Variation of the Echo Amplitude with Pulse Separation .	86
4.11	Dependence of the Echo Amplitude on Strength of RF Pulses	87

Figure		Page
4.12	Dependence of the Echo Amplitude on Intensities of the RF Electric Pulses	88
4.13	Dependence of the Echo Amplitude on RF Pulse Intensity for $h_1 = h_2$	90
4.14	Amplitude of the Second and First Echo for Ni Powder for Different RF Field Intensities	90
4.15	Relative Echo Spectrum	93
4.16	Echo Amplitude as a Function of Time From a Fresh Sample	93
4.17	Echo Amplitude as a Function of H for Various Values of h_1, h_2	96
4.18	Echo Amplitude as a Function of H for Various Metals .	97
4.19	Dependence of the Echo Amplitude of H for high Field Intensities	97
4.20	Block Diagram of the Direct Excitation of Ultrasonic Waves in Bulk Metal	99
4.21	Amplitude of the "Direct Excitation" Signal From Al as a Function of H	99
4.22	Dependence of the Echo Amplitude on the Relative Angle Between h and H	100
4.23	Temperature Dependence of the Echo Amplitude for Al as a Function of Particle Size and Frequency.	100
4.24	Echo Amplitude as a Function of Temperature (Al, Cu Au) .	102
4.25	Echo Amplitude as Function of Temperature (Mg)	102

Figure		Page
4.26	Relaxation Time of Echo From Al Powder as a Function of Biasing Magnetic Field	103
4.27	Dependence of the Echo Amplitude, X-ray Line Breadth and Electrical Resistivity on Annealing Time	105
4.28	Echo Amplitude and Relaxation Time as a Function of Biasing Magnetic Field	108
4.29	Echo Amplitude as a Function of Biasing Field for Bulk and Powdered Ferrite	110
4.30	Relaxation Time of Echo from Bulk Ferrite as a Function of Frequency	110
4.31	Echo Amplitude as a Function of the Biasing Field (Co) . .	112
4.32	Echo Amplitude as Function of the Biasing Field in Fe for Annealed and Deformed Powder	114
4.33	Echo Amplitude as a Function of the Biasing Field for YCo_5	115
4.34	Relaxation Time of Annealed Ni as a Function of Biasing Field	116
4.35	Relaxation Time as a Function of the Biasing Field for Deformed and Annealed Ni Powder	117
4.36	Relaxation Time of Annealed and Deformed Fe Powder as a Function of Biasing Field	117
4.37	Relaxation Time of the Free Induction and an Echo from $\alpha - Fe_2O_3$	119

Figure		Page
4.38	Relaxation Time of Ferrite as a Function of the Biasing Field.	119
4.39	Echo Amplitude as a Function of Temperature for Various Materials	121
4.40	Echo Amplitude as a Function of Sweep Speed of Biasing Field ($NdCo_5$)	121
4.41	Echo Amplitude for YCo_5 Annealed in Hydrogen and Vacuum.	123
4.42	Echo Amplitude as a Function of Sweep Speed of Biasing Field YCo_5	124
4.43	Relaxation Time of $NdCo_5$ Powder Before and After Vacuum Annealing	124
4.44	The Amplitude and the Relaxation Time of the First Echo as a Function of Temperature (Rochelle Salt)	125
4.45	Dependence of the Echo Amplitude on the Biasing Electric Field	127
4.46	Modulation of the Echo Shape by the Transients	138
4.47	Skin Depth as a Function of Temperature	147
4.48	Magnetic Contribution to the Loss for Al Powder	150
4.49	Plot of Losses For Spherical Particle	151
4.50	Magnetostructive Stress Amplitudes as a Function of the RF Field Intensity	160
4.51	Electromechanical Coupling Coefficient as a Function of Magnetic Induction for Ni	163

Figure		Page
4.52	Magnetic Contribution to Logarithmic Decreament of Ni Sample at Various Temperatures	169
4.53	Dependence of the Echo Amplitude on the Sweep Speed for YCo_5	178
4.54	Temperature dependence of the Various Components of the a Tensor for Rochelle Salt.	182

Chapter I

INTRODUCTION

The term "echo" refers to a partial reradiation of energy from a sample some time after the application of a two (or more) RF-pulse excitation. There are many different processes in solids which can lead to an echo and some of them become valuable tools for the study of different material properties. The best known of these is the spin-echo which is used to study spin dynamics in materials.

It was assumed for a long time, after Hahn's discovery and description of spin echoes[1], that echo formation was a property of a quantum system. In the early 1960's the discovery of a photon echo[2], arising from a transition between energy levels in a 2 level system, was not surprising due to the formal identity between a spin ½ and a 2 level energy system[3].

In 1965 a cyclotron echo from an ionized plasma was observed[4]. This system is classical (the energy of each "oscillator" written in the form $n \hbar \omega$, requires a very large n) and its discovery stimulated interest in echo phenomena more general than the spin echo, which resulted in a number of echo models (see, for example, Refs. (5-7)). The basic principle involved in all these models is that energy can be stored in a system in different modes and pulse excitation, under favorable conditions, leads to a spontaneous reradiation, or an echo.

Echoes involving many different modes in solids have been observed or described. Some examples of these are: magnetostatic modes[8],

fluxoid modes in type II superconductors[9], polarization modes[10], and various elastic modes in bulk[11-13] or powder[14-17] materials.

In this work a mechanical (elastic) echo observed from powder materials in a wide range of temperature, frequency, and particle size is discussed. This kind of echo certainly is not new. It is observed quite often in pulsed NMR experiments, when powder samples are used, and effort is usually directed towards its elimination. This echo has been reported for many substances at fixed frequencies. While all observers agree that the modes, required to store energy, are elastic in nature the actual microscopic mechanism which leads to echo formation is not known. In order to familiarize the reader with the problem of the echo formation from powder substances a short summary of the reported observations and conclusions regarding the echo origin is presented.

An echo from piezoelectric powders was mentioned by Livingstone[18] in connection with NQR pulse experiments where this echo obstructed the spin-echo. He pointed out its mechanical origin, i.e. refocussing of the elastic modes of particles, and suggested the submersion of powders in liquids as a means of the echo's elimination. He did not attempt to explain its origin.

In 1968 Stauss and Rubinstein[15] reported this echo from ferromagnetic substances. They observed a relationship between the particle size and the echo appearance, as well as a correlation between the frequency ranges of the presence of the absorption lines in CW (continuous wave) and the echo in pulse experiments. For the echo process, they proposed the refocussing of single particle modes excited by magnetostriction.

This suggestion was strongly supported by the observed dependence of the echo amplitude on the biasing magnetic field, which passes through a maximum and continuously disappears above magnetic saturation.

They discussed the echo formation in terms of parametric mode mixing by an amplitude dependent driving force. This echo process was discussed previously by Hermmann and Whitmer[19] in connection with the cyclotron echo.

Echoes from the normal metals were first reported by Alloul and Froidevaux[14] at a low temperature and fixed frequency. They observed an H^2 dependence of the echo amplitude on the biasing magnetic field, H, and different relaxation times of the first and second echoes after a two-pulse excitation. They did not discuss the echo origin. In 1970 Snodgrass[20] reported a strong echo from AgNi, AgMn (< 0.1%) which was absent in pure Ag without attempting to explain its origin. An echo from different metals at 16MHz was reported by Pacult et al[16]. They also observed an H^2 dependence of the echo amplitudes, and a dependence of the echo amplitude on the repetition rate. They observed the echo from particles smaller than the minimum size required for free vibrations and later reported[21] that the decrease of the echo amplitude after mixing the powder of normal metals with inactive powder is size dependent. These observations led them to the conclusion that collective vibrational modes are responsible for an echo. They suggested that the driving force was the torque, due to the interaction of the eddy currents, induced by the RF magnetic field, with the static magnetic field. They did not attempt to explain the echo mechanism.

Table 1.1 lists the normal metals for which an echo has been reported.

Table 1.1

Material	Ref (16) 16 MHz	Ref (14) 5 MHz
In	---	yes
Cu	yes	yes
Zn	yes	---
Sn	---	yes
Al	yes	---
V	yes	---
Pb	no	yes
CuCo	yes	---
Pb Hg	---	yes
Ag	yes	---

Apart from the fact that some kinds of elastic modes in powders are responsible for the echo, it is not clear how and which elastic modes lead to an echo. The purpose of this study is to compare the echoes from different materials, identify the character of the elastic vibrations and their excitation mechanism, and determine the echo formation process. The aim of this study is also to investigate the usefulness of this effect for the study of material properties.

The experimental evidence indicates that elastic vibrations in the sample ultimately lead to the observed echo. The sample, therefore,

can be represented by a set of nondegenerate oscillators (resonance modes) which somehow partially refocus after a two pulse excitation leading to the observed echo.

It should be stressed that a linear system's (simple harmonic oscillator's) response to a multi-pulse sequence does not lead to an echo. This follows because a linear system's total response is the direct sum of the linear responses from the individual pulses and this provides no possibility for the eventual echo formation. A nonlinearity in the system, which is effective during or after the application of the second pulse, can provide the proper mixing of elastic modes, which then leads to an echo.

The energy reradiated during the echo is only a small fraction (10^{-10}) of the energy pumped into the system by the RF pulses. Therefore the nonlinearity which is required to form the echo can be small. This suggests that these echo phenomena could form a powerful new tool in solid state physics.

This thesis is organized as follows:

In Chapter II various nonlinear processes which can lead to an echo from a multioscillator system are discussed. The discussion leads to the developement of a simple model which can describe all the experimental data, if simplifying restrictions are relaxed. The model can relate the relaxation time of individual echoes to the anelastic losses of the particles, and it also aids in the selection of physical nonlinearities which can lead to an echo. Neither the relaxation time nor the origin of the required nonlinearities have been discussed prior to this

work. This chapter also includes a short discussion of the elastic properties of the powders and possible coupling mechanisms between the RF field and elastic modes of the sample.

Chapter III describes the apparatus used for the echo observation and lists the samples.

Chapter IV lists the experimental results and their discussion. Both are divided into the following groups:

A. Properties common to all powders

B. Properties specific to normal metals

C. Properties specific to ferromagnetic materials

D. Properties of the one piezo and ferroelectric substance Rochelle salt.

E. Experiments related to the identification of the elastic modes involved.

This division is more illustrative than the list of the properties according to the materials, because the majority of the echo properties are identical in all powders but some of the materials are more suitable than others to demonstrate a given effect. The final conclusions are in Chapter V.

Chapter II

ECHO FORMATION PROCESSES

2.1. Classical Echo Processes

In the well known vector model for a spin-echo the origin of the echo can easily be visualized as a flipping and refocussing of spins in a rotating frame of reference. A similar pictorial model of oscillator echoes was proposed by Gould[30]. The basic idea of his model is that a classical system, in some ways, can be viewed as a set of nondegenerate oscillators with closely spaced frequencies in the bandwidth of an exciting pulse. In the presence of nonlinearities a two pulse excitation leads to a periodic phase refocussing, and hence an echo. This model was originally proposed for cyclotron echoes where the oscillators are electrons moving in circular paths and the degeneracy is removed by inhomogenities in the static magnetic field. After the application of a pulse of electric field intensity $\mathcal{E}$ and duration t_w the electrons gain a velocity $v = \frac{e}{m}\mathcal{E}t_w$ and move in a circular path $v_x^2 + v_y^2 = v^2$ where z is the direction of the static magnetic field in real space.

By the canonical transformation $(v_x, v_y) \rightarrow (q, p)$ (q, p are canonical coordinates) the motion of any linear oscillator can be described by a closed path in phase space.

For example, a harmonic oscillator can be described by the closed path $(p/\sqrt{m})^2 + (q\,\omega\sqrt{m})^2 = 2\mathcal{F}$ where $\mathcal{F}$ is the energy and $\omega = \sqrt{k/m}$, the natural frequency of the oscillator.

A necessary condition for echo formation is a memory in the

system, i.e., the system at the time of application of additional pulses must remember the initial excitation. This is guaranteed by the high resonance Q, quality factor of the oscillators.

Since oscillator interaction can be important to an echo process, it is necessary to distinguish between echoes due to the nonlinear response of individual oscillators to pulse excitation and those due to mutual oscillator interaction. In the first case the echo origin can be studied as the response of one oscillator and the echo amplitude is the sum of responses for all oscillators. In the latter case a many-body approach is necessary[22]. In the present study no evidence of multi-mode interaction was observed.

The term "oscillator" refers to one resonance mode which need not be spatially localized.

Gould's model of echo formation can also be used to visualize the formation of elastic echoes.

The model is based on the fact that all oscillators, having particular coordinates $(q, p)_{\tau'}$, at time τ' after a coherent excitation, will rephase at the same position $(q, p)_{2\tau'}$ at time $2\tau'$ independent of their frequencies. This is a necessary but not sufficient condition for the formation of oscillator echoes.

Let us assume a linear two pulse excitation. After the first pulse, at $t = 0$, all oscillators have the same energy and the same phase. After the second pulse (II) $(t = \tau)$ their energies will depend on what their phase, θ, was prior to pulse II. Because the energy increments due to pulse II for all oscillators with the same phase θ are equal, it

is convenient to introduce the term "θ - class" referring to the subset of oscillators with phases in the interval θ to θ + Δθ.

One can introduce the term "moment of θ - class" to refer to the sum of coordinates of all members of a θ - class (N_θ) as

$$\mu_\theta = \Sigma_{i \epsilon N_\theta} \mu_i \qquad (2.1)$$

$$\mu_i = A_i = \omega\sqrt{m}q + \{i/\sqrt{m}\}p$$

(where the symbol ε means contained in). Because the different members of a θ - class have different resonance frequencies they defocus quickly. (In a time $\frac{2\pi}{\Delta\omega}$ where $\Delta\omega$ is the angular frequency distribution of the oscillators).

At times $t > \frac{2\pi}{\Delta\omega}$, after the pulses, the members of a θ - class are approximately equally distributed along a constant energy curve in phase space and

$$\mu_\theta = 0$$

The members of a θ - class rephase at times $n\tau$ where n is an integer and only at these times is $\mu_\theta \neq 0$. It must be emphasized that this rephasing by itself, does not lead to an echo because the total moment of the sample,

$$\mu = \sum_{\text{all } \theta} \mu_\theta = \sum_{i \epsilon N} \mu_i \equiv 0 \qquad (2.2)$$

(where N is the number of oscillators) is identically zero. However, certain nonlinearities can destroy this balance between different θ - classes and an echo can appear.

The process described above is shown schematically in Fig. 2.1. Prior to pulse I, the energy of all oscillators is zero and the system is described by a point at the origin. (δ - pulse excitations are assumed (infinite bandwidth)).

Figure 2.1a shows the situation immediately after pulse I. defocussing at $t > \frac{2\pi}{\Delta\omega}$ leads to an equal distribution of oscillators along a constant energy curve Figure 2.1b. Because of this homogeneous distribution,

$$N_\theta = \frac{\Delta\theta}{2\pi} N \tag{2.3}$$

the effect of a second pulse at $t = \tau$ is a shifting of the entire distribution in a particular direction, Figure 2.1c. (Points 1-20 represent particular θ - classes).

All members of a θ - class travel through an angle $2\pi n + \theta$ in the time τ, where n is an integer.

Immediately after pulse II they have a new phase and amplitude (A', θ'). The new amplitude is given by the sum of the amplitudes due to pulse I and II.

$$A'_\theta = A_I e^{i\theta} + A_{II} \tag{2.4}$$

i.e. in the special case in Figure 2.1c.

$$|A'_\theta| = \sqrt{(A_{II} + A_I \cos\theta)^2 + (A_I \sin\theta)^2}$$

and (2.5)

$$\cos\theta' = \frac{A_I^2 - A_{II}^2 - A_\theta^{12}}{2A_2 A'_\theta}$$

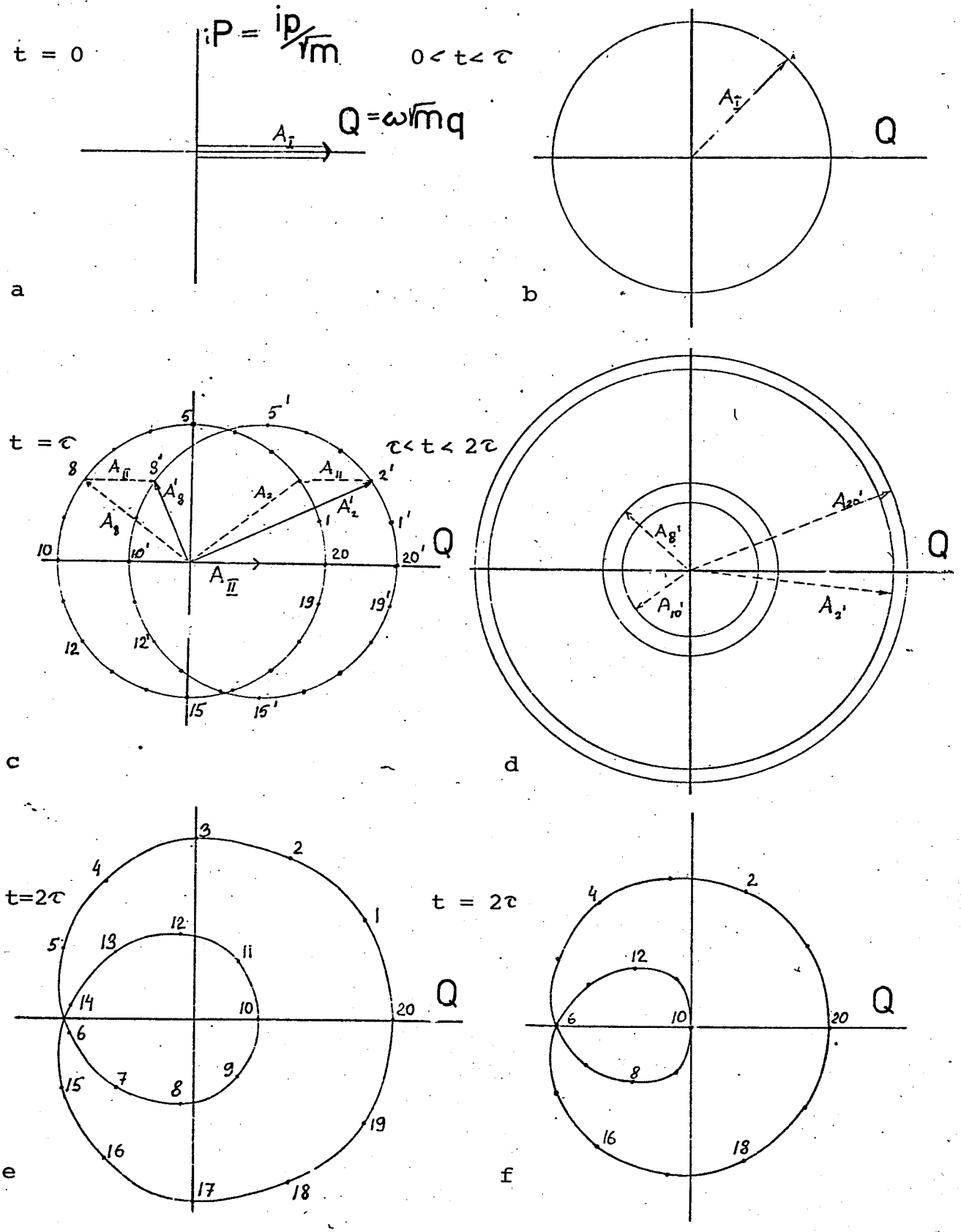

Figure 2.1: Gould's Model of Echo Formation (See-text)
($A_{II} = \frac{1}{2} A_I$)

At time $t > \tau$, $t \neq n\tau$ each θ - class is defocussed and its members are equally distributed on a constant energy curve. Figure 2.1d shows four θ - classes at $2\tau > t > \tau$, which are completely defocussed.

A_2', A_8', e.t.c. represents the amplitude of the individual members of the particular θ - class.

Figure 2.1e shows the entire distribution at time $t = 2\tau$, when all θ - classes are refocussed in position $\theta' + \theta$ and have moments

$$\mu_\theta = N_\theta \mu_o \tag{2.6}$$

Where μ_o is a moment of one particle.
The total moment is

$$\mu = \sum_{\text{all } \theta} \mu_\theta = \frac{N}{2\pi} \int_o^{2\pi} d\theta \, A_\theta' \, e^{i\theta}$$

$$= \frac{N}{2\pi} \int_o^{2\pi} (A_I e^{i\theta} + A_{II}) e^{i\theta} d\theta = 0 \tag{2.7}$$

where a uniform phase distribution of θ - classes

$$n(\theta) = \frac{N}{2\pi} \tag{2.8}$$

was assumed. Different processes which can lead to an echo will now be discussed.

As can be seen all θ - classes mutually compensate their moments in this two-pulse linear model. If the shift of the energy curve due to pulse II differs from θ - class to θ - class, due to a nonlinear interaction, $\mu(2\tau)$ can be different from zero and an echo occurs. For example figure 2.1f indicates the distribution of θ - classes at $t = 2\tau$

assuming that the second pulse has the form $A'_{II} = A_{II}(1 - \cos\theta)$. In this case

$$A'_\theta = A_1 e^{i\theta} + A_{II}(1 - \cos\theta) \tag{2.9}$$

and

$$\mu(2\tau) = \frac{N}{2\pi}\int_o^{2\pi} A_{II}(1 - \cos\theta)e^{i\theta}\, d\theta = \frac{N}{2} A_{II} \tag{2.10}$$

In the mechanism described above the echo originates from the incomplete compensation of moments of different θ - classes. The fact that μ_θ is non zero only at $t = n\tau$, $n = 2,3 \ldots$ clearly puts a restriction on possible echo times. The origin of this incomplete compensation of different θ - classes can be either the properties of the oscillators themselves or the nature of the driving force. In both cases the echo is a result of a nonlinearity in the system. Different processes which can lead to an echo will now be briefly discussed.

(a) If the relaxation rate depends on amplitude[6,23], then the moment of a particular θ - class is given by

$$\mu_\theta(2\tau) = \sum_{i\varepsilon N_\theta} \mu_i(2\tau) = \mu_\theta(\tau)e^{-\frac{\tau}{T(\theta)}} \tag{2.11}$$

and generally

$$\mu(2\tau) = \frac{N}{2\pi}\int_o^{2\pi} \mu_\theta(2\tau)d\theta$$

$$= \frac{N}{2\pi}\int_o^{2\pi} d\theta(A_1 e^{i\theta} + A_{II})e^{i\theta}\, e^{-\frac{\tau}{T(|A_1 e^{i\theta} + A_{II}|)}} \neq 0 \tag{2.12}$$

However, for a zero pulse separation the term causing the echo disappears and therefore this echo increases with pulse separation.

(b) The resonance frequency of individual oscillators may depend on their[24,25] amplitude. Then different θ - classes, because of their different amplitude, exhibit a different additional frequency shift $\Delta\omega_\theta(A'_\theta)$. Thus at time $t = 2\tau$ they will have phase $\theta' + \theta + \Delta\omega_\theta\tau$ which leads to an incomplete compensation of their moments and

$$\mu(2\tau) = \frac{N}{2\pi}\int_o^{2\pi} d\theta(A_I e^{i\theta} + A_{II})e^{i\theta + i\Delta\omega(A'_\theta)\tau} \neq \theta \qquad (2.13)$$

Again, this echo increases with increasing pulse separation.

In addition, because the different members of a particular θ - class have different resonance frequencies, the frequency shift varies from member to member and therefore leads to a partial defocussing of the θ - class.

The moment of the θ - class is given by

$$\mu_\theta(2\tau) = \sum_{i\epsilon N_\theta} |\mu_i| \cos(\Delta\omega_i\tau) =$$

$$= |\mu_o| \sum_{i\epsilon N_\theta} \cos\,\Delta\omega_i\tau < N_\theta|\mu_o| \qquad (2.14)$$

Thus it should be stressed that these amplitude dependent processes, (a) and (b), require time to develop and therefore the echo amplitude will increase with pulse separation (neglecting relaxation effects). The specific form of the dependence of the echo on the amplitudes A_I and A_{II} depends strongly on the chosen relationship $T(A)$ or $\omega(A)$.

Two specific cases were discussed in the literature:

a) the attenuation linearly proportional to the amplitude[26]. In this case

$$\mu\alpha A_I A_{II} \tau \qquad (2.12a)$$

b) the frequency shift proportional to the square of the amplitude[24] leading to

$$\mu \alpha A_I A_{II}^2 \tau \qquad 2.13a)$$

c) another possible origin of incomplete compensation is nonlinear (parametric) coupling of the amplitude of the oscillators due to pulse I to the external periodic RF field during the pulse II. In this case the effect of the RF pulse II at time $(t = \tau)$ depends on the phase of the oscillators and is different for different θ - classes. The physical interaction leading to a possible echo in the sample occurs during the second pulse. Unlike the previous processes, this process does not require time between pulses to develop and the echo amplitude is independent of τ (neglecting relaxation effects). According to experimental evidence, this mechanism seems to play a dominant role in the formation of elastic echoes from solids and will be discussed in greater detail.

2.2 Echo due to parametric mixing

Let us demonstrate this process with two examples:

a) an oscillator with the restoring constant dependent on the RF

field h.

The equation of motion of the oscillator has the following form

$$\ddot{x} + \omega^2(1 + \varepsilon f(h))x = 0 \qquad (2.15)$$

where $\varepsilon << 1$ and $f(h)$ represents some function expressing the dependence of the restoring constant on h.

The simplest form of $f(h)$, for x and h having approximately the same time dependence $e^{i\omega t}$, leading to an echo, has the form

$$f(h) = h^2$$

b) An oscillator excited by an amplitude dependent force.

The equation of motion has the form

$$\ddot{x} + \omega^2 x = F(1 + \varepsilon f(x)) \qquad (2.16)$$

where again $\varepsilon << 1$ and $f(x)$ express the dependence of the force on the amplitude x.

For the same time dependence of x and F the simplest form of $f(x)$ leading to an echo is

$$f(x) = x^2$$

Case a is a classical example[27] of a parametric oscillator and its function as a parametric amplifier is discussed in the literature[28].

Case b was analyzed in great detail by Hermmann and Whitmer[19]. In both cases the parametric mixing occurs during the second pulse, because the response of the oscillator to the second pulse is modulated

by the elastic vibrations excited by the RF pulse I.

To illustrate the echo formation it is convenient to use the normal mode formalism (appendix I). The advantages is that in the equation of motion for mode $a = a_o e^{i\omega t}$ only terms varying as $e^{i\omega t}$ are of interest. Therefore, the derivation is more illustrative and can be easily extended to higher order echoes.

In case a the first RF pulse of intensity h_{10} and duration t_{w1} produces a force $f_{10} = dh_{10}$ # on the i-th oscillator, generating the mode

$$a_i = a_{iI} e^{i\omega_i t} = d\, h_{10}\, t_{w1}\, e^{i\omega_i t} \tag{2.17}$$

which interacts with the RF field, h_2 due to an interaction of the type

$$H_{int} = \frac{1}{2} \sum_i \varepsilon' (a_i + a_i^*)^2 (h_2 + h_2^*)^2 \tag{2.18}$$

where H_{int} represents the nonlinear term in the interaction $(x^2 h^2)$ and

$$h_2 = h_{20} e^{i\omega_o (t - \tau)} \quad \text{for } \tau < t < \tau + t_{w_2}$$

$$= 0 \quad \text{otherwise} \tag{2.19}$$

The hamiltonian of the system has the following form (Appendix I)

$$H = \sum_i a_i a_1^* + \frac{\varepsilon'}{2} \sum_i (a_i + a_i^*)^2 (h + h^*)^2 + \text{RF Energy}$$

The equation of the motion for mode a_i has the form (Appendix I)

$$\dot{a}_i = i\omega_i \frac{\partial H}{\partial a^*} = i\omega_i (a_i + \varepsilon' (a_i + a_i^*)(h + h^*)^2) \approx$$

$$\approx i\omega_i (a_i + \varepsilon' (2a_i\, hh^* + a_i^* h^2)) \tag{2.20}$$

Footnote: Factor d is used to relate the force acting on the oscillator to the RF field intensity.

where we neglected terms with time dependence other than $e^{i\omega t}$.

Seeking a solution of Eq. (2.20) of the form

$$a_i = \sum_{n=o}^{\infty} a_{in} \varepsilon^{n} \tag{2.21}$$

and comparing the terms of equal power of ε, one obtains a family of equations, from which we need only the first two to describe the echo.

$$\dot{a}_{io} - i\omega_i a_{io} = 0 \tag{2.22}$$

$$\dot{a}_{i_1} - i\omega_i a_{i_1} \doteq a^*_{io} h^2_0 e^{i2\omega(t - \tau)}{}_i \quad \text{for} \quad \tau < t < \tau + t_{w_2}$$

$$= 0 \quad \text{otherwise}$$

where in the second equation we neglected the term $a_i hh^*$ which does not contribute to the echo.

The solution of Eq's. (2.22) have the form

$$a_{io} = a_{iI} e^{i\omega_i t}$$

and (2.23)

$$a_{iI} \sim i\omega_o a^*_i h^2_{20} e^{\omega_i (t - 2\tau)} t \quad \text{for} \quad \tau < t < \tau + t_{w_2}$$

$$\approx i\omega_o a^*_{io} h^2_{20} e^{i\omega_i (t - 2\tau)} t_{w_2} \quad \text{for} \quad t > \tau + t_{w_2}$$

In the second equation we neglected the frequency difference $\omega_o - \omega_i$ during the second pulse of the duration t_{w_2}.

The sum of amplitudes of all modes $\sum_i a_i$ is

$$\mu'(t) = \sum_i a_i(t) = \sum_i (a_{io} + \varepsilon' a_{iI}) =$$

$$= i\varepsilon' \omega_o h_{20}^2 t_{w_2} \sum_i a_{iI} e^{i\omega_i(t - 2\tau)}$$

i.e. it is zero at $t \neq 2\tau$ and equal to

$$\mu'(2\tau) = i\varepsilon' \omega_o a_I h_{20}^2 N t_{w_2} \tag{2.24}$$

for $t = 2\tau$, in Eq. (2.24) we assumed that $a_{iI} = a_I$ for all i.

Using Eq. (2.17) Eq. (2.24) can be written as

$$\mu'(2\tau) = 2\varepsilon' \omega_o t_{w_1} t_{w_2} dh_{10} h_{20}^2 N \tag{2.25}$$

The second example is the amplitude dependent driving force.

The equation of the motion for the i-th mode has the form

$$(\frac{\partial}{\partial t} - i\omega) a_i = f_2 (1 + \varepsilon' f(a,a^*)) \tag{2.26}$$

with $f_2 = dh_2$, where h_2 is given by Eq. (2.19).

Let $f(a,a^*) = aa^*$, then the term

$$dh_{20} e^{i\omega t} (1 + \varepsilon' aa^*)$$

on the right side of Eq. (2.26) can lead to an echo. Prior to the second pulse, the a_i has the form

$$a_i = a_{iI} = a_{iI}(0) e^{i\omega t} = f_{10} t_{w_1} e^{i\omega_i t}$$

Solving Eq. (2.26) with the substitution (2.21) and comparing the terms

of equal power of ε' one obtains the family of the equations, the first two of which are

$$\left(\frac{\partial}{\partial t} - i\omega_i\right) a_{io} = f_{20}\, e^{i\omega_o (t - \tau)} \qquad \text{(a)} \quad (2.27)$$

and

$$\left(\frac{\partial}{\partial t} - i\omega_i\right) a_{i1} = f_{20} e^{i\omega_o (t - \tau)}\, a_{i0}\, a_{i0}^{*} \qquad \text{(b)}$$

The solution of Eq. (2.27)a for $t > \tau + t_{w_2}$).

$$a_{io} \doteq a_{iI} + f_{20}\, t_{w_2}\, e^{i\omega_i (t - \tau)} =$$

$$= a_{iI} + a_{iII}$$

where we introduced the $a_{iII} = f_{20}\, t_{w_2}\, e^{i\omega_i (t - \tau)}$ and neglected the frequency difference $\omega_o - \omega_i$. during the second pulse. The solution of Eq. (2.27)b has the form for $t > \tau + t_{w_2}$.

$$a_{iI} = f_{20}\, t_{w_2} (a_{iI}\, a_{iI}^{*} + a_{iII} a_{iI}^{*} + a_{iII}^{*}\, a_{iI} + a_{iII}\, a_{iII}^{*})\, e^{i\omega_i (t - \tau)} \qquad (2.28)$$

$$= a_{iI}\, a_{iI}^{*}\, a_{iII} + a_{iI}^{*}\, a_{iII}^{2} + a_{iI}\, a_{iI}^{*}\, a_{iI} + a_{iI}^{*}\, a_{iII}^{2}$$

the term

$$a_{iI}^{*}\, a_{iII}^{2}$$

has the time dependence

$$e^{i\omega_i (t - 2\tau)}$$

and therefore

$$\mu'(t) = \sum_i a_i = \sum_i (a_{io} + \varepsilon' a_{iI}) - \tag{2.29}$$

$$= 0 \qquad \text{for} \quad t \neq 2\tau$$

$$= N\varepsilon' a_I^* a_{II}^2 = N\varepsilon' t_{w_1} t_{w_2}^2 h_1 h_2^2 d^3 \quad \text{for} \quad t = 2\tau$$

The third equation in the expansion of Eq. (2.26) in equal powers of $\varepsilon'(\varepsilon'^2)$ has the form

$$(\frac{\partial}{\partial t} - i\omega_i) a_{i2} = f_{20} e^{i\omega_o(t - \tau)} [(a_{iI} + a_{iII}) a_{i1}^* + (a_{iI} + a_{iII})^* a_{i1}] \tag{2.30}$$

and contains a term

$$a_{iI}^{*2} a_{iII}^2 \tag{2.31}$$

which leads to a component of a_{i2} of the form

$$a_{iI}^{*2} a_{iII}^3$$

varying as $e^{i\omega_i(t - 3\tau)}$ and leads to an echo at time $t = 3\tau$.

This echo is of the order ε'^2.

As can be seen, the formation of the simplest echo at $t = 2\tau$ is a third order process. Different interaction terms lead to echoes at different times with different dependence on h_1 and h_2. For example: a term of the form $a^2 a^{*2} h_2$ in Eq. (2.26) leads to an echo at $t = 3\tau$ (linear in ε') or a term of the form $a^* h_2^* h_2^3$ in Eq. (2.20) to an echo at $t = 2\tau$ varying

as $h_1 h_2^4$ with the RF pulses intensities. As can be seen, the echo is produced by the products of the elastic modes generated by pulse I.

$$a_I \alpha dh_1 \, t_{w_1} \, e^{i\omega t}$$

with the elastic modes generated by pulse II

$$a_{II} \alpha dh_2 \, tw_2 \, e^{i\omega(t - \tau)}$$

or the RF field $h_2 = h_{20} e^{i\omega(t - \tau)}$. Let a_1 represents a_I which varies as $a_1 = a_1(o) e^{i\omega t}$ and a_2 represents a_{II} or h_2, dependent on the character of the echo process, and varies as $a_2 = a_2(\tau) e^{i\omega(t - \tau)}$. Then a parametric mixing of a_1 and a_2 forms terms of the form (for the i-th oscillator).

$$a_{i1}^{\ell} \, a_{i1}^{*m} \, a_{i2}^{k} \, a_{i2}^{*n} \qquad (2.32)$$

where ℓ, m, k, n are integers, which will refocus for all oscillators when

$$\ell t - mt + k(t - \tau) - n(t - \tau) = 0 \qquad (2.33)$$

The lowest term leading to an echo at time $t = n\tau$, after the two pulse excitation, has the form

$$a_1^{*(n - 1)} \, a_2^{n}$$

higher order terms contributing to the same echo are formed by multiplying the basic term by $(a_1 a_1^*)^s$ and $(a_2 a_2^*)^r$ where s, r are integers.

The above formalism can be easily extended to the mixing of

modes with various frequencies or traveling waves. For example, let

$$a_1 = a_1(o)e^{i\omega t}$$

and $$a_2 = a_2(\tau)e^{i2\omega(t - \tau)}$$

then

$$a_1^* a_2 = a_1^*(o)\ a_2(\tau)\ e^{i\omega(t - 2\tau)} \tag{2.34}$$

will form an echo at $t = 2\tau$, or let $a_1 = a_1(o)e^{i(\omega t - \vec{b}_1 \vec{x})}$ and

$$a_2 = a_2(\tau)\ e^{i(\omega(t - \tau) - \vec{b}_2 \vec{x})} \tag{2.35}$$

then the term

$$a_1^*\ a_2^2$$

will form an echo at $t = 2\tau$ with the $\vec{b}$ vector

$$\vec{b} = 2\ \vec{b}_2 - \vec{b}_1$$

Secondary echoes can be formed by the higher order approximations in the solution of the equation of motion (Eq. 2.31), or higher order terms in the hamiltonian Eq. (2.31), or by allowing the echo to play the role of a pulse. The first and last possibilities are of higher order in ε (ε^2).

3 Pulse Echo:

After the application of 3 pulses at time $t = o, \tau, T$ the so-called "stimulated echo" is excited (Figure 2.2) at $t = \tau + T$ (this corresponds to a spin lattice relaxation measurement in the spin echo case

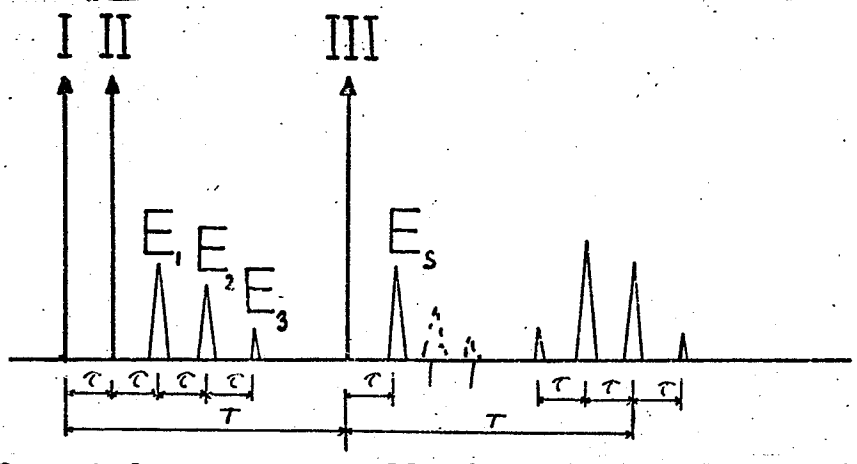

Figure 2.2: Echo Pattern Following the 3 Pulse Excitation

This echo, in the lowest order, is produced by a 3rd order process of the form

$$a_1^* a_2 a_3 = a_1^*(o)\ a_2(\tau)\ a_3(T)\ e^{-i\omega t}$$

$$\times\ e^{i\omega(t - \tau) + i\omega(t - T)}$$

$$= a_1^*(o)\ a_2(\tau)\ a_3(t)\ e^{i\omega(t - \tau - T)}$$

where a_1, a_2, a_3 have the same generalized meaning as in Eq. (2.32) with time variation $a_1 = a_1(o)\ e^{i\omega t}$, $a_2 = a_2(\tau) e^{i\omega(t - \tau)}$ and $a_3 = a_3(T)\ e^{i\omega(t - T)}$. This echo is hard to visualize in terms of rephasing of oscillators. However, Gould presented a graphical representation of this process involving a 3-dimensional distribution[29]. The 3-pulse echo is discussed in great detail by Herrmann and Whitmer[19].

The information leading to a 2-pulse echo is stored in the phases of

the oscillators, while in the 3 pulse case two mechanisms of information storage are possible: One is similar to that in the 2 pulse echo and involves phases of oscillators, the second involves their energies[19]. In the first case the elastic modes a_1 and a_2 are mixed together during the pulse III, in the second, the modes a_1 and a_2 are mixed during the second pulse to form a DC mode, which after mixing with a_3 leads to an echo.

2.3. The Relaxation Time

In the previous discussion we neglected the finite Q of the oscillators. The presence of losses will manifest itself through relaxation. Formally this can be described through the introduction of a complex frequency

$$\omega' = \omega_o\left(1 + \frac{i}{2Q}\right) \tag{2.36}$$

The equation of motion has the form (Appendix 1)

$$\dot{a} = i\omega' \frac{\partial H}{\partial a} \qquad \dot{a}^* = -i\omega'^* \frac{\partial H}{\partial a^*} \tag{2.37}$$

and the normal modes for a harmonic oscillator are

$$a = a(o)e^{i\omega' t} \qquad a^* = a^*(o)e^{-i\omega' t}$$

$$a = a(o)e^{-\left(\frac{\omega_o t}{2Q}\right)}e^{i\omega_o t} \qquad a^* = a^*(o)e^{-\left(\frac{\omega_o t}{2Q}\right)}e^{-i\omega_o t} \tag{2.38}$$

i.e. the normal modes relax with a characteristic relaxation time given by

$$T_o = \frac{2Q}{\omega_o}$$

T_o is linearly related to the quality factor, Q, of the oscillator. Experimentally the logarithmic decrement, δ, is measured as an indication of the Q factor, where δ is defined as

$$\delta = \frac{\pi}{Q} = \frac{\Delta W}{2W} = \ln \frac{a_n}{a_{n+1}} \qquad (2.39)$$

here ΔW is the energy loss per cycle, W is the total energy and a_n is the amplitude of the n-th cycle.

Pictorially, the relaxation can be represented in Figure 2.1 by allowing the radii of the individual energy curves to decrease with time.

2.4. Relaxation Time of the Echoes

Substituting (2.36) into (2.32) immediately leads to an expression for the echo relaxation time. Mode interaction takes place only during the short interval t_{w2} at the time of application of the second pulse. At that time

$$a_1 = a_1(0)\, e^{-\tau/T_o} \qquad (2.40)$$

The term contributing to an echo, $a_1^* a_2^2$, has the form

$$a_1^*(0)\, e^{-\tau/T_o}\; a_2(t)^2 \qquad (2.41)$$

and after pulse II it relaxes with the relaxation time of the oscillator. At the time of the echo the term $a_1^* a_2^2$ has the form

$$a_1^*(0)\, a_2^2(\tau)\, e^{-2\tau/T_o} \qquad (2.42)$$

and the echo decay can be described by

$$E(t) = E_o e^{-t/T_1} \tag{2.43}$$

Comparing Eq. (2.42) with (2.43) for an echo at $t = 2\tau$ leads to

$$T_1 = T_o \tag{2.44}$$

The first echo relaxes with a relaxation time, T_1, identical with those of the oscillators. Similarly, the lowest term leading to an echo at time $t = 3\tau$ has form $a_1^{*2}\, a_2^3$. Mixing takes place at time τ

$$a_1^{*2}\, a_2^3 = (a_1^*(o)\, e^{-\tau/T_o})^2\, a_2^3(\tau) \tag{2.45}$$

and at $t = 3\tau$ this term has the form

$$a_1^{*2}(o)\, a_2(\tau)^3\, e^{-4\tau/T_o} \tag{2.46}$$

Comparing Eq. (2.46) with Eq. (2.43) gives

$$T_2 = 3/4T_o = 3/4T_1 \tag{2.47}$$

The second echo relaxes with an increased rate. Similarly, the stimulated echo, for a phase sensitive process, relaxes with the characteristic time

$$T_s = T_o/2 \tag{2.48}$$

This is obtained from the mixing of modes a_1 and a_2 with a_3 at $t = T$ (T is variable) then

$$a_1^*(o)e^{-T/T_o}\, a_2(\tau)e^{-(T-\tau)/T_o}\, a_3(T))\; e^{-\tau/T_o} = E_s e^{-(T+\tau)/T_s} \tag{2.49}$$

which leads immediately to $T_s = \frac{T_o}{2} = \frac{1}{2} T_1$ (τ is held constant)

2.5. Echo Patterns Produced by Parametric Coupling

As was seen, the amplitude of the i-th oscillator, neglecting the linear response, contains terms proportional to

$$\sum_{\substack{m,\ell=0}}^{\infty} \sum_{n=2}^{\infty} a_{i\,10}(o)^m\, a_{i\,10}^*(o)^{m+n-1}\, a_{i\,20}(\tau)^{\ell+n}\, a_{i\,20}^*(\tau)^{\ell} \times e^{i\omega_i(t - n\tau)} \tag{2.50}$$

$$+ \text{C.C.} + \text{terms varying as } n\omega,\ n \geq 2$$

which are produced by the appropriate term in the hamiltonian or by higher order approximations in the solution of the equation of motion. The sum of amplitudes of all oscillators, $\sum_i a_i$, is nonzero only at $t = n\tau$ when it is proportional to

$$N \sum_{\substack{m=o\\ \ell=o}}^{\infty} a_{10}(o)^{2m+n-1}\, a_{20}(\tau)^{2\ell+n}\, e^{-\left(\frac{2(m+n-1)\tau}{T_o}\right)} \tag{2.51}$$

The subsequent echoes relax with different rates.

If one assumes weak coupling, i.e., the energy transfer between modes per cycle is small, one can neglect all the time-dependent terms in the system's hamiltonian. Then for the phase dependent processes (3 pulse echo formed by mixing a_1 and a_2 with a_3 at $t = T$) one can identify

Table 2.1

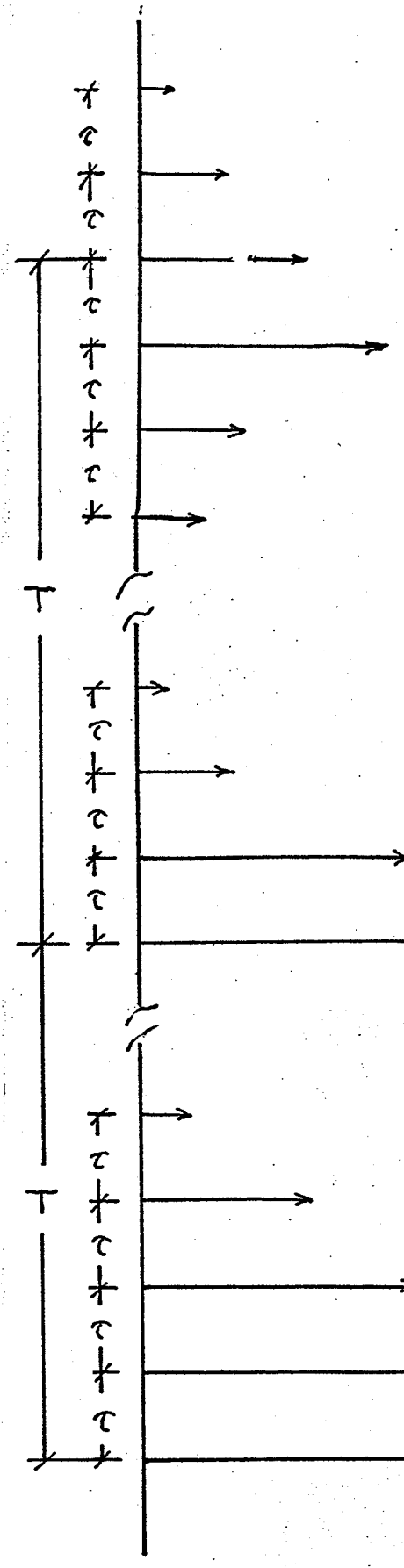

Time of echo t_e	Echo relaxation Re	Echo amplitude Ee(0)
$2T + 2\tau$	$\frac{7T + 2\tau}{T_0}$	$a_1^{*3} a_2^2 a_3^2$
$2T + \tau$	$\frac{5T + \tau}{T_0}$	$a_1^{*2} a_2 a_3^2$
$2T$	$\frac{2T}{T_0}$	$a_1^* a_3^2$
$2T - \tau$	$\frac{2(T-\tau)}{T_0}$	$a_2^* a_3^2$
$2T - 2\tau$	$\frac{4(T-\tau)}{T_0}$	$a_1 a_2^{*2} a_3^2$
$2T - 3\tau$	$\frac{6(T-\tau)}{T_0}$	$a_1^2 a_2^{*3} a_3^2$
$T + 3\tau$	$\frac{6T}{T_0}$	$a_1^{*3} a_2^3 a_3$
$T + 2\tau$	$\frac{4T}{T_0}$	$a_1^{*2} a_2^2 a_3$
$T + \tau$	$\frac{2T}{T_0}$	$a_1^* a_2 a_3$
Pulse III		
4τ	$\frac{6\tau}{T_0}$	$a_1^{*3} a_2^4$
3τ	$\frac{4\tau}{T_0}$	$a_1^{*2} a_2^3$
2τ	$\frac{2\tau}{T_0}$	$a_1^* a_2^2$
Pulse II		
Pulse I		

the origin of the individual echoes in the complex echo pattern. This is shown in Table 2.1 up to the 7-th order interaction. T_o is the relaxation time of the oscillators.

The echo amplitude as a function of time is formally described as

$$E_e(t_e) = E_e(o)\ e^{-R_e} \tag{2.52}$$

2.6. Other Echoes Descriptions

It has already been shown, Eq's. (2.12) and (2.13) that the echo results from the incomplete compensation of the θ - classes, due to some kind of phase or amplitude dependent nonlinearity $Q(A)$ which multiplies the μ_θ in Eq. (2.7), i.e.

$$\mu = \frac{N}{2\pi} \int_o^{2\pi} \mu_\theta\ Q(A)\ d\theta \tag{2.53}$$

The amplitude of the member of the θ - class after pulse II is related to the phase

$$A = A_I e^{i\theta} + A_{II} \tag{2.54}$$

i.e.

$$|A|^2 = A_I^2 + A_{II}^2 - 2A_I A_{II} \cos\theta$$

and therefore $Q(A)$ can be replaced by $Q(\theta)$. The echo formation due to the amplitude dependent frequency or attenuation has been shown in Eqs. (2.12) and (2.13). The nonlinear driving force can be described by

$$Q(A) = (1 - \varepsilon A^2) \tag{2.55}$$

leading to an echo given by

$$\mu \propto A_1 A_{II}^2 \, N \, \varepsilon \tag{2.56}$$

This approach can easily be extended to a 3-pulse echo.

The amplitude of a particular oscillator at $t = \tau$ is

$$A(\tau) = A_I e^{i\vartheta} + A_{II} \, .$$

At time T this oscillator will have a phase ψ and therefore the amplitude at $t = T$ is

$$A(T) = A(\tau) \, e^{i\psi} + A_{III} \tag{2.57}$$

During the time interval τ it travels through an angle $2\pi n + \theta$ and therefore

$$A(T + \tau) = A(T) \, e^{i\theta} =$$

$$= ((A_1 e^{i\theta} + A_{II}) e^{i\psi} + A_{III}) \, e^{i\theta} \tag{2.58}$$

the moment μ has the following form

$$\mu(T + \tau) = \int_0^{2\pi} d\theta \int_0^{2\pi} d\Psi \, n(\psi) \, n(\theta) \, A(T + \tau) \tag{2.59}$$

where $n(\theta) = n(\psi) = \frac{N}{2\pi}$.

Again

$$\mu(T + \tau) = 0 \tag{2.60}$$

and a nonlinearity $Q(A)$ or $Q(\theta,\psi)$ multiplying A in (2.59) will produce the echo.

2.7. Phase Relationship Between RF-Pulses and Echoes

Phase relations between coherent RF-pulses and echoes were discussed by Goldberg et al[9]. Phase shifts between the RF-pulse and the echo signal are: $\pi/2$ for oscillators with an amplitude dependent frequency shift, π for oscillators with a nonlinear attenuation, and 0 or π for oscillators parametrically coupled to the driving force.

The experimental arrangement used here produces noncoherent pulses and therefore phase relationships could not be experimentally determined.

2.8. Consequences of the Various Echo Mechanisms

Now we are in the position to discuss the expected behavior of the echo produced by the various echo mechanisms.

I. Dependence on the pulse separation:

For an amplitude dependent attenuation or restoring constant the amplitude of the echoes is expected to increase with pulse separation. Parametric mixing predicts an exponential decay of the echoes amplitude with characteristic amplitude independent relaxation times.

II. Dependence on the strength of the RF-pulses.

The echo amplitude for the amplitude dependent processes depends on the particular choice of the relationship between the oscillator amplitude, A, and the relaxation time, $T(A)$, or restoring constant, $\omega^2(A)$, respectively. For the simple choices in Eq's. (2.12a or 2.13a)

the first echo depends linearly on the first pulse and linearly (T(A)) or quadratically (ω(A)) on the second. In the case of parametric mixing the dependence of the echo amplitude on the intensity of the RF pulses has a special significance, because according to Eq's. (2.50,51) the echo can depend on h_1 and h_2 as $h_1^n h_2^m$, where $m + n$ gives the order of the process involved in the echo formation.

To be concrete, the simplest first echo can be formed by the term $a_1^* a_2^2$ Eq. (2.27) therefore it is expected to vary as $h_1 h_2^2$. The higher (5-th order) processes leading to the first echo are

$$(a_1 a_1^*)(a_1^* a_2^2) \quad \text{or} \quad a_1^* a_2^2 (a_2 a_2^*)$$

i.e., they vary as $h_1^3 h_2^2$ or $h_1 h_2^4$ respectively. It is important to note that this relationship between the echo amplitude and the intensities of the RF pulse is not dependent on the actual mixing process.

In all echo processes discussed it was assumed that all oscillators interact with the second pulse. Artificial choices of interactions in which only certain θ - classes interact with pulse II, can also lead to an echo. A rather trivial case can be visualized by assuming that only one θ - class interacts with pulse II. Then this θ - class will refocus in regular time intervals τ, giving rise to the subsequent echoes.

2.9. Echo from a Real System

The real system (set of particles) differs in many ways from the ideal oscillator system assumed until now.

a) Particles have a finite Q and therefore if driven at

resonance their amplitudes saturates. The amplitude of an ideal oscillator, driven by an external force $f = f_o\ (e^{i\omega t} + c\ c)$, at resonance, increases with time without limit while a damped oscillator has a final amplitude of $A = \frac{f_o Q}{\omega^2}$. Therefore an oscillator can be considered to be "ideal" only if the pulse duration t_w is less than Q/ω.

b) Particles are not identical, therefore they will have different amplitudes and relaxation times.

c) The RF-pulse is not a δ pulse but has a finite duration i.e. finite bandwidth.

Let us discuss the points (b) and (c) in greater detail.

b) Amplitude and the relaxation time of the non-identical oscillators.

Let each oscillator be defined by its amplitude, A_i, resonance frequency, ω_i, and the relaxation time T_i.

$$A_i = A_i(o)\ e^{i\omega_i t}\ e^{-t/T_i} \tag{2.61}$$

The moment of the particular θ - class at $t = 2\tau$ is

$$\begin{aligned}
\mu_\theta\ (2\tau) &= \sum_{i \varepsilon N_\theta} A_i \\
&= \sum_{i \varepsilon N_\theta} (A_{I_i}(o)\ e^{i\theta}\ e^{-\tau/T_i} + A_{II_i}(\tau)) e^{i\theta} e^{-\tau/T_i} \\
&= e^{2i\theta} \sum_{i \varepsilon N_\theta} A_{I_i}(o)\ e^{-2\tau/T_i} + e^{i\theta} \sum_{i \varepsilon N_\theta} A_{II_i}(\tau) e^{-\tau/T_i}
\end{aligned} \tag{2.62}$$

This expression is complicated, because of the unknown distribution of A_{Ii}, A_{IIi} and T_i through the system.

A large simplification can be achieved by assuming that all A_I and A_{II} are the same and by introducing a distribution function of the relaxation times $P(T)$ such, that $P(T)dT$ represents the probability of finding the oscillator with relaxation time in the interval T to $T + dT$.

Obviously

$$\int_o^\infty P(T)\ dT = 1$$

Then Eq. (2.62) has the form

$$\mu_\theta(2\tau) = A_I\ N_\theta e^{2i\theta} \int_o^\infty P(T)\ e^{-2\tau/T}\ dT + A_{II}\ N_\theta\ e^{i\theta} \int_o^\infty P(T)\ e^{-\tau/T}\ dT \qquad (2.63)$$

The integrals in the last expression are usually written as

$$\int_o^\infty P(T)\ e^{-t/T}\ dT = 1 - G(t) \qquad (2.64)$$

where $G(t)$ is the so-called relaxation function. $G(t)$ varies between 0 and 1 with increasing t.

The form (2.63) for μ_θ should be used for calculating the total moment $\mu(2\tau)$ (Eq. (2.53)).

$G(t)$ is often used to describe the relaxation of multicomponent systems. Extensive discussion of the usage and calculation of $G(t)$ for various distributions $P(T)$ appears in the book of Nowick and Berry[31] Distribution of T_i leads to an nonexponential decay described by $G(t)$.

c) The response of the oscillator system to one pulse of finite length.

Assuming the system is initially at rest let us apply a force pulse $F(t)$ at $t = 0$. The linear response of an individual oscillator is

$$\mu_i(t) = K_i \int_{-\infty}^{t} F(\tau)\, e^{i\omega_i(t - \tau)}\, d\tau \qquad (2.65)$$

where K_i is a coupling coefficient.

Let

$$F(t) = e^{i\omega t} \qquad 0 < t < t_w \qquad (2.66)$$

$$= 0 \qquad t > t_w$$

For $t > t_w$ we can write

$$\mu_i(t) = Ke^{i\omega_i t} \int_{-\infty}^{\infty} F(\tau)\, e^{-i\omega_i \tau}\, d\tau \qquad (2.67)$$

Defining

$$F_i(\omega) \equiv \int_{-\infty}^{\infty} F(t)\, e^{-i\omega_i t}\, dt \qquad (2.68)$$

At this point it is convenient to define the amplitude spectrum $\mu_i(\omega)$ as

$$\mu_i(\omega) = K\, F_i(\omega) \qquad (2.69)$$

i.e.

$$\mu_i(\omega) = \mu_i(t)\, e^{-i\omega_i t} \qquad (2.70)$$

The system's response is

$$\mu(t) = \sum_i \mu_i(t) = K\, N \int_{-\infty}^{\infty} n(\omega)\, F(\omega)\, e^{i\omega t}\, d\omega \qquad (2.71)$$

where N is the number of oscillators and $n(\omega)$ the normalized

distribution function, giving the probability that the oscillator has the resonance frequency between ω and $\omega + d\omega$,

$$\int_{-\infty}^{\infty} n(\omega)\, d\omega = 1 \tag{2.72}$$

Writing

$$n(t) = \frac{1}{2\pi} \int_{-\infty}^{\infty} n(\omega)\, e^{i\omega t}\, d\omega \tag{2.73}$$

Eq. (2.71) can be written as the convolution of $F(t)$ and $n(t)$

$$\mu(t) = 2\pi\, KN \int_{-\infty}^{\infty} F(t')\, n(t - t')\, dt' =$$

$$= 2\pi\, KN\, F(t) * n(t) \tag{2.74}$$

Theoretically it is possible, by studying the response after 1 pulse, to determine $n(\omega)$. (This is the basis of high resolution N M R.) Typical echoes from powder samples are observed in the frequency range of 10 - 50 MHz: i.e., $n(\omega)$ is constant and $n(t) \approx \delta(t)$.

Therefore $\mu(t) \propto F(t)$

and

$$\mu(t) = 0 \qquad \text{for} \quad t > t_w$$

and one does not expect any free induction.

The experimentally observed free induction, has a form of spikes decreasing in amplitude and can be visualized as a reduction in an otherwise broad distribution $n(\omega)$. or as a result of a discrete (or discontinuous) spectrum.

The Fourier transform of the pulse $F(t)$ Eq. (2.65) is

$$F(\omega) = F_o \frac{\sin(\omega_o - \omega)t_w/2}{\omega_o - \omega} \tag{2.75}$$

If one assumes that only the oscillators inside the bandwidth of the pulse are excited such, that $\mu_i(\omega) \approx$ const. for ω satisfying

$$|\omega - \omega_o| < \frac{1}{t_w}$$

then the response, Eq. (2.74), has the form

$$\mu(t) \propto e^{i\omega t} \frac{\sin(t/tw)}{t} \tag{2.76}$$

which qualitatively resembles the observed induction.

Similarly, if the spectrum consists of separate lines (or gaps)

$$n(\omega) = \frac{1}{N} \sum_{i=1}^{N} \delta(\omega - \omega_i) \tag{2.77}$$

Then

$$\mu(t) = K \sum_{i=1}^{N} \int_{\infty}^{\infty} F(\omega)\, e^{i\omega t}\, \delta(\omega - \omega_i)\, d\omega$$

$$K \sum_{i=1}^{N} F(\omega_i)\, e^{i\omega_i t} \tag{2.78}$$

can differ from zero. Billmann et al[12] showed that the dependence of the echo width on the length of the RF pulses t_{w_1} and t_{w_2} can give information about the order of the mixing process causing the echo.

The echo amplitude is always expressed as a product of the responses to individual RF pulses.

For example, let $\mu_i(t)$ have the form

$$\mu_i(t) = F_1^{\ell}(\omega_i)\, F_2^{m}(\omega_i)\, e^{i\omega_i(t - \tau)} \tag{2.79}$$

Then from Eq. (2.73)

$$\mu(t) = \sum_i \mu_i(t) = \int_{-\infty}^{\infty} n(\omega)\ F_1^{\ell}(\omega)\ F_2^{m}(\omega)\ e^{i\omega(t - r\tau)}\ d\omega$$

$$= 2\pi n\ (t - r\tau) * F'(t - r\tau) \qquad (2.80)$$

where

$$F'(t) = \underbrace{F_1(t) * F_1(t) * \ldots * F_1(t)}_{\ell\text{-times}} * \underbrace{F_2(t) * \ * F_2(t)}_{m \text{ times}}$$

Because the convolution of the two square pulses of the duration t_w has a duration $2t_w$ the duration of $F'(t)$ is approximately ℓt_{w_1} $m\ t_{w_2}$ where t_{w_1} and t_{w_2} are the durations of the force pulses I and II. Thus the dependence of the echo width on the pulse duration can give, theoretically, additional information about the mixing process.

2.10. Nonresonant Excitation

In the previous discussions it was assumed that a spectrum of resonance modes was excited and the echo resulted from destructive interference at all times except $t = n\tau$ at which time there was a net moment. An echo has also been observed from a continuous medium[11-12]. In this case, instead of simple oscillator modes, one can introduce propagation modes. These have the form

$$A = a(x,t) = A(x)\ e^{i(\omega t - \vec{b}x)} \qquad ((2.81)$$

and the equations of motion are[32]

$$\frac{\partial a}{\partial x} = -i\beta \frac{\partial p}{\partial a^*} \tag{2.82}$$

$$\frac{\partial \bar{a}}{\partial x} = i\beta \frac{\partial p}{\partial \bar{a}^*} \tag{2.83}$$

where a and $\bar{a}$ represent forward and reverse travelling modes, p is the linear momentum, and β parameter relating a to A.

Expanding p in terms of a_i's we have

$$p = a_1^* a_i + \bar{a}_i^* \bar{a}_i + K a_i a_r^* \bar{a}_s + \text{similar terms} \tag{2.84}$$

From Eqs. (2.82, 2.83) one obtains a set of equations for a and $\bar{a}$. Parametric terms in the momentum will lead to an echo. This is analogous to the echo process for oscillator modes.

The quantum mechanical analogue of the discussion, also called "phonon echo", was described in great detail by A. Billmann and coworkers[12] and is briefly outlined in Appendix II.

A different echo origin was proposed by Lu and Fedders[33]. Their model is based on the following idea: Pulse I generates a short travelling wave

$$u(x\ t) = a \cos \omega(t - \frac{x}{v})$$

for $$\left|(t - \frac{x}{v})\right| < \tfrac{1}{2} t_{w1}$$

$$= 0 \quad , \text{otherwise} \tag{2.85}$$

Interaction of the type $u^2 h^2$ during the second RF-pulse leads to reversal of the propagation vector and the echo is produced by the backward-travelling wave. This process does not require the presence and superposition of

many modes. Formation of an echo due to travelling modes is unlikely in powders because of their small size.

2.11. Elastic Properties of the Particle

Free vibrations of an isotropic elastic body must satisfy the Navier equation

$$\nabla \cdot \nabla \vec{u} + \frac{1}{1 - 2\sigma} \nabla (\nabla \cdot u) = \frac{2(1 + \sigma)}{E_m} \vec{F} \qquad (2.86)$$

where u is a displacement, σ the Poisson ratio, E_m the elastic modulus, and $\vec{F}$ the volume force. For free vibrations $\vec{F}$ is given by

$$\vec{F} = \rho_D \frac{\partial^2 \vec{u}}{\partial t^2} \qquad (2.87)$$

where ρ_D is the mass density. The resonance modes can be obtained by solving (2.86) and (2.87) for proper boundary conditions: $\frac{\partial \vec{u}}{\partial \vec{n}} = 0$, for a free, and $u = 0$, for a fixed, surface ($\vec{n}$ is the vector normal to the surface). The calculation of the actual elastic modes using (2.83) and satisfying the boundary condition is a difficult 3-dimensional problem and has no immediate value at this time.

An elastic body has a spectrum of elastic modes satisfying (2.86) The spectrum has a low cut off frequency but no upper limit (in the continuum approximation). Many different modes involve both transverse and longitudinal displacements. Generally, they can not be decoupled and resonance modes contain a combination of both.

For example, an isotropic sphere has two types of resonance modes[34]; Class I modes having purely transverse displacements and Class II having

a combination of transverse and longitudinal components. Some simple modes for a sphere of radius, a, are given below

Class I: Rotational modes with frequencies

$$f = \tfrac{1}{2}a\sqrt{\frac{\mu_M}{\rho_D}}\ k \qquad k = 1.83;\ 2.98;\ 3.92\ \ldots$$

Class II: Radial modes where

$$f = \tfrac{1}{2}\ a\sqrt{E_M/\rho_D}\ \ h \qquad h = 0.82;\ 1.92;\ 2.93\ \ldots$$

and a spheroidal mode for which

$$f = .084\ a\sqrt{E_M/\rho_D}$$

here μ_M is the shear modulus.

It can be shown[31] that at a frequency close to a particular resonance mode a multiresonant system is equivalent to a harmonic oscillator, vibrating at the frequency of the resonance mode; therefore, the system of particles can be represented by the set of closely tuned oscillators discussed in Chapter II.

The lowest resonance frequency, corresponding to the basic modes of vibrations of the particles, occurs when its diameter is approximately equal to half of the acoustic wavelength. Elastic constants of the small particles can differ from these of bulk material. Even "ideal" whisker crystals exhibit reduced elastic moduli (90% of the bulk[35] values) and larger reductions can be expected from the "nonideal" particles.

Therefore the low "cut off" frequency of an echo from powders can be less than that expected from the bulk elastic modulus.

For highly irregular particles, there exist low frequency torsional or bending modes, whose resonance frequency depends more on the actual geometry of particles than their size.#

Simple oscillator behaviour of the particles can be expected only as long as individual resonances in the particle spectrum are well defined, i.e. untill the individual resonance lines do not start to overlap (due to finite Q), which requires the separation of the resonance modes to be larger than the resonance line width.

$$\omega_n - \omega_{n-1} > \frac{\omega_n}{Q}$$

For a spectrum of the form $\omega_n = n\,\omega_o$ the former leads to the limit $n < Q$. Because $\omega_o \approx 10\text{MHz}$, $Q \approx 10^3$ ω_n is above the experimental limit.

Collective Properties of the Particles:

Collective vibration of particles was recently proposed as a possible mechanism for the modes responsible for echo formation[16]. Thus it is worthwhile to consider the elastic properties of a large conglomerate of loose particles. The interaction between particles is very weak and measurements[36] as well as theoretical estimations[37] indicate a sharp

Footnote:# For example, the frequencies of the bending modes of a uniform circular bar are

$$f = \frac{1}{2\pi}\,\frac{R^2}{e^2}\,\sqrt{E/\rho_o}\;\;\alpha^2$$

where R is the radius, e the length of the rod and $\alpha = n \pm \frac{1}{2}$

n - integer. For $R/e \ll 1$ this frequency can be low.

decrease of the elastic constants (10^{-4} of the bulk modulus), a large loss, and a very strong dependence on the particle environment (pressure, presence of the other substances, etc.) for a large conglomerate of loose particles.

The acoustic velocity in this loose medium is typically comparable with the velocity of sound in gases, which makes the existence of a collective mode unlikely, since λ for collective mode would be less than a particle diameter.

2.12. Various Echo Mechanism in Powders

All mechanisms discussed previously are possible in powders.

(a) Amplitude Dependent Frequency

The elastic potential energy of solids can be expanded in terms of strain e as follows

$$\mathcal{F} = \alpha_1 e^2 + \alpha_2 e^3 + \alpha_3 e^4 + \ldots$$

where the α_m correspond to the $(m + 1)$ order elastic constants. α_2 leads to thermal expansion while α_3 "softens" the stress-strain relation and leads to the amplitude dependence of the frequency. The solution for the frequency of an anharmonic oscillator is readily available[38] and can be written as

$$f = \frac{1}{4\sqrt{2}} \int_0^{\pi/2} \frac{d\rho}{2\alpha_1 + \alpha_3 A^2 + \alpha_3 A^2 \sin^2 \rho}$$

where A is the amplitude of the oscillations, for

$\alpha_3 A^2 \ll 1$ the equation above leads to -

$$f = fo\ (1 + \frac{\alpha_3 A^2}{2\ \alpha_1}) \qquad (2.87)$$

i.e. the resonance frequency varies with the square of the amplitude. The fourth order elastic constants of the materials are not known. For a simple estimation, let us assume $\alpha_3 = \alpha_1$ and $A \approx 10^{-5}$, for this case the resultant frequency shift $(f_o \times 10^{-10})$ is negligible. This rules out one amplitude dependent process for echo formation outlined in Eq. (2.13).

(b) Amplitude Dependent Attenuation

This process plays a dominant role in the cyclotron echo in gases. In powders it is difficult to imagine that external losses, due to collision or friction, are strongly amplitude dependent. As far as intrinsic losses are concerned there are always hysteresis losses present, and these are strongly amplitude dependent. Some examples are: irreversible motion of domain walls in ferromagnetic powders and unpinning of dislocations in other materials. Many defects move under the influence of elastic deformations and the character of this motion differs for small and large amplitudes. However, a qualitative estimation of this effect indicates that it is negligible and rules out the other amplitude dependent process for echo formation outlined by Eq. (2.11). (The echo envelope in ferromagnetic and normal metals is similar, while the amplitude dependent losses differ by orders of magnitude).

(c) Nonlinear coupling of the elastic modes of the particles to R.F. field.

The existence of terms of the form e^2h^2 or eh^3 or higher in

the hamiltonian immediately leads to an echo in the pulse excitation.

The interaction between the RF field and the elastic vibrations can be expanded into the general series.

$$F(h,e) = g_{11}\, he + g_{12}\, he^2 + g_{21}\, h^2 e + \ldots \qquad (2.88)$$

Physically, two illustrative cases can be obtained by grouping the terms in equal power of e or h. i.e.

$$F(h,e) = (g_{11}e + g_{12}e^2 + \ldots)h + (\quad\quad)h^2 \qquad (2.89)$$

or

$$F(h,e) = (g_{11}h + g_{21}h^2 + \ldots)e + (\quad\quad)e^2 \qquad (2.90)$$

then individual terms can be visualized as amplitude dependent coupling constants or field dependent coupling and elastic constants.

All previously discussed echo processes are possible in the solids. They can exist simultaneously but the last one is expected to be dominant.

2.13. Origin of the Loss

The time, for which the particles are able to store the elastic energy depends on their quality factor Q (Eq.(2.36)).

The Q is determined by the type of particle material, Q_i, and also by the particles environmental Q_e.

$$\frac{1}{Q} = \frac{1}{Q_i} + \frac{1}{Q_e}$$

For pure crystalline solids the Q_i is very high $\simeq 10^5$ but sharply decreases in the presence of defects.

Extrinsic losses, Q_e, are dependent on the particles' shape and size, type of their contact and presence of the attenuation media.

Two extremes are of interest:

$$Q_e >> Q_i$$

in this case the $Q \sim Q_i$ and the intrinsic properties of the material are reflected on the echo relaxation,

$$Q_e << Q_i$$

in this case the echo relaxation reflects only the properties of the environment or particles' geometry.

The anelastic losses in solids often have a relaxation character, i.e., they depend on frequency and are accompanied by a change of the elastic modulus. They can be described by the complex elastic modulus E_M

$$E_M = E_{Mo} \frac{(1 - k_1\omega^2) + ik_2\omega}{\omega_\gamma^2 - \omega^2}$$

where ω_γ is the characteristic frequency and k_1 and k_2 are constants.

The real part of E_M represents the modulus and the imaginary part the losses.

2.14 Driving Force

In all previous discussions the echo was expressed as the product of the amplitudes of the oscillations, excited by the linear driving force, multiplied by some factor expressing the nonlinearity leading to an echo.

Therefore the variation of the amplitude and the relaxation time of the echo with the variation of the external parameters reflects both the linear coupling mechanism between the RF field and the elastic vibrations and also the echo process.

The RF field produces a force $f = dh$ which excites the oscillators. The amplitude of the elastic mode has the form

$$a \alpha ft = dht_w$$

where d depends on the mass of the particle, i.e. the echo amplitude depends on a higher power of d.

For example, a term $a_I^* a_{II}^2$, where a_I and a_{II} are elastic modes, which leads to an echo at $t = 2\tau$ (Eq. (2.29)) has the form

$$a = \varepsilon a_1^* a_2^2 = \varepsilon d^3 h_1 h_2^2 t_{w_1} t_{w_2}^2 \qquad (2.91)$$

The experimentally observed quantity, however, is not the sum of the amplitudes $\sum_i a_i$ but the effective electric or magnetic moment, m, inducing the voltage in the pick up system.

m_i is related to the oscillator amplitude by the inverse process to the excitation, therefore

$$m_i \alpha d\mu_i \alpha da_i$$

and at the time of the echo

$$m = \Sigma m_i = d\mu \qquad (2.92)$$

i.e. in the example above, Eq. (2.91) the observed echo E_1, depends

on the 4-th power of d. This makes it very difficult to extract some information about ε from the observations of m, since d is not known in detail.

In different materials different driving forces are dominant, i.e. d behaves differently and this is reflected in the echo characteristics.

For all three types of powders (normal metals, piezoelectrics or ferromagnetics) the RF field produces both torque, rotating the otherwise rigid particles, and a volume force causing deformation of the particles.

The experimental evidence to be presented favours the latter in all cases.

Normal metals:

The excitation of the elastic modes and formation of the echo requires the presence of a static magnetic field.

The RF field induces eddy current, $\vec{i}$, in the particle which interacts with the static magnetic field $\vec{H}$ to produce the torque $|\vec{B} = \vec{H}|$

$$\vec{T} = \frac{1}{c}\int (\vec{i} \times \vec{B}) \times \vec{r}\, d^3r \qquad (2.93)$$

This excitation process was suggested by the Pacult et al[16]. The same interaction produces the Lorentz force.

$$\vec{F} = \frac{\vec{i} \times \vec{B}}{c} \qquad (2.94)$$

acting on the particle which causes its deformation.

It is necessary to point out that the latter is a macroscopic approximation of so-called "direct" excitation of the acoustic waves in metals where the RF-energy is directly converted into acoustic waves inside the metal[39]. The effect has been extensively studied in recent

years from both microscopic[40-45] and macroscopic[46-51] points of view. This effect certainly is not new, since eddy current excitation was used in 1940 for elastic measurements,[52] and many different experimental arrangements have been used. Direct excitation is a consequence of the coupling of electron and ionic motions in the presence of a static magnetic field.

In the limit $q\ell << 1$ (q is the acoustic wave vector and ℓ is the electron mean path) the excitation process is well described by a simple macroscopic model, where the acoustic waves are excited by a Lorentz force from the interaction between surface eddy currents and an external magnetic field.

The force in equation (2.86) can be written as

$$F \sim \frac{\vec{i} \times \vec{B}}{c} + \rho_D \frac{\partial^2 u}{\partial t^2} \qquad (2.95)$$

Eq. (2.86) and (2.95) must be solved for proper boundary conditions. This solution is greatly simplified if the skin depth

$$\Delta = \frac{c}{(2\pi \sigma_e \omega)^{\frac{1}{2}}} \qquad (2.96)$$

where c is the speed of light and σ_e the electrical conductivity, is far less than the diameter of the particle a. Than the eddy currents and therefore Lorentz force are limited to the surface.

Eq's (2.86) and (2.95) are solved in the literature for the simple one dimensional case[47,20,51].

Gaerttner and Maxfield[48] pointed out that the solution for the vibrational amplitude depends on the boundary conditions[48].. i.e. it differs for the fixed and free surface.

In particles the Lorentz force (Eq. 2.94) excites predominantly longitudinal waves for $B \parallel h$ and transversal waves for $B \perp h$. (See Figure 2.3).

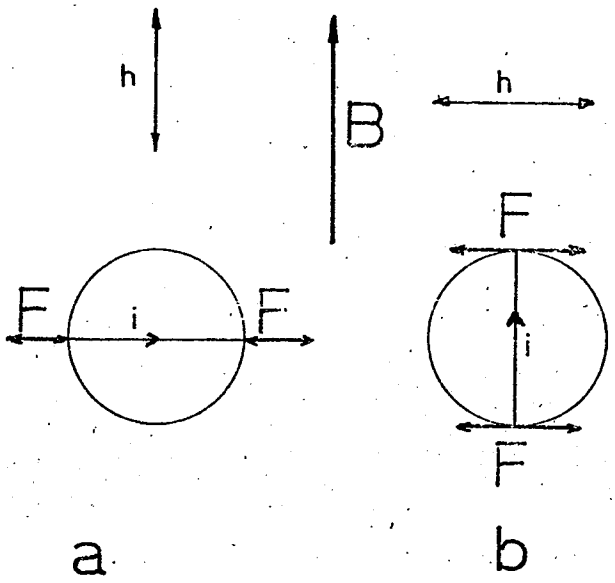

Figure 2.3: "Direct Excitation Process" by Eddy Currents (Schematically) (a) Longitudinal (b) Transversal Excitation. ($H \doteq B$)

The vibrational amplitude depends on the material only through its mass density (ρ_D) electrical conductivity and elastic constants.

The static magnetic field also affects the elastic properties of conductors by introducing increments to the elastic losses, $\Delta\gamma$, and moduli, ΔC which can be written as[51,53]

$$\gamma = \gamma_o + \Delta\gamma\ (B)$$

$$C = C_o + \Delta C(B) \qquad (2.97)$$

where

$$\Delta\gamma(B) = \frac{1}{1+\beta^2}\,\frac{B^2 \sin^2\varphi}{4\pi c}$$

and

$$\Delta C(B) = \frac{1}{1+\beta^2}\,\frac{B^2 \sin^2\varphi}{4\pi} \qquad (2.98)$$

φ is the angle between B and the propagation vector of the elastic waves. ΔC, and $\Delta\gamma$ also depend on frequency through β since

$$\beta = \frac{2\pi c^2 \omega}{v^2 \sigma_e} \qquad (2.99)$$

making variations in ω and σ_e as well as those in B and ρ affect C and γ. The fractional change in the resonance frequency of the particle (H = 10KOe) $(\frac{\Delta C}{C})^{\frac{1}{2}} \approx 10^{-6} - 10^{-5}$ [53] which is less than the resonance line width and will therefore be neglected.

Exact relationship between a surface force distribution and a particular mode is not known, but it can be assumed that there is a linear relationship between amplitude and force.

d in Eq. (2.86) has the form $d \alpha H$ and the mode amplitude is

$$a \alpha d\, h\, t_w = H\, h\, t_w \qquad (2.100)$$

For the same size particles, with the same electrical conductivity, the absolute amplitude of the vibrations depends only on the mass density and elastic constants of the particles.

Piezoelectric and ferroelectric materials:

The RF-electric field, h_1 # produces a torque on the particle

Footnote: h indicates both , the magnetic and electric RF field. There is no ambiguity in the notation, because the RF magnetic field is used to excite the echo from ferromagnetic or normal metals, while the electric field is used to excite the echo from piezoelectric material.

posessing a constant electric moment $\vec{m}_o$.

$$\vec{F} = \vec{m}_o \times \vec{h} \tag{2.101}$$

Piezoelectrics do not have a spontaneous moment but the torque can result from the polarization or the shape anisotropy.

The electric field $\vec{E}$, static or RF, causes the deformation of the piezoelectrics. There is a relationship[54] between the mechanical variables (stress $\tilde{\sigma}$, strain $\tilde{e}$) and the electrical variables (electric field intensity $\vec{E}$ and electric displacement $\vec{D}$) given by

$$\begin{aligned} \tilde{\sigma} &= \tilde{c}_E \tilde{e} - \tilde{d}\vec{E} \\ \vec{D} &= \tilde{d}\tilde{e} + \tilde{\varepsilon}_e \vec{E} \end{aligned} \tag{2.102}$$

where $\tilde{c}_E$ represents the elastic constant tensor at constant field, $\tilde{\varepsilon}_e$ the electric permittivity tensor at constant strain and $\tilde{d}$ the piezoelectric constant.

The RF electric field $\vec{h}$ produces a stress $\tilde{\sigma} = \tilde{d}\vec{h}$ which acts as a volume force on the particle. No simple relationship exists between the temperature or biasing electric field $\vec{E}_o$ and the value of $\tilde{d}$.

Ferromagnetic Materials:

The interaction of the RF-magnetic field $\vec{h}$ with the permanent magnetic moment of the particle $\vec{m}(H)$, produces a torque

$$\vec{T} = \vec{m} \times \vec{h}$$

The RF field also deforms the particle by the direct coupling of $\vec{h}$ to

$\tilde{\sigma}$ (stress). Formally it can be described analogously as in the piezoelectrics, replacing $\vec{D}$ and $\vec{E}$ by the $\vec{B}$ and $\vec{H}$ (magnetic induction and field intensity) and $\tilde{\varepsilon}_e$ by $\tilde{\mu}_e$ (magnetic permeability).

Physically, however, the linear relationship between $\tilde{e}$ and $\vec{h}$ is not a true piezomagnetic effect but the result of the biased magnetostriction. It is not a result of the deformation of the lattice by the applied field but originates in the rearranging of the magnetic domains which are deformed due to magnetic ordering. Therefore a strong dependence of $\tilde{d}$ on the biasing magnetic field is expected.

The external electric or magnetic field also affects the elastic properties of the piezoelectric or ferromagnetic materials, namely the elastic modulus, E_m, and elastic losses, δ.

All ferromagnetic conductors show a strong dependence of the relaxation times of the echoes on the biasing field, which results from the domain structure. Elastic losses in ferromagnetic conductors are usually divided into macroeddy, microeddy and hysteresis losses. The loss mechanisms are treated in detail by Bozorth[55] and only a brief outline, necessary for understanding the properties of the echo from ferromagnetic powders, will be given here (for details see Ref's (55, 56, 57).

a) Macroeddy Currents

The stress (σ) induced change in the net intensity of magnetization (ΔM) is given by the following equation analogous to (2.102), and can be written as

$$\Delta M = \left(\frac{\partial M}{\partial \sigma}\right) \sigma \qquad (2.103)$$

This variable magnetization induces eddy currents in the sample, and leads to losses which can be represented as a relaxation process. The loss passes through a maximum and the elastic modulus changes its value for some characteristic frequency f_c. f_c is shape dependent and is given by

$$f_c = \frac{g(s)}{a^2} \frac{10^{-2}}{\sigma_e \mu_r 2\pi} \tag{2.104}$$

where σ_e is the electric conductivity (℧/cm)

a - diameter of the particle (cm),

μ_r - relative permeability.

and $g(s)$ is a function of shape and is of the order of unity. f_c increases inversely with the square of the radius and for small particles it can be in our experimental range.

For, $\sigma_e \approx 10^4 - 10^8$ ℧/cm, a ≈ 50 μm, and $\mu_r \approx 10$

f_c is $5 \times 10^2 - 5 \times 10^6$ Hz.

(f_c increases with decreasing conductivity).

These losses are zero for the full demagnetized and the fully saturated states.

(b) Microeddy Currents

Microeddy currents result from energy dissipation by eddy currents induced by the variation of the magnetization due to the motion of individual domain walls[58] or the rotation of the magnetization inside of the individual domains[59]. In contrast to the previous process, there is no net change of the magnetization. This process also has a relaxation character, with the characteristic frequency

$$f_{c1} = \frac{1}{10\mu_r \sigma_e \xi} \tag{2.105}$$

where ξ is the domain wall spacing (cm). The relaxation frequency is different for domain wall displacment and domain rotation and since domain wall displacement is much larger than domain rotation, for a given stress, the characteristic frequency for wall displacement is well below that for domain rotation (there is a different effective μ_r for the two loss processes discussed above).

If one introduces a distribution of domain dimensions, then the losses can be expressed as the sum of losses for different domain dimensions and different process. The logarithmic decrement is given by:

$$\delta(f) = \sum_{ij} K_{ij} \frac{(f/f_{ij})}{1 + (f/f_{ij})^2} \quad \text{(a)} \tag{2.106}$$

and the change in the elastic modulus ΔE_M by

$$\Delta E_M = \sum_{ij} K'_{ij} \frac{1}{1 + (f/f_{ij})^2} \quad \text{(b)} \tag{2.107}$$

where the summation includes the two processes (i) (Wall displacement and domain rotation) and the different domain sizes (j). The coefficients K_{ij} are linearly related to the elastic and magnetoelastic constants and to the susceptibility of the material. (For details see[59]) δ has a maximum for the demagnetized state (maximum density of domains) and decreases to zero as the magnetization increases. In contrast to the macroeddy current losses, microeddy current losses are not shape dependent, as long as the shape does not affect domain structure.

Experimental qualitative verification of the loss mechanisms outlined

above has been presented by many authors[19,60,61]. However, recent measurements, comparing the variation of susceptibility with elastic losses or ΔE_M, indicate a lack of detailed quantitative agreement between theory and experiment[62,63].

Microeddy and macroeddy losses are amplitude independent because of the linear relationship between magnetization change and the amplitude of vibrations, x, and therefore stress σ. Since the induced eddy currents, i, are linearly related to the change of magnetization, the ratio of the dissipated energy ($\sim i^2$) to the total elastic energy ($\sim x^2$) is constant.

In relaxation processes the variation of $\delta(f)$ is related to a corresponding change in ΔE_M; therefore, for multiparticle samples, different particles are tuned to resonance at different stages of magnetization.

(c) Hysteresis Losses

Hysteresis losses are present in all ferromagnetic substances and result from the irreversible motion of domain walls (or domain rotation). This loss per cycle is proportional to the area enclosed by the stress-strain curve, which is analogous to magnetic hysteresis loss due to the fact that both are linearly related[55]. Hysteresis losses depend on the amplitude of the stress and for low amplitudes the logarithmic decrement is linearly proportional to the amplitude (Rayleigh loop). For frequencies below the characteristic frequencies of microeddy currents, hysteresis losses are frequency independent and decrease with increasing magnetization.

Chapter III

APPARATUS

3.1 Electronics

All the data are taken on a noncoherent variable frequency NMR pulse spectrometer. Figure 3.1 is a block diagram of the apparatus. Its function is straightforward. Pulses from a pulse generator modulate the Matec spectrometer,# the pulses from which are applied to the sample, placed inside a coil. A single coil arrangement was used for most of the experiments. The echo signal, after detection

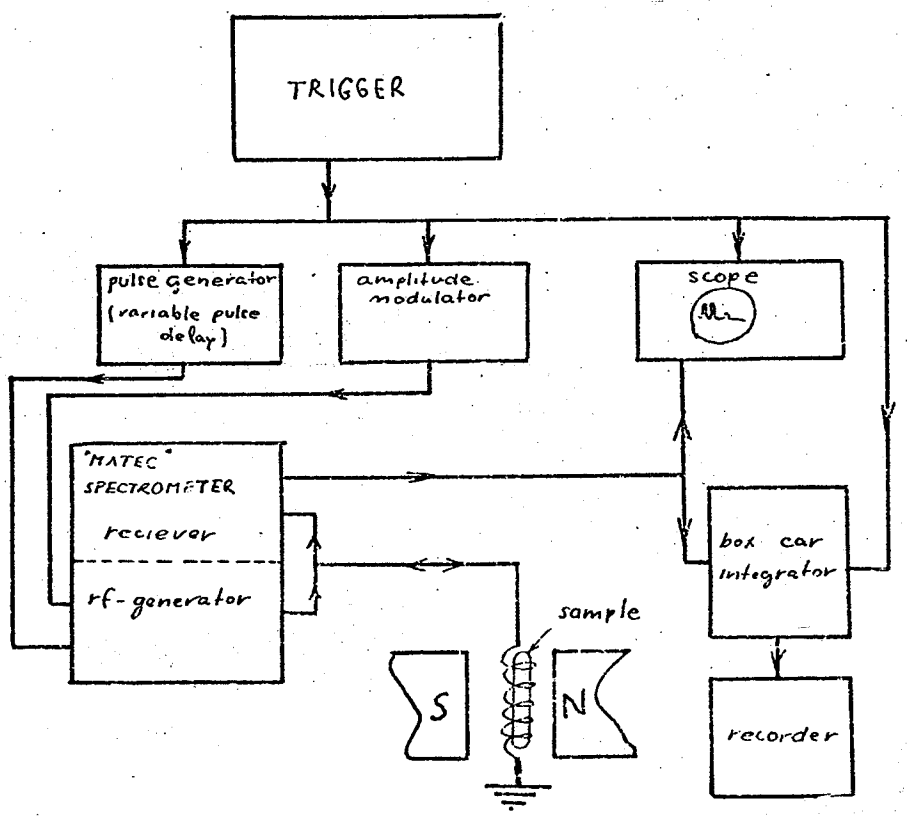

Figure 3.1: Block Diagram of the Pulse Spectrometer

#Footnote:Model 6600 with plug in units model 760 and 765 Matec Inc. Warwick R.I. 02886

and amplification, was displayed on an ocsilloscope and, after processing by a box-car integrator, was plotted on either an X-Y or a chart recorder.

For some measurements, instead of a single coil, an inductively coupled resonant LC-circuit was used. Since the built-in modulator of the spectrometer generated pulses whose maximum widths were too short, an external modulator producing longer pulses leading to stronger echoes was used.#

The tuning of the spectrometer was somewhat ambiguous. First, the receiver unit of the Matec spectrometer was tuned to an external frequency generator and the RF-pulse generator was tuned for maximum echo amplitude. Because the echo spectrum is continuous and, the Matec receiver has poor selectivity the method described above did not guarantee proper tuning. In the frequency range (10-30 MHz) it was possible to tune the RF-generator by observing a beat signal from the superposition of the outputs from both the pulse generator and the calibrated RF-generator.

The pulse repetition rate was variable, but any rate above 500 Hz overloaded the Matec generator.

Besides the noncoherency of the RF-pulses, another shortcoming of the spectrometer is a strong crosscoupling between the RF generator and the receiver, which are both part of one unit.

The receovery time for the receiver was approximately

Footnote: To excite and observe the echo from Rochelle salt a holder in the form of a plate capacitor was used.

6 microseconds (Fig. 4.9) and the receiver output was linear for all input voltages ranging from 5% to 90% of the saturation value.

The sample coil was placed inside a custom made glass helium dewar placed in a magnetic field (11KOe) produced by an electromagnet. Some of the measurements were made using a superconductive magnet with a maximum field of 50KOe, in which case a stainless steel insert dewar was used.

3.2 RF Magnetic Field Calibrations

For some measurements it was necessary to estimate and vary the amplitude of the RF-field. In these cases a single coil arrangement was used and the RF-magnetic field was measured by:

(a) Measuring the voltage induced in a second small coil , placed inside the sample coil,

(b) Measuring the RF-current through the sample coil and calculating the RF magnetic field from the coil geometry. The results of a and b agreed to better than 15%. In experiments where relative values of the RF field intensity were considered the uncertainty was less than 5%.

3.3 Measuring the Echo Spectrum

The power output of the RF-generator and the input sensitivity of the receiver vary drastically with frequency. Some attempts to compensate for this were made by keeping the

receiver input and generator output at the same level. This was done by comparing each of the above with the output from a calibrated frequency generator. The above procedure did not compensate for the frequency variation of the coils impedance; therefore, the echo spectrum, defined as a dependence of the initial echo amplitude on frequency, has only a qualitative character. More reliable information is obtained from relative measurements, where the amplitudes of echoes from various samples are compared with the same "standard" sample.

3.4 Cryogenic System

Both the glass and stainless steel dewars were of a standard design. The temperature range from 77^{o} to $300^{o}K$ was achieved by putting exchange gas into the helium dewar vacuum space (between the liquid nitrogen and the sample). Blowing cold He gas over the sample produced temperatures in the range of 4.2^{o}- $77^{o}K$. Temperatures below $4.2^{o}K$ were obtained by pumping on the He bath.

The temperature was measured by a Cu-constantan thermocouple referenced at either $273^{o}K$ or $77^{o}K$, depending on the temperature range being used. Below $4.2^{o}K$ the temperature was determined from the known P-T diagram for liquid He.

3.5 Miscellaneous

To study the effect of ordering (in alloys) on the

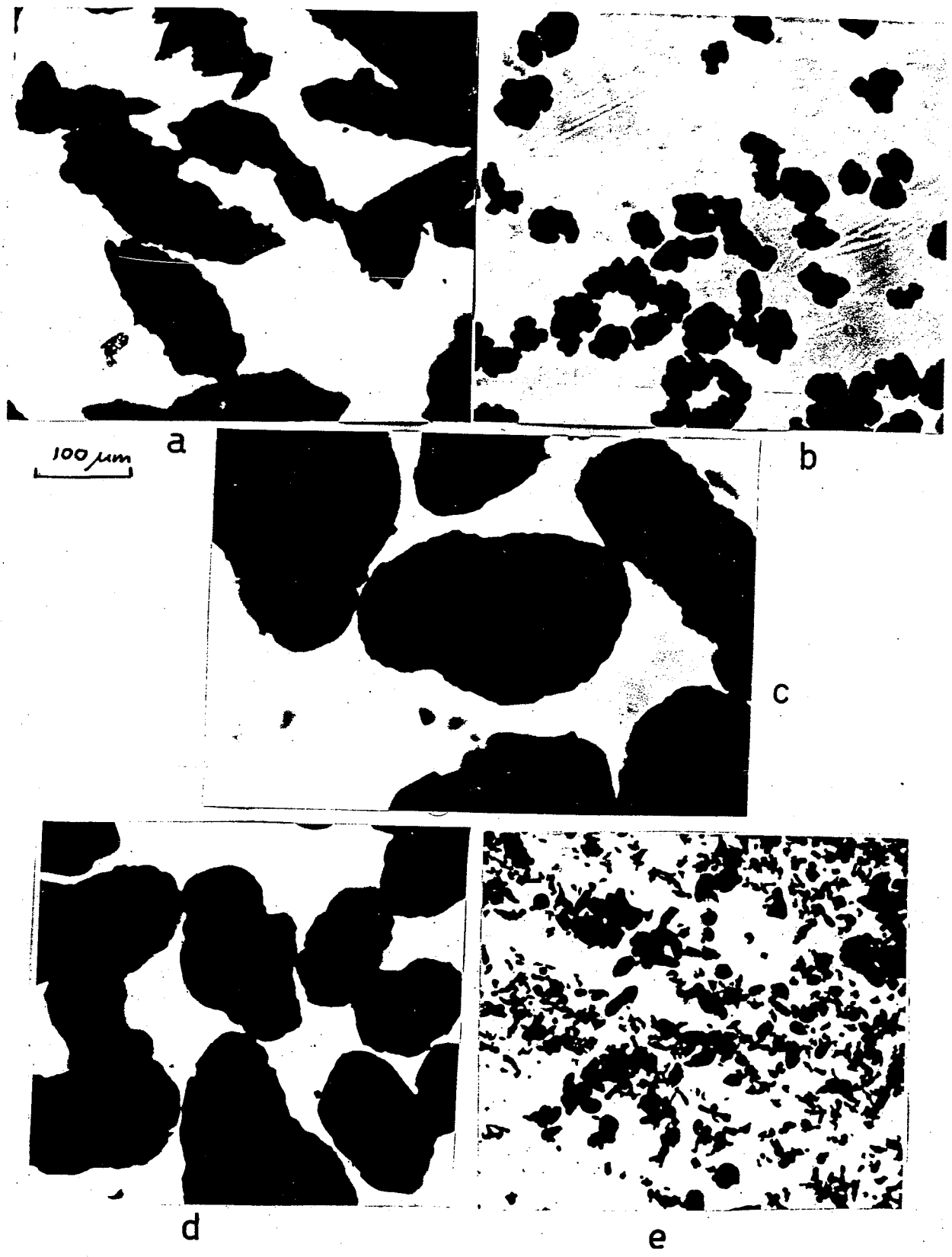

Figure 3.2 Examples of the powder samples a) Cu filings 100-200 mesh, b) commercial Ni, c), d), e), Al mesh 60-100, 100-200, 240-320.

echo properties, diffraction line widths and the electrical resistivity (4 probe technique) of the samples were measured. The magnetization measurements were performed using a vibrating sample magnetometer.

3.6 Sample Preparation

All the samples were in powder form with diameters of 10-200 μm. Most of the powders were filed from bulk samples. These were highly irregular in shape and therefore the effective size was difficult to define. See Fig. 3.2a To allow some kind of comparison all the data were taken from powders sieved through a 100-200 range mesh.. (NBS standard sieves).

Some commercial powders, which were more regular in shape were also used (Al, Ni). These were used for a study of the size dependence of the echo spectrum. They were separated using the standard seives in the range of 60-320 mesh. Fig. 3.2b. Shows the 50 μm Ni powder, while 3.2c,d,e shows the different sizes of Al powder.

Dilute alloys were prepared by melting in an argon arc-furnace. A master sample was initially prepared and later diluted. This method was satisfactory for more concentrated alloys ($>1\%$) but unsatisfactory for dilute alloys, when the dilute component either had a much lower melting point or oxidized readily. In the later cases the total melting losses were approximately 30-50 mg which was an order of magnitude greater than the total amount of dilute component.

Therefore, data for these cases should be taken with reservation. The actual samples consisted of approximately 1 g of powder sealed in a evacuated glass tube (4 cm in length and 7 mm in diameter).

Table 3.1 contains a list of the samples.

The normal metal samples were chosen with the expectation of finding a direct relationship between the echo characteristics and the electronic structure. No such direct relationship was found.

The magnetic samples used represent 3 major groups of magnetic solids:

Cubic with the "easy magnetic direction" along the ⟨111⟩ crystallographic direction, Ni.

Cubic with "easy direction" along ⟨100⟩ crystallographic direction, Fe.

Uniaxial with the "easy direction" along the hexagonal c axis, Co and RCo_5 (R is Nd or Y).

The RCo_5 compounds are uniaxial with a very large anisotropy energy (10^7 erg/cc)[65,66] and the ferrites used were high frequency commercial ferrites of unknown composition.

The purpose was to compare the echo properties of the magnetic conducters with those of insulators. The ferromagnetic metals exhibit large acoustic losses depending strongly on the domain structure. These can be reflected in the echo relaxation time.

Hematite α-Fe_2O_3 #was used only for a comparison of the echo relaxation time from the single crystaline powders with the relaxation of the free induction from the bulk single crystal.

α-Fe_2O_3 possess a net magnetic moment only above 260°K (Morin transition[67]) and therefore the observation which was made was performed at room temperature only.

RCo_5 materials exhibit a strong aftereffect which can affect the echo properties.

Ferrities also show an echo in bulk form and a comparison was made between the echoes from both bulk and powder materials.

Both ferrites and RCo_5 were sintered materials prepared by an unknown technique.

Rochelle salt represents the piezo and ferroelectric material.[68](Ferroelectric between $\approx$ -19.5°C and +24.5°C.) The single crystals were prepared by growing from a water solution and afterwards crushed. The echo from piezoelectric materials has not been studied previously. The purpose was to compare the echo properties with those from other powders (normal metals and ferromagnetics) as well as to compare the echo in the piezo and ferroelectric region.

#Footnote: Synthetic α-Fe_2O_3 was grown by J.A. Eaton[64].

TABLE 3.1

Normal Metals Material	Purity	Structural	T max # H = 10KOe	Comment
Ag	(Spec pure) 5N (Alfa Inorg)	fcc	no echo	Echo was observed at 77°K only in a high magnetic field H > 30 KOe
Al	5N	fcc	180°K	Very strong echo and independent on purity (impurities < 0.5%)
	2N5 (commercial) metal		no echo	
Au	5N	fcc	30°K	Strong echo at 4.2°K. Gradual decrease with temperature
Cd	5N5	hex	no echo	
Cr	unknown	bcc	20°K	Very weak echo
Cu	Spec pure	fcc	100°K	Very strong echo Constant at low temperature, Gradual decrease with temperature
Mg	unknown	hex	4.2°	Very strong dependent on temperature
Mn	3N	cubic	no echo	
Zn	m5N+	hex	100°K	Strong echo Gradual decrease with temperature

TABLE 3.1 (Continued)

Normal Metals Material	Purity	Structure	T max # H = 10KOe	Comment
$Ag_x Mn_{1-x}$		fcc	200°K	Echo observed for $0.99 < x < 99.99$, very strong
$Ag_x Cu_{1-x}$		fcc	150°K	Echo observed only after annealing for $x < 0.2$
$Au_x Mn_{1-x}$		fcc	no echo	$0.9 < x < 1$
$Al_x Mn_{1-x}$		fcc	200°K	$x > 0.99$ echo depends strongly on thermal history $x < 0.9$ no echo
Ferro and Piezoelectric Material				
Rochelle Salt	unknown	orthorombic	300°K	Echo strongest in the ferroelectric region (between -20 and +24°C) single crystal powder

T_{max} is the upper temperature for the observation of the echo at 10 MHz (at H=10 KOe for normal metal powders and optimal bias for ferromagnetic powders).

Table 3.1 (Continued)

Ferromagnetic Materials Material	Purity	Structure		T_{max} Optimal bias (H)	Comment
		Crystalic	Magnetic		
Fe	5N 2N5	bcc	easy direction <100>	300°K	Commercial powder 99.5 and filings from high purity Fe had the same properties (after annealing)
Co	5N	hex	uniaxial	250°K	Filed from bulk
Ni	Spec pure 3N5	fcc	easy direction <111>	300°K	Filed from bulk. Commercial powder has identical properties.
$NdCo_5$ $Y\ Co_5$	unknown unknown	hex hex	uniaxial	220°K	Ground from polycrystaline block
Ferrite	unknown	cubic (from x-ray)		300°K	Sintered poly-crystaline bulk or powder
$\alpha\ Fe_2\ 0_3$	unknown	hex	planar	300°K	Echo only above Morin transition single crystal powder

3.7 Echo Detection

The echo is observed through the voltage induced in a coil by the oscillating net moment, m, of the sample. From Faraday's law the voltage induced in the coil by the time varing moment $m = m_o e^{iwt}$ is given by

$$V = 4\pi\omega m_o S \tag{3.1}$$

where S is the effective area of the coil

$$S = \pi r^2 n \tag{3.2}$$

n - number of turns and r - radius of the coil.

If the coil is only partially filled by the sample, the induced voltage V_i is

$$V_i = MV \tag{3.3}$$

where M is a filling factor defined as ratio of the volume of the sample to that of the coil.

V_i is induced in the coil, which is part of a resonance circuit of quality factor Q, which gives an output voltage of

$$V_r = QV_i \tag{3.4}$$

The voltage induced by a typical echo at 10 MHz in a coil where n = 20, r = 0.4 cm is approximately 10-100 μV, corresponding to $m_o = 10^{-5} - 10^{-4}$ emu/cc cc $\sim 10^6 - 10^7$ particles).

3.8 Effect of Repetition Rate

The conversion of RF energy into elastic vibrations is a very inefficient process, most of the RF

energy is dissipated as heat. Since the particles are in a vacuum and the heat conductivity of the system is very low, the samples tend to warm up during the application of RF-pulses. To reduce this effect the repetition rate must be low, especially in cases where the echo properties are strongly temperature dependent. At low temperatures the heat capacity of the sample is small and the effect is much more noticable (Figure 3.3). A drastic example of this internal heating of the sample was observed from powders immersed in liquid He below its λ point. There was a critical repetition rate, depending on pulse intensity and shape, beyond which the echo suddenly disappeared. (The echo is observable from powders immersed in superfluid He but not from powders immersed in normal He.)

The presence of gas in the sample tube changed the echo characteristics (relaxation time and temperature dependence of the echo amplitude). A compromise between losses due to the presence of gas and good thermal conductivity resulted in the use of partially evacuated sample tubes (pressure 5-10 torr at room temperature)

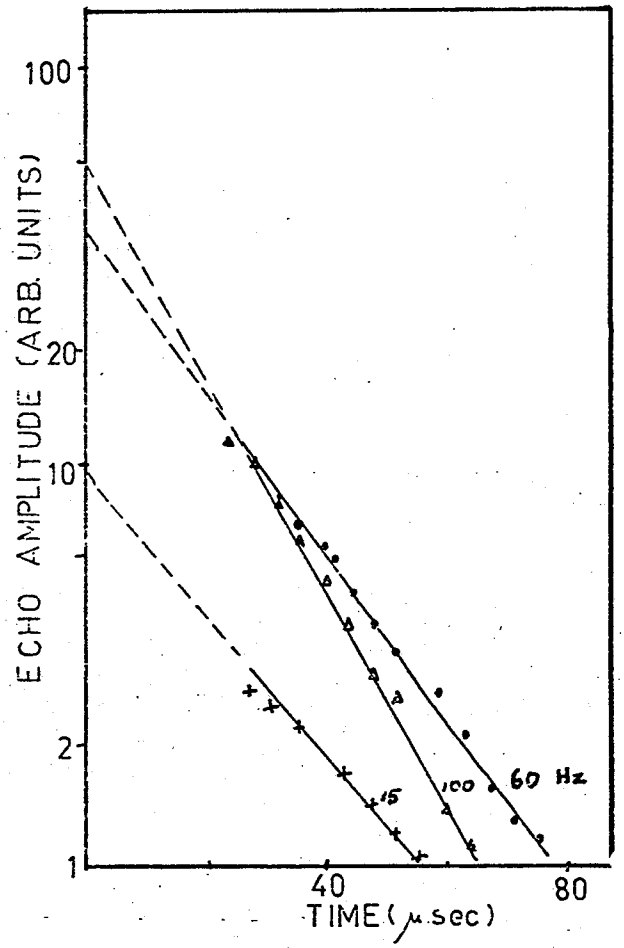

Figure 3.3: Echo Amplitude as a Function of Pulse Separation for Different Repetition Rate (Repetition rate is a parameter) (Cu 2.1°K)

Indicating the warming effect of an increased repetition rate.

CHAPTER IV

EXPERIMENTAL RESULTS AND DISCUSSION

4.1 Introduction

Prior to discussing the experimental results it is necessary to mention that all data related to the echo amplitude are relative. They depend on the sensitivity of the apparatus, the quality of the pick-up coil, which is temperature dependent and the filling factor of the coil, which differs for different sizes of particles.

It has a low reproducibility (there are differences up to 20% after subsequent removal and reinsertion of the sample in the spectrometer). The observations of the echo amplitude as a function of the various external parameters have a purely qualitative character and therefore they will be illustrated only on some examples. A majority of the echo properties is common to a large group of samples, but some samples are more suitable to demonstrate the effects than others.

The different echo models discussed in Chapter II relate the echo amplitude to the intensity of the driving pulses. Therefore its dependence on the external parameters is investigated, but the implications of the experiments should not be overblown.

In cases where the sample is not moved during the investigation or otherwise disturbed, the reprodictibility the echo amplitude is 5%.

The relaxation time of the echo, on the other hand, is an absolute parameter. It is measured as a decrease of the echo amplitude with the pulse separation. Therefore the error in its measurement depends on its magnitude (Long relaxation time allows more measuring points.).

The fact that the echo decays exponentially with increasing pulse separation points out that some kind of parametric coupling is responsible for the echo (see section 2, Chapter II).

It is convenient to divide the properties of the echo into two groups A: and B,C,D.

A describes the variation of the echo amplitude and relaxation time with RF pulse strength, length separation and frequency and the particle size. These properties in a large degree depend only on the echo formation process and are similar for the all powders.#

Footnote: The amplitude of the echo depends on the presence and magnitude of the external biasing electric or magnetic field as well as temperature, but these affect the magnitude and not the character of the effect.

B,C,D describes the echo parameters as a function of the temperature and the biasing field.

These properties depend on the coupling mechanisms between the RF field and elastic vibrations and therefore will be discussed separately for each group of materials.

4.2 Experimental Results

A Common properties of the echo from powders.

The following properties do not depend on the character of the driving force and are common to all powders.

A1 Induction following one pulse.

A2 Exponential echo decay.

A3 Sensitivity to the enviroinment.

A4 Echo pattern following a 3 pulse excitation.

A5 Decrease of the echo relaxation times with frequency.

A6 Complex dependence of the echo shape on pulse width.

A7 Dependence of the echo amplitude on the intensity of the RF pulses.

A8 Dependence of the echo on the particle size.

A1 Response to one force pulse

All powders, even those which did not exhibit the echo phenomena, have the same response to one RF-pulse;# this is a series of spikes, following the pulse, with roughly exponentially decreasing amplitudes.

#Footnote: Normal metals require, in addition to RF, the presence of a static magnetic field.

The exact structure of this signal is well defined for a particular experimental set-up, but it is not reproducible. The spikes are more intense for large particles and almost completely disappear for small ones.

A2 Echoes. following a two or more pulse excitation, decay approximately exponentially with the pulse separation.

This can be seen in Fig. 3:3.

For short pulse delay the echo amplitude does not decay exponentially, but rather has a gaussian envelope. For a pulse separation longer than $T_1/2$ the echo decay can be fitted to the exponential relation

$$E(t) = E_0 e^{-t/T_1}$$

Figure 4.1 a shows the echo decay (Linear scale) for a Ni sample in different biasing magnetic fields. The deviation from exponential is clearly visible. Figure 4.1b shows the echo amplitude for Al (10 MHz, 10 KOe, and size 170 μm) for various RF pulse intensities. As can be seen, the shape of the echo envelopes does not depend on the amplitude of the driving force. This deviation from exponential decay was also observed for other powders, (for example Cu at 4.2K or Ni) only at low frequencies, where the relaxation time was large. The shortest pulse delay in our apparatus is limited by the dead time of the receiver and further observations close to zero delay are desirable.

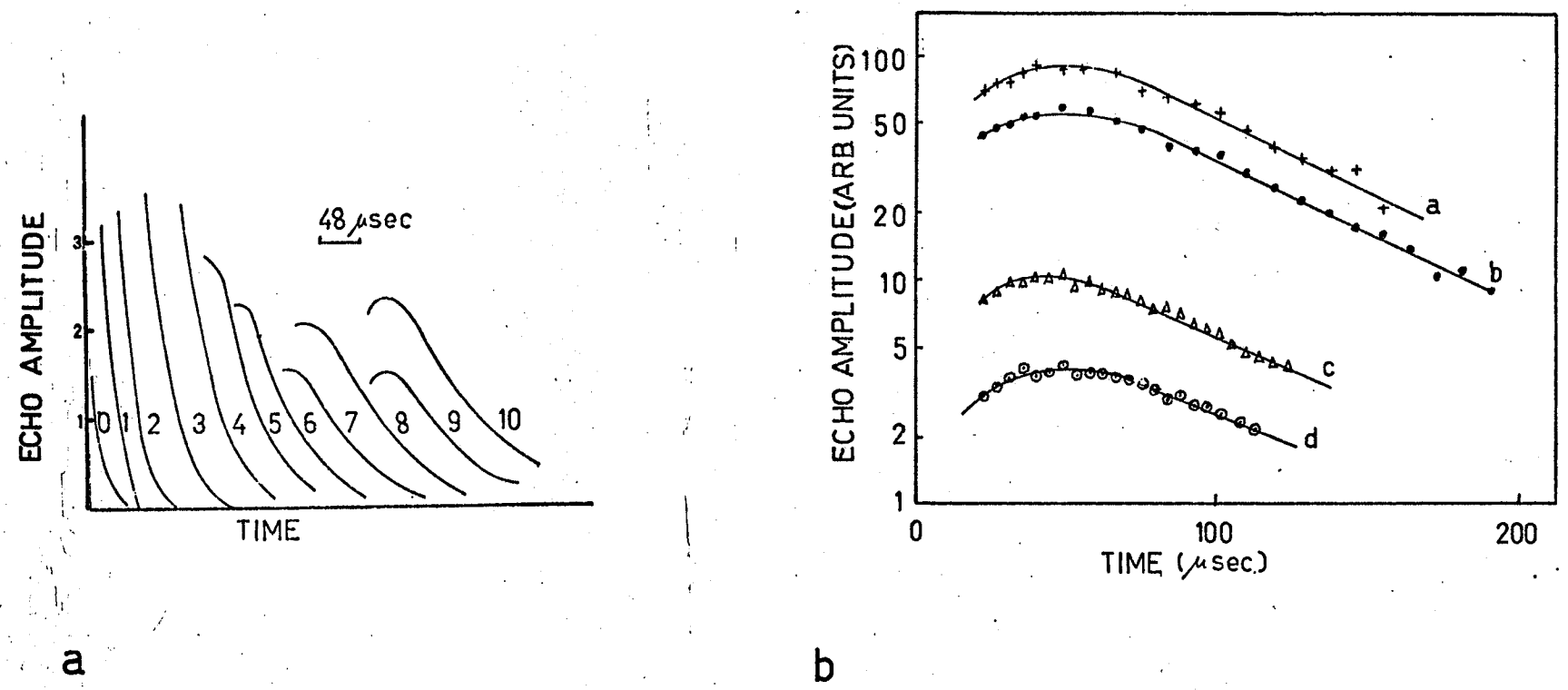

Figure 4.1 : Echo Envelope (a) Ni Powder in Different Biasing Field (20 MHz , 77°K). All Curves begin 24 μsec After the First Pulse (Parameter is Biasing Field in KOe) (b) Al Powder (10 MHz , 4.2°K) for Different RF-Pulse Intensities and Duration. a) 100 Oe, 10 μsec, b)50 Oe 10 μsec; c)100 Oe, 5 μsec, d)50 Oe 5 μsec.

It is necessary to point out that at short pulse delays the echo amplitude interferes with the induction signal following the pulses, and therefore the true echo envelope is not known.

In this study it will be assumed, that the echo decay is exponential and echo amplitudes refer to the extrapolated amplitudes from the exponential decay region ($T_1/2 < t \lesssim 5T_1$) to zero delay.

A3 Variation of the particles environment affects the echo

The echo phenomena is extremely sensitive to all forms of attenuation.

The following illustrations are given:

α) Compression of the powder in the sample tube reduces both the echo amplitude and its relaxation time.(Figure 4.2) A normal sample consists of the sample tube incompletely filled by powder.

Compression of the powder with a plunge affects the echo. Excessive compression (above $\approx$ 0.5 – 1 kg) completely eliminates the echo.

β) Immersion of the powder in liquids also eliminates the echo (with the exception of superfluid He). Pacult and coworkers observed an echo from powder immersed in liquid He[16].

γ) Freezing in ice also leads to a complete disappearance of the echo.

δ) Varying the gas pressure in the sample tube affects the relaxation time, Figure 4.3.

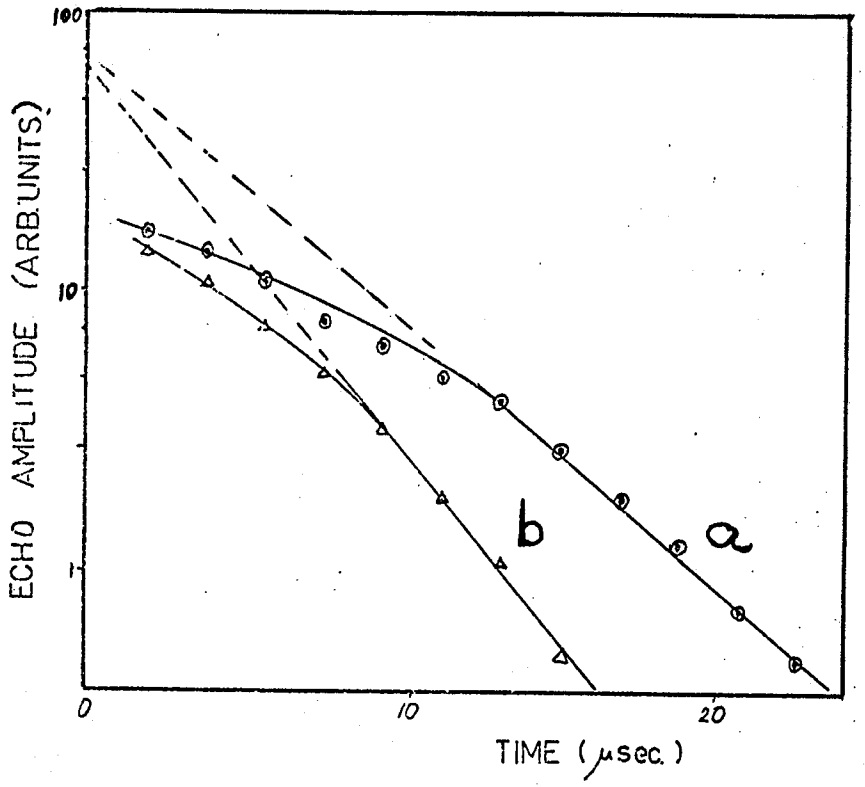

Figure 4.2 Echo Envelope for Loose (a) and Compressed Powder (b)

(Al. 20MHz , 77°K)

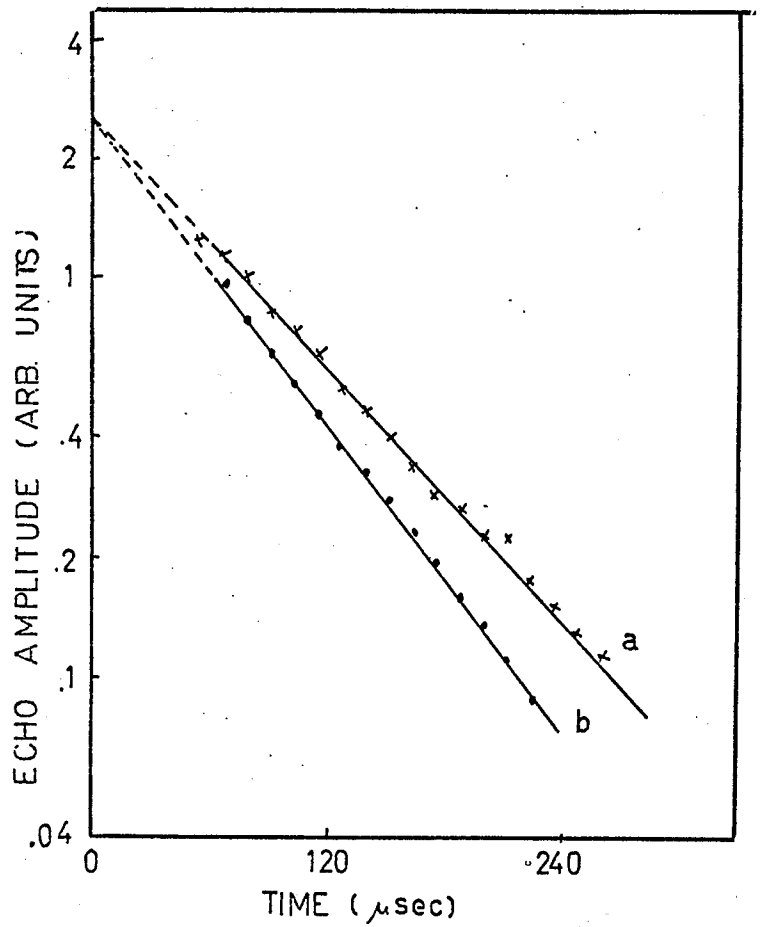

Figure 4.3: Echo Envelope for Different Gas Pressures (He) in the sample tube, (a) 10^{-1} torr (b) Atmospheric Pressure (Al. powder)

Another example of the effect of the environment on the echo properties is the dependence of the relaxation time on particle size and shape, Figure 4. 4 a & b. Relaxation times, obtained from filings (Fig. 4.4b), are shorter than those obtained from smooth commercial powders (Fig. 4.4a).

All these observations indicate that elastic vibrations are storing the energy and eventually lead to an echo.

A4 The two-pulse excitation (pulse at $t = 0, \tau$) leads to more than one echo, each having a different relaxation. time.

The secondary echoes are very weak and quantitative observations can be made only on samples with a strong echo and long relaxation time. The ratio of the initial amplitudes of the first and second echoes depends on the relative RF pulse intensity. For $h_1 = h_2$ it is approximately 10:1 and varies only slightly between samples. The third pulse at $t = T$ leads to the stimulated echo E_s at $t = T + \tau$. Fig. 4.5. shows the echo pattern following the three pulse excitation from Ni (77^0K). A similar pattern from the Rochelle salt at 290^0K is shown in Fig. 4.6.

E_1 and E_2 shown in Fig. 4.5 indicate first and second echo following pulses I and II. E_{II-III} and E_{I-III} indicate the two-pulse echo produced by the pulses II and III and I and III respectively.#

#Footnote: In the higher orders of the echo formation the E_{II-III} and E_{I-III} can involve all three pulses.

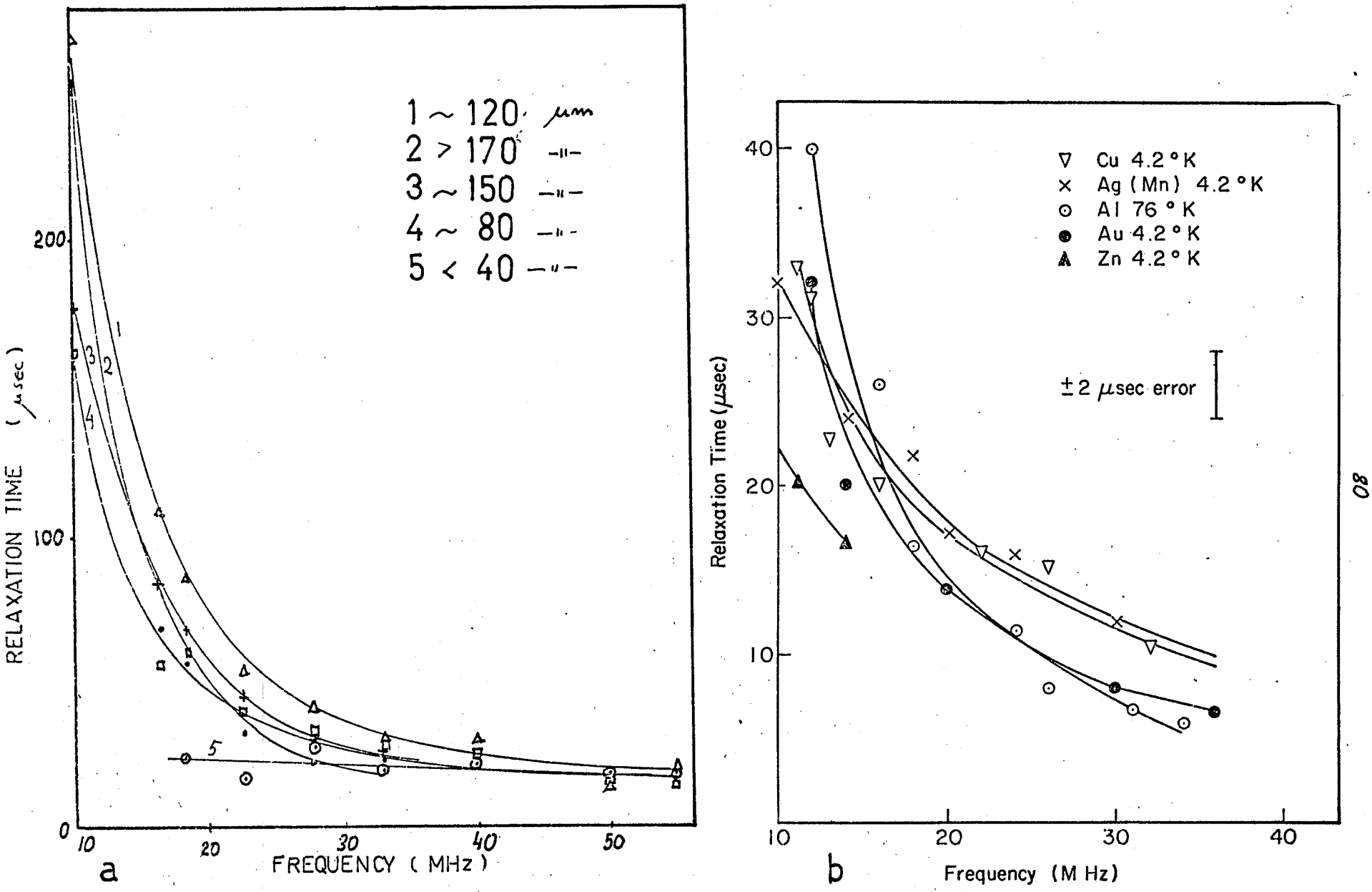

Figure 4.4: Relaxation Time as a Function of Frequency (a) Al Powder of Different Size (Commercial Powder) (b) Different Materials (Filed from Bulk)

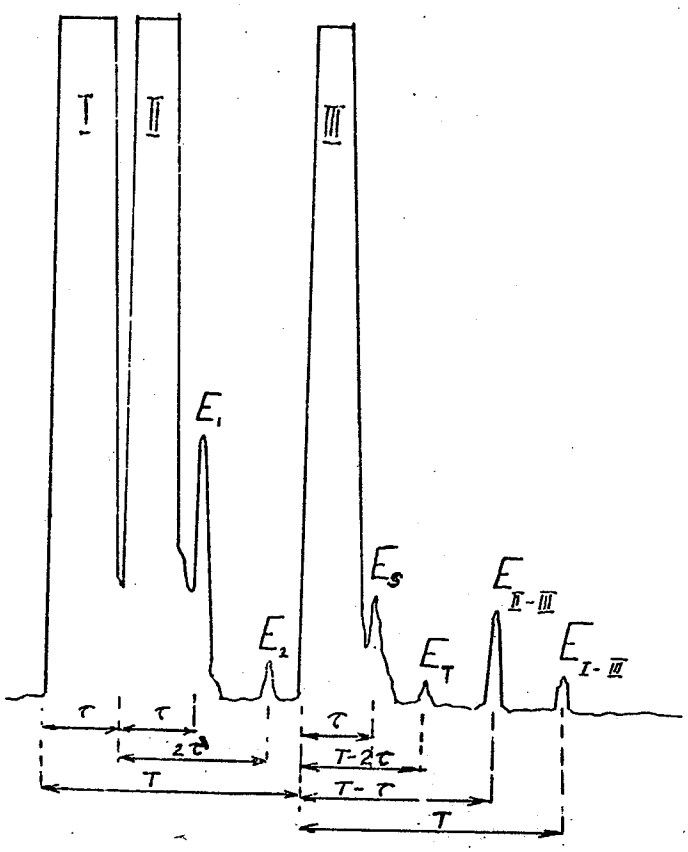

Figure 4.5 Box-car Trace of the Echo Pattern from Ni Powder

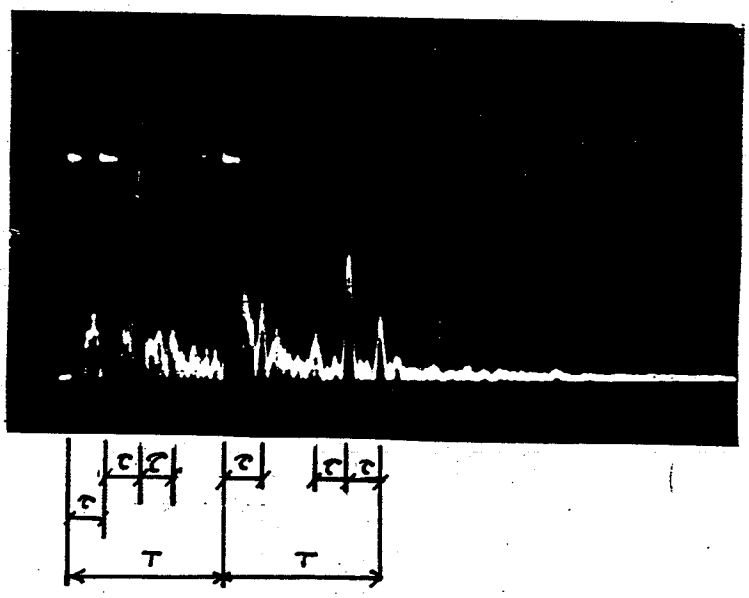

Fig. 4,6 Echo Pattern Following a Three Pulse Excitation. (The Echoes of t = 3τ and 2T - 2τ , Produced by a 5-th Order Process are Clearly Visible.)

Formation of E_s and E_τ involves all three pulses.

The relaxation times of the first, second and stimulated echo (T_1, T_2, T_s) for some selected samples are presented in Tab. 4.1. These relaxation times are independent of the intensity of the RF pulses.

There is a reasonable agreement between the experimental ratios T_2/T_1 and T_s/T_1 and the theoretical values 0.75 and 0.5, Eq.'s (2.47) and (2.48).

A5 The relaxation times of the echoes decay approximately inversely with the frequency.

This is illustrated in Fig. 4.4 where the relaxation time of the first echo is plotted as a function of the frequency for a, different sizes of particles of the same material (Al), b, particles of the same size and shape (filings) of the different materials.

A similar $T_1(f)$ dependence is observed from Rochelle salt (Fig. 4.7) or ferromagnetic powders, the latter has already been shown by Rubinstein and Stauss.[15]

A6 The echo shape depends on the pulse length.

The echo has a regular shape for narrow pulses of the same width. Increasing the pulse width leads to a complex echo shape. An example of such a complex echo shape is shown in Fig. 4.8, where the first long and second short RF pulse (displayed in the LH low corner) produces the echo consisting of four peaks.

TABLE 4.1

Relaxation Time	Al. 60 μm# 16MHz, 22°K	Ni, 50 μm 27MHz, 77°K	Al. 40 μm 12MHz, 4.2°K	Cu 100 μm 15MHz, 4.2°K	Al. 40 μm 10MHz, 77°K	Pb* 16MHz, 4.2°K
T_1	116	86	63	35	117	60
T_2	77	60	39	25	77.5	45
T_s	60	42	30	16	60	--
T_2/T_1	0.67	0.71	0.62	0.71	0.66	0.75
T_s/T_1	0.52	0.48	0.49	0.46	0.51	--

* Ref. (14)

Size of particles refers to the mean, of the size distribution actual size varies $\pm$ 50% of the mean.

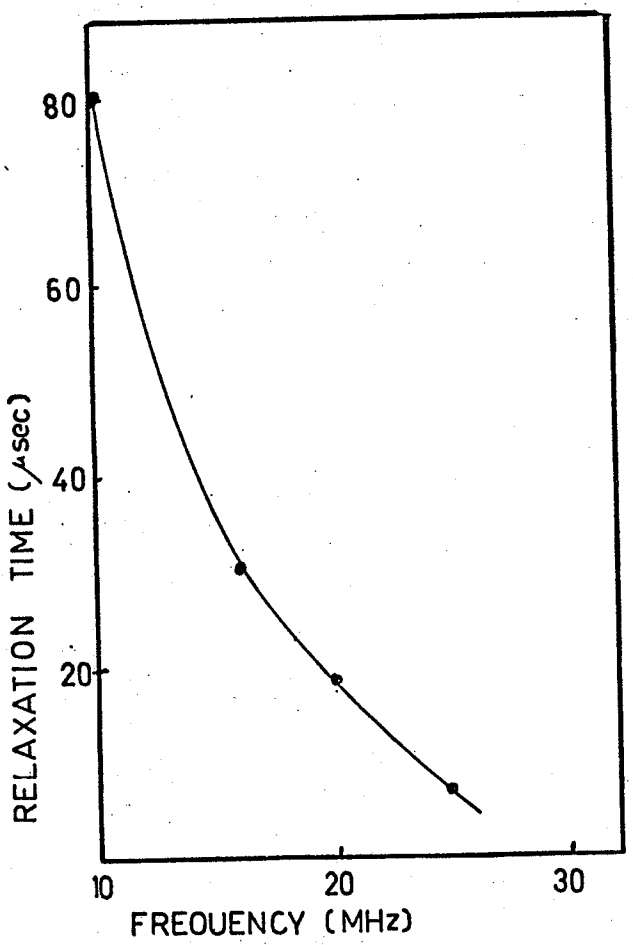

Figure 4.7: Relaxation time of the Rochelle salt as a Function of the Frequency (10MHz, 293°K).

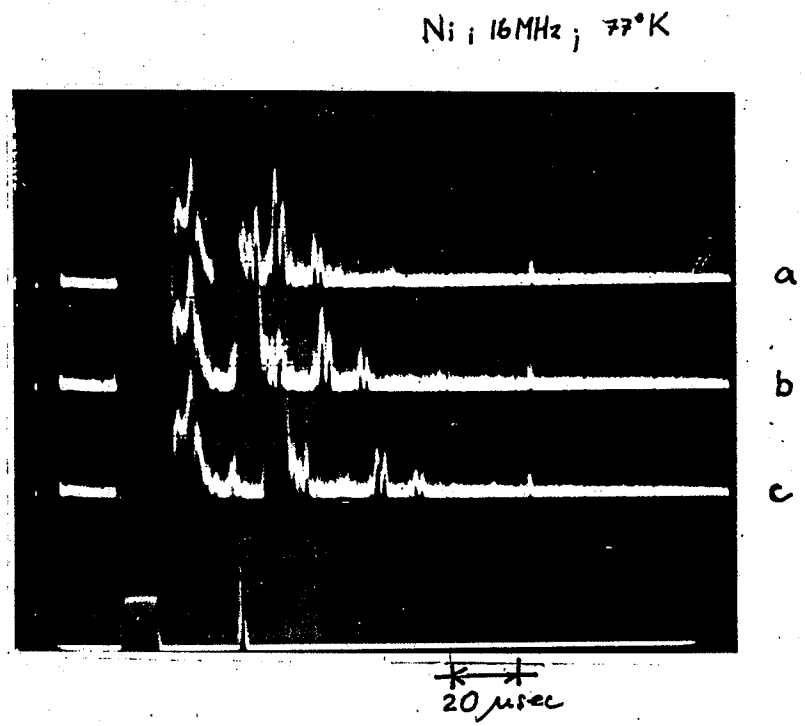

Figure 4.8: Complex Echo Shape Following the Excitation by 2 RF-Pulses of Different Width (Displayed in Low LH Corner) for Increasing Pulse Separation a,b,c.

The fact that these four peaks form the echo is apparent from their constant arrangement for the 3 different pulse separations (Fig. 4.8 a,b,c).

After the first pulse of "infinite width" (continuous signal) a second short pulse excites a very weak echo.

An echo can also be seen after only one pulse. It is superimposed on the induction following the pulses and appears at a time equal to two pulse widths after the beginning of the pulse (See Figure 4.9), For comparison, the pulse width as observed from the receiver output is also plotted. Its length is longer (≈ 6 μsec), corresponding to the recovery time of the receiver.

For the particles with long relaxation time and long RF pulses, continuous variation of the delay between pulses results in a periodic modulation of the echo signal. This is demonstrated in Fig. 4.10, where the echo amplitude from Ni powder (77^{o}K, H = 10 KOe , f = 10 MHz) is monitored while the pulse delay is slowly swept.

A7 At low RF field intensities the echo amplitude varies approximately linearly with the intensity of the first and quadratically with the intensity of the second pulse.

These dependencies are illustrated in Fig's. 4.11 for Cu and Ni and 4.12 for Rochelle salt. In Fig. 4.11

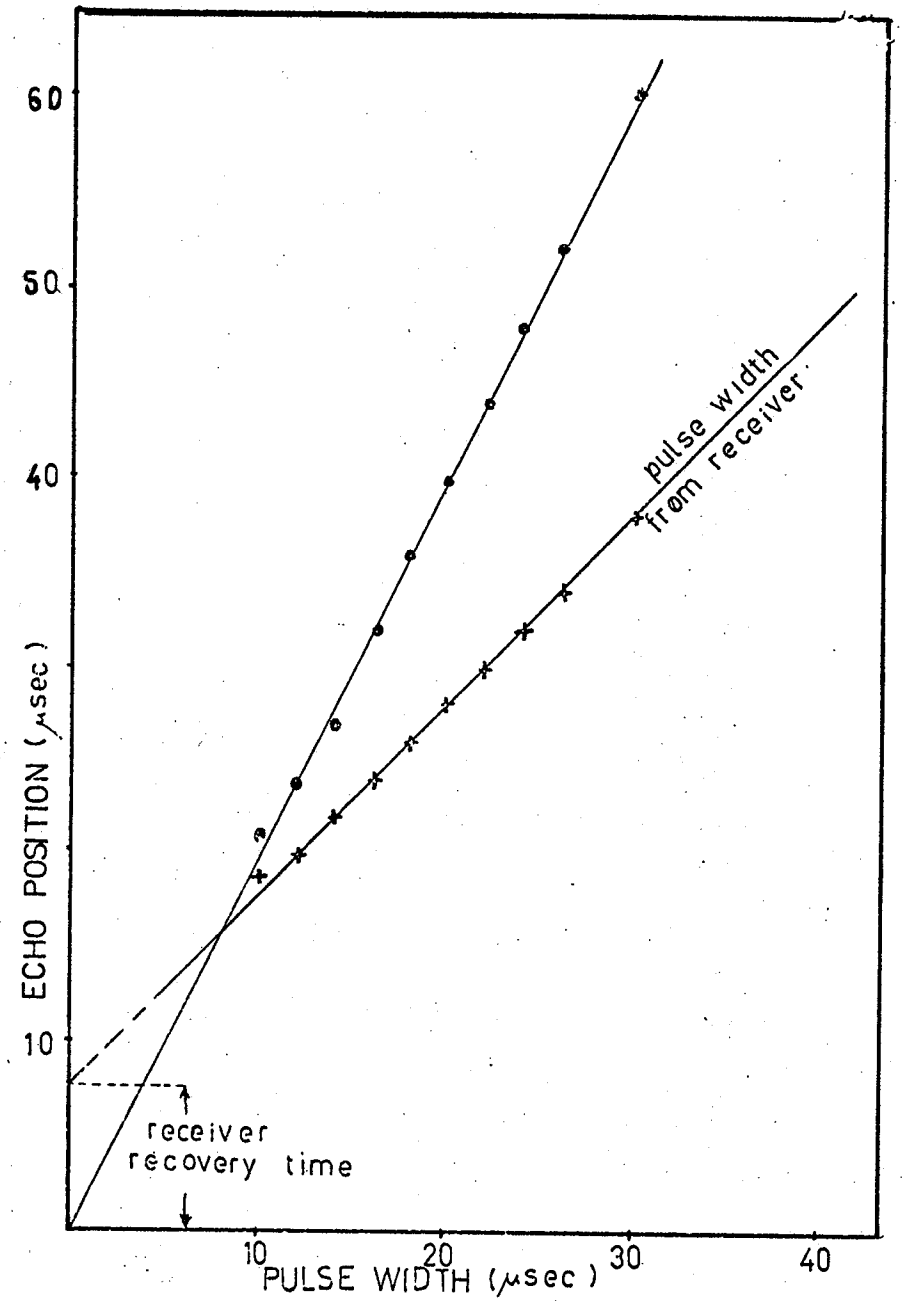

Figure 4.9 Position of the Echo Following 1 Pulse as Function of Pulse Width.

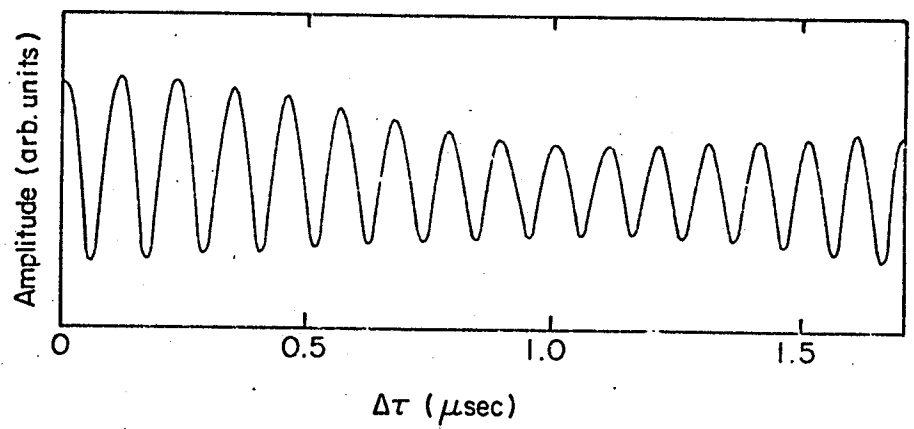

Figure 4.10: Variation of the Echo Amplitude with Pulse Separation.

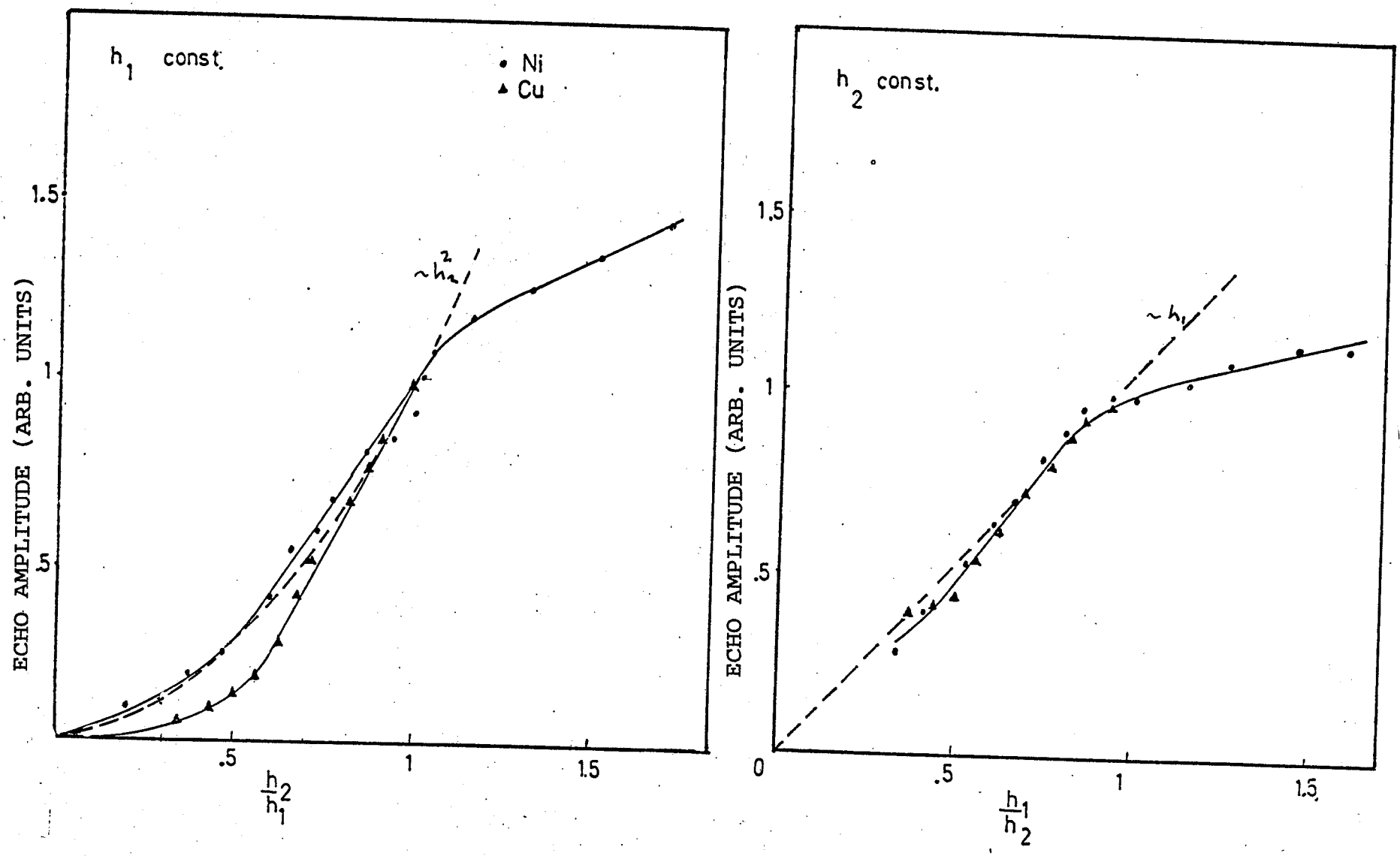

Figure 4.11: Dependence of the Echo Amplitude on Strength of RF Pulses ($h_{max} \approx 100$ Oe) Dotted lines are theoretical expectations.

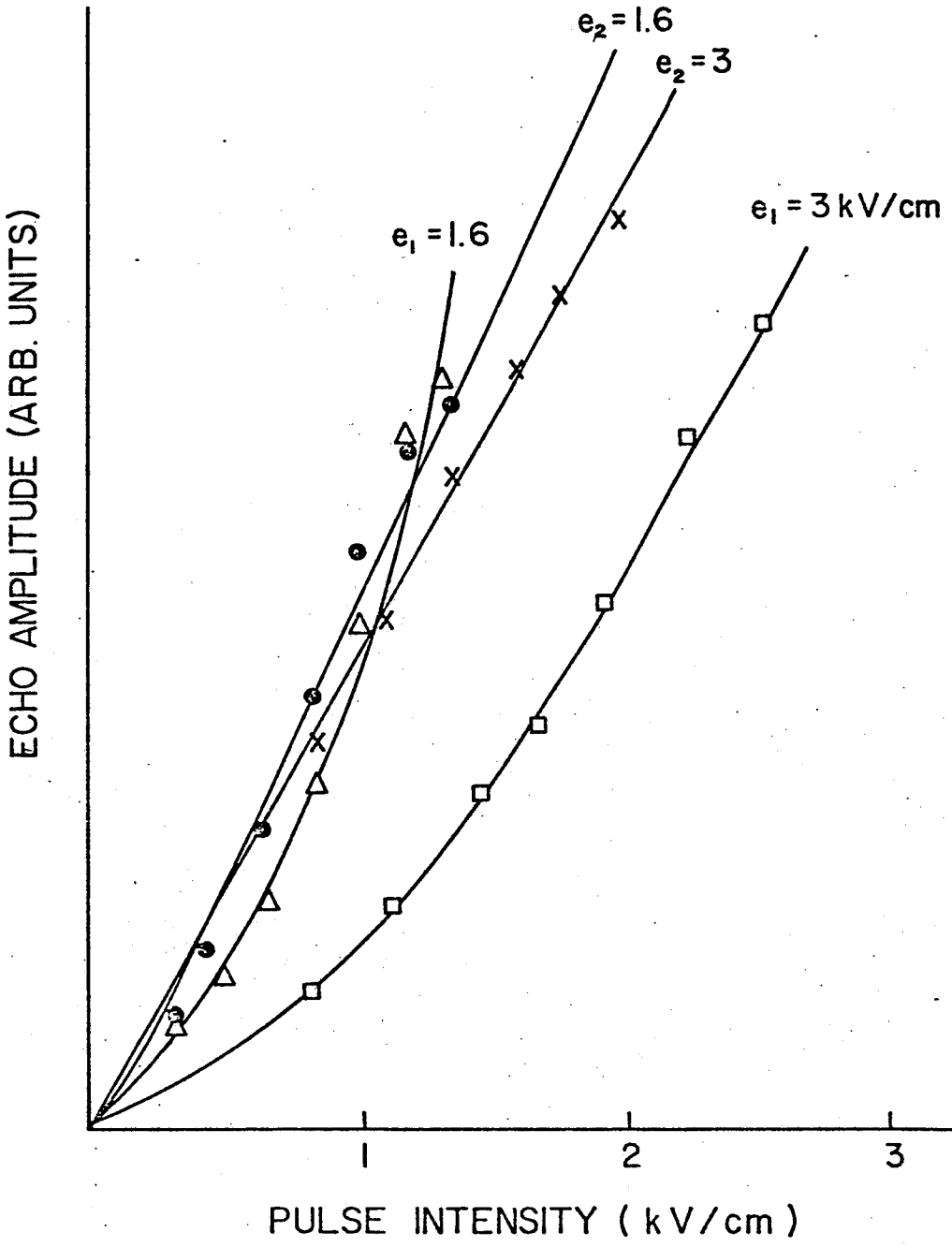

Fig.4.12: Dependence of the Echo Amplitude on Intensities of the RF Electric Pulses. (One Pulse Variable, Second Constant.(Parameter on curves.))

the echo amplitude is plotted as a function of the relative strength of the RF pulses h_1 and h_2, keeping one constant. As can be seen in Fig. 4.11 this relationship is highly nonlinear and for $h_1 = h_2$ the simple relationship

$$E_1 \propto h_1 h_2^2 \qquad (4.1)$$

does not hold. For $h_1 = h_2 = h$ the echo amplitude varies approximately linearly with h (Fig. 4.13) i.e.

$$E_1 \propto h \qquad (4.2)$$

The secondary echoes are too weak to warrant a study of their amplitude dependence on the driving pulses. Theoretically, it is expected that they will vary as $h_1^2 h_2^3$. Although one expects the ratio E_{2/E_1} to vary as h^2, for $h_1 = h_2$, a linear relationship between E_2 and E_1 is observed, Fig. 4.14. However, for small amplitudes the data can be fitted to $E_2 = E_1^{5/3}$ which is expected for $E_1 \propto h^3$ and $E_2 \propto h^5$.

A8 The frequency range of the echo observation depends on the particle size.

For all samples, the highest frequency for which the echo can be seen increases with decreasing particles size.

The only systematic study of this effect was performed on commerical Al powders, because the filings were highly irregular.

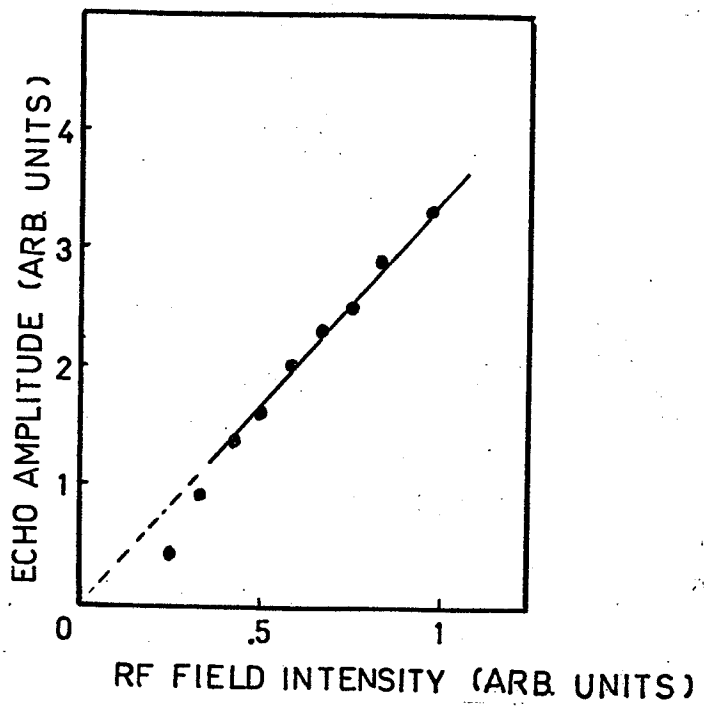

Figure 4.13: The Dependence of the E_1 on the RF pulses intensity for $h_1 = h_2$. (Al, 16MHz, 77°K 10KOe).

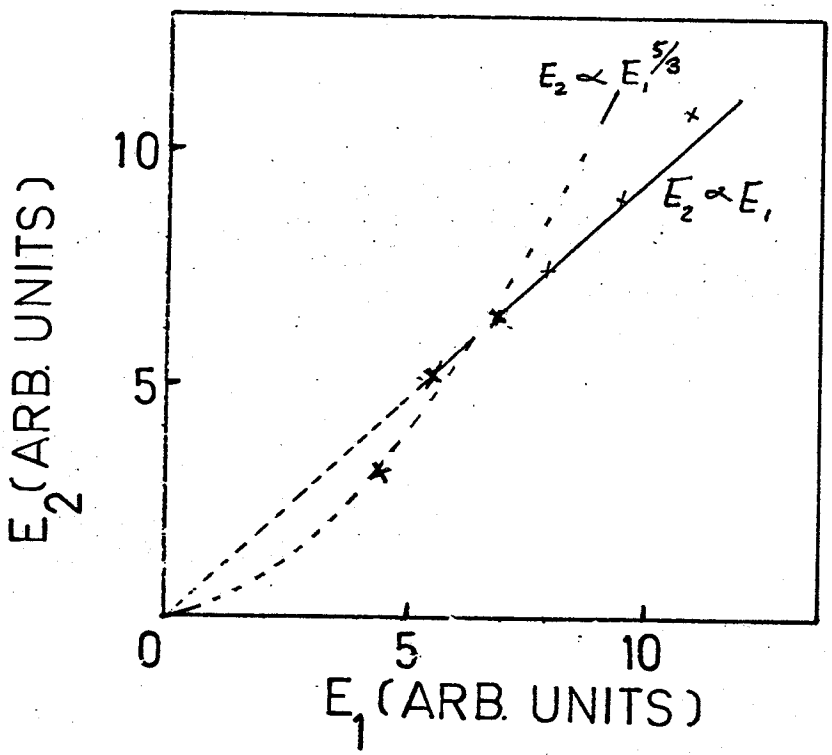

Figure 4.14: Amplitude of the Second and First Echo for Ni Powder for Differnet RF Field Intensities (H = 4KOe, T = 292°K, f = 26 MHz).

As was mentioned in Chapter III, absolute measurements at different frequencies are unreliable. Therefore, relative measurements were employed. Figure 4.15 shows the relative echo amplitude for different size Al powders as a function of frequency. In Figure 4.15 the echo amplitude peaks at different frequencies for different particle sizes. #1 For the $\approx$ 170 μm sample the amplitude peaks below and for the 40 μm above the experimental range (not to be confused with absolute amplitudes, which decrease with frequency for all samples).

Similarly for Ni powders, there seemed to be a maximum in the echo signal at 17MHz for 100-150 μm size and at approximately 27 MHz for 30-70 μm (absolute amplitude). #2

No echo was observed from particles larger than 500 μm for either material.

The samples consisting of big particles showed a very strong free induction but no echo.

The single crystal of Rochelle salt was crushed into smaller and smaller particles and when the size of the particles was smaller than approximately 500 μm an echo appeared. The aim of this experiment was to

#Footnote 1: In ferromagnetic powders Stauss and Rubinstein observed a correlation between the frequency interval for the echoes' appearance and the presence of the absorbtion lines in cw experiments.(15)

#Footnote 2: Particle size refers to the mean of the particle sizes' distribtion. Particle size varies approximately $\pm$ 50% of the mean.

produce an echo from particles big enough for a comparison of the echo amplitude with the free induction from one particle.

A9 No dependence of the echo amplitude on the repetition rate was observed except for alignment effects.

The echo shape is not constant. Using a low repetition rate (10^{-3} Hz) the individual echoes following a single pulse train vary in both amplitude and shape. The experimental data are average values for many excitations. In our experimental range (10^{-3} - 10^{2} Hz) the echo is not a function of the repetition rate. No dependence of the echo appearance on the repetition rate as reported by Palcut et al. [16], was observed.

If pulses are applied to a fresh sample, the echo gradually develops with a rate depending on the pulse repetition rate, Figure 4.16 This process takes more time for ferromagnetic than for normal metal powders. Once the echo is established its amplitude no longer depends on the repetition rate.

Additional effect of particles alignment, so called permanent echo, is described in appendix III.

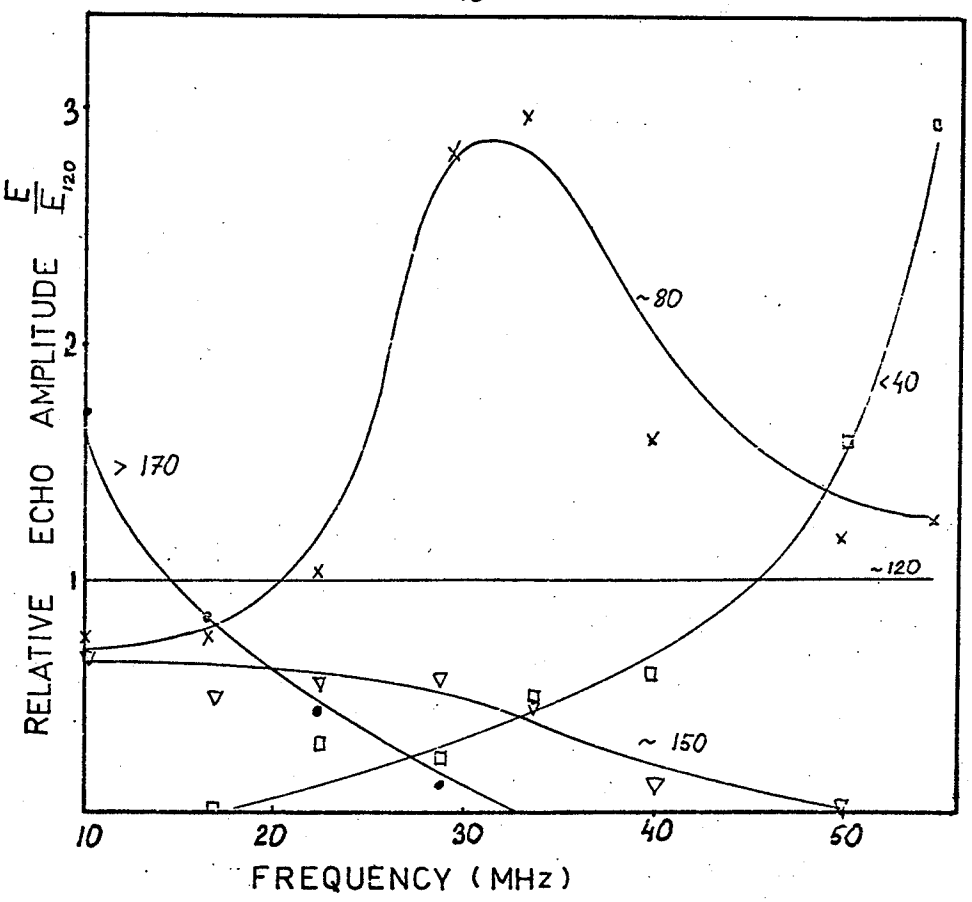

Figure 4.15: Relative Echo Spectrum (Al, H = 10KOe)

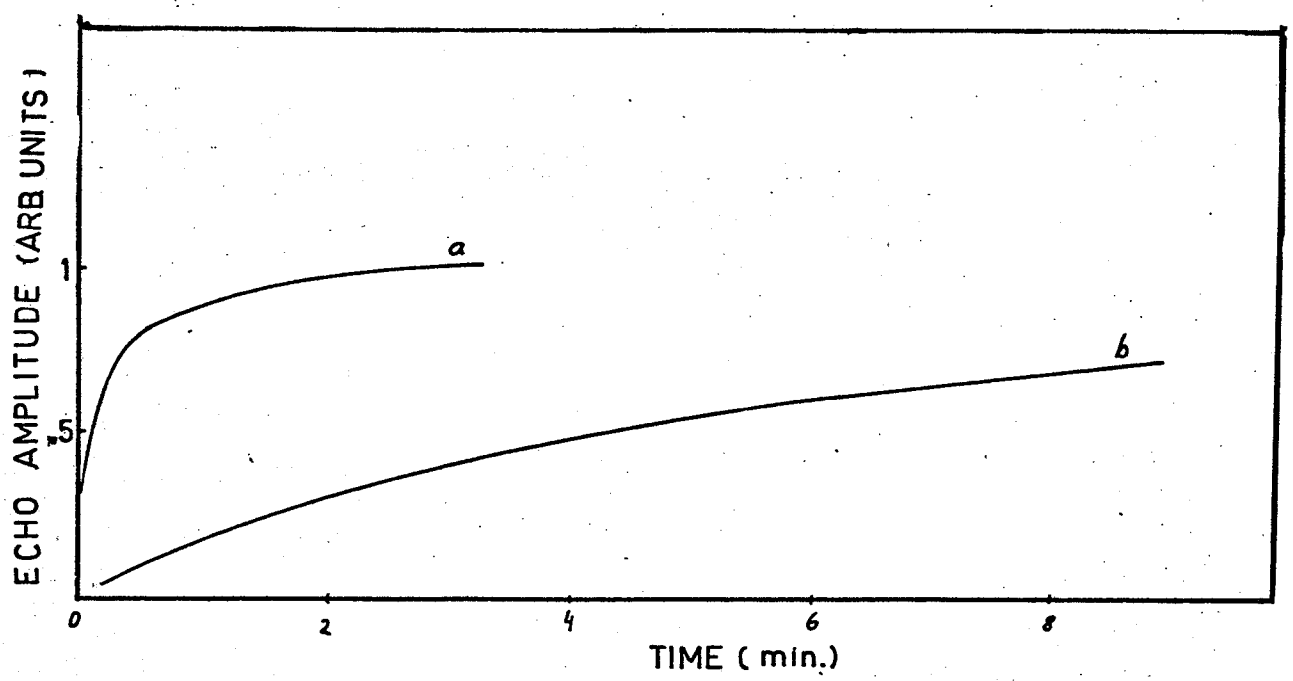

Figure 4.16: Echo Amplitude as Function of Time from a Fresh Sample ($Nd Co_5$ H = 8KOe, T = 77°K, f = 10 MHz) For Various Pulse Repetition Rate a, 30 Hz b, 10^{-1} Hz.

B Echoes from normal metals.

The echo formation requires RF pulses of duration of 5 - 15 μsec. The optimal echo was observed for pulses of a duration of t_w = 10 μ sec.

The absolute echo amplitude at 4.2°K varies from sample to sample. The strongest echo is observed from Al followed by Cu, Au, Zn, Mg, Cr.

Regular particles of Al showed a stronger echo than irregular powder.

Al or Cu powders are the only samples warranting the study of the echo amplitude for various pulse strength or length since they have a signal to noise ratio $\approx$ 100. In other powders the signal to noise ratio is $\approx$ 10-20 . (At 10 MHz and 10 KOe)

All measurements, unless stated otherwise are performed on filings of the "same size" (in the 100 to 200 range of the standard mesh).

The following properties were common to all samples of normal metal powders.

B1 The presence of a static magnetic field, H is necessary for the excitation of both the free induction and the echo. Both increase with increasing magnetic field. The explicite dependence varies and the echo amplitude E_1 as a function of H depends on the intensities of the RF pulses h_1 and h_2 the magnitude of H and on

the material.

B2 In all samples the echo amplitude decreases with increasing temperature. This dependence varies drastically from sample to sample and depends also on frequency and particle size.

B3 At low field intensity, H, the relaxation time of the echoes is not field dependent.

The statements above are illustrated in details below.

B1 The echo amplitude as a function of H for various ratios of h_1/h_2 and h_2/h_1 for Al is plotted in Fig. 4.17. As can be seen, the echo amplitude cannot be expressed by a simple universal power dependence of the form.

$$E_1 \propto H^{\beta} \qquad (4.3)$$

with β constant, but β varies between 2 and 4. To make a comparison between the various metals the echo amplitude at $h_2 = \frac{1}{2}h_1$ is plotted as a function of H in Fig. 4.18. The curves in Fig. 4.18 are vertically shifted for a clearer demonstration of the variation of β.

The optimal echo amplitude is for $h_1 = h_2$. In this case all the samples show the $E_1 \propto H^2$ dependence (H = 10KOe) which is a consequence of the $E_1 \propto h$ dependence shown in Fig. 4.13.

Fig. 4.19 shows the echo amplitude at $h_1 = h_2$ for some samples at large magnetic field intensities. The echo increases with H up to 50 KOe and in some cases there is an indication of saturation.

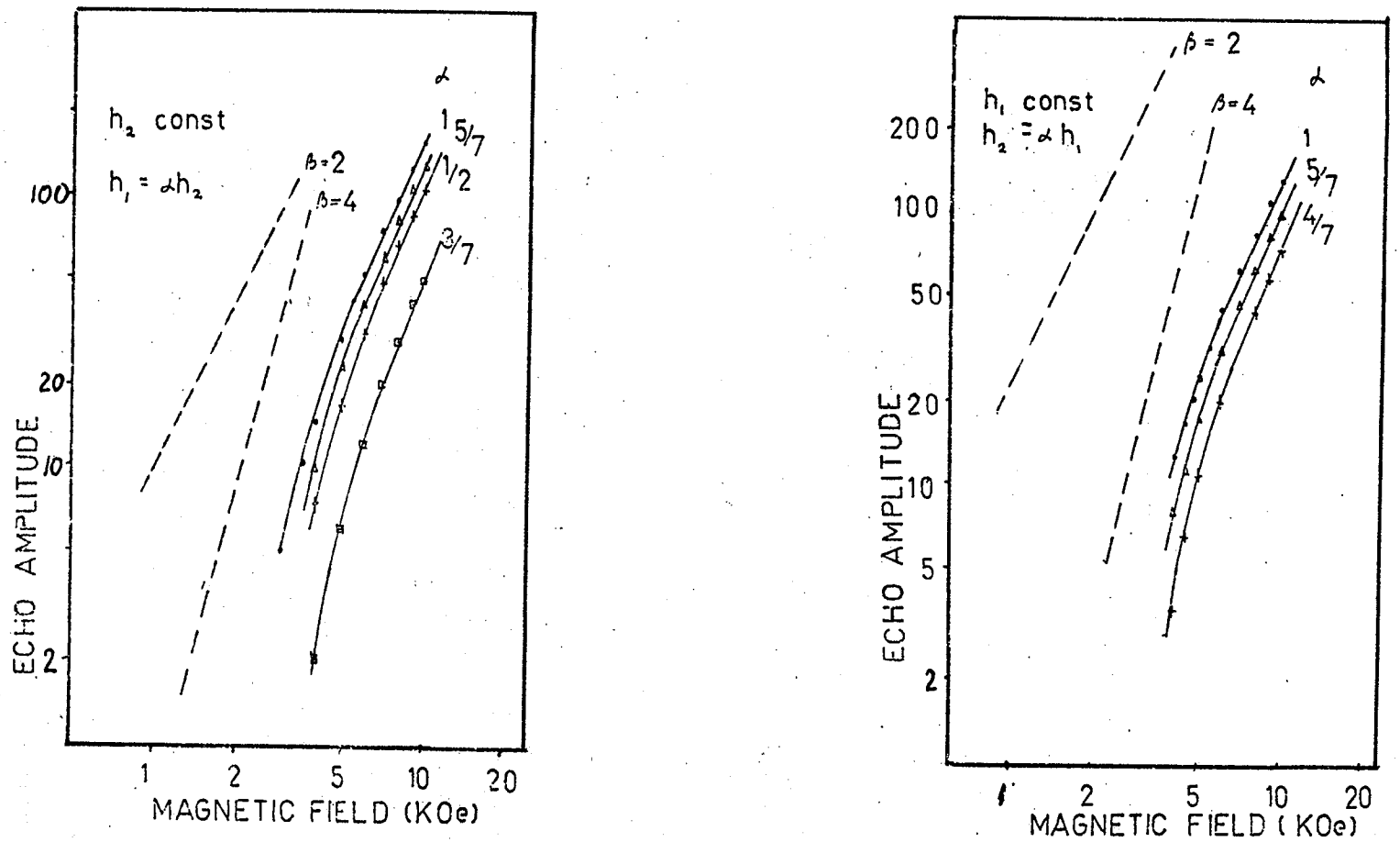

Figure 4.17: Echo Amplitude as a Function of H for Various Values of h_1/h_2 dotted line Indicates the Slope of H for Comparison (Al).

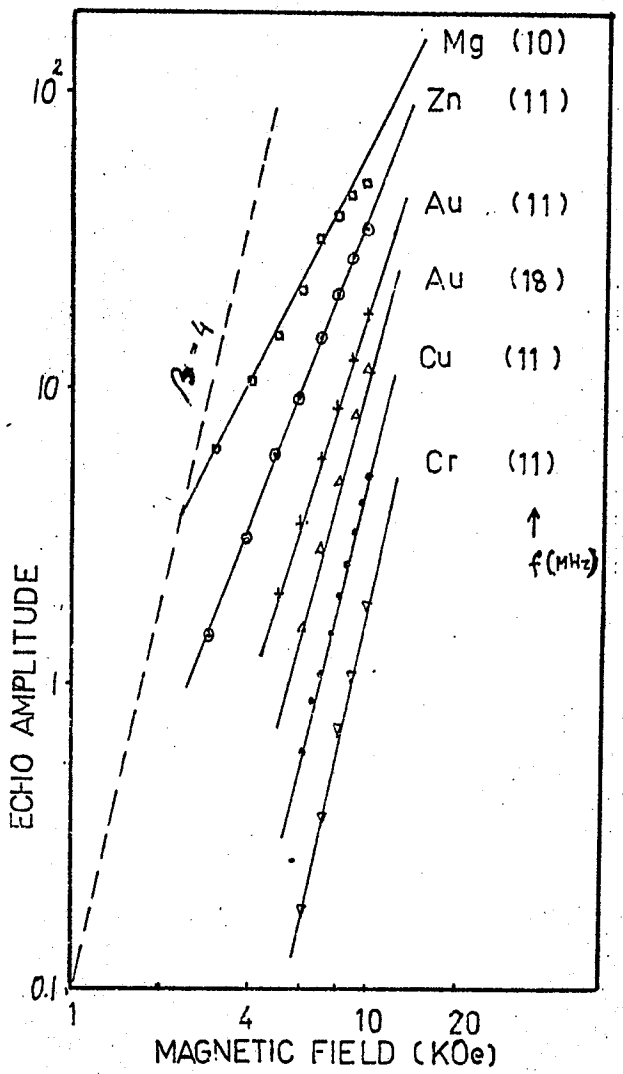

Figure 4.18 Echo Amplitude as a Function of H for Various Metals ($h_2=\frac{1}{2}h_1$) (4.2°K) (Frequency is the Parameter.

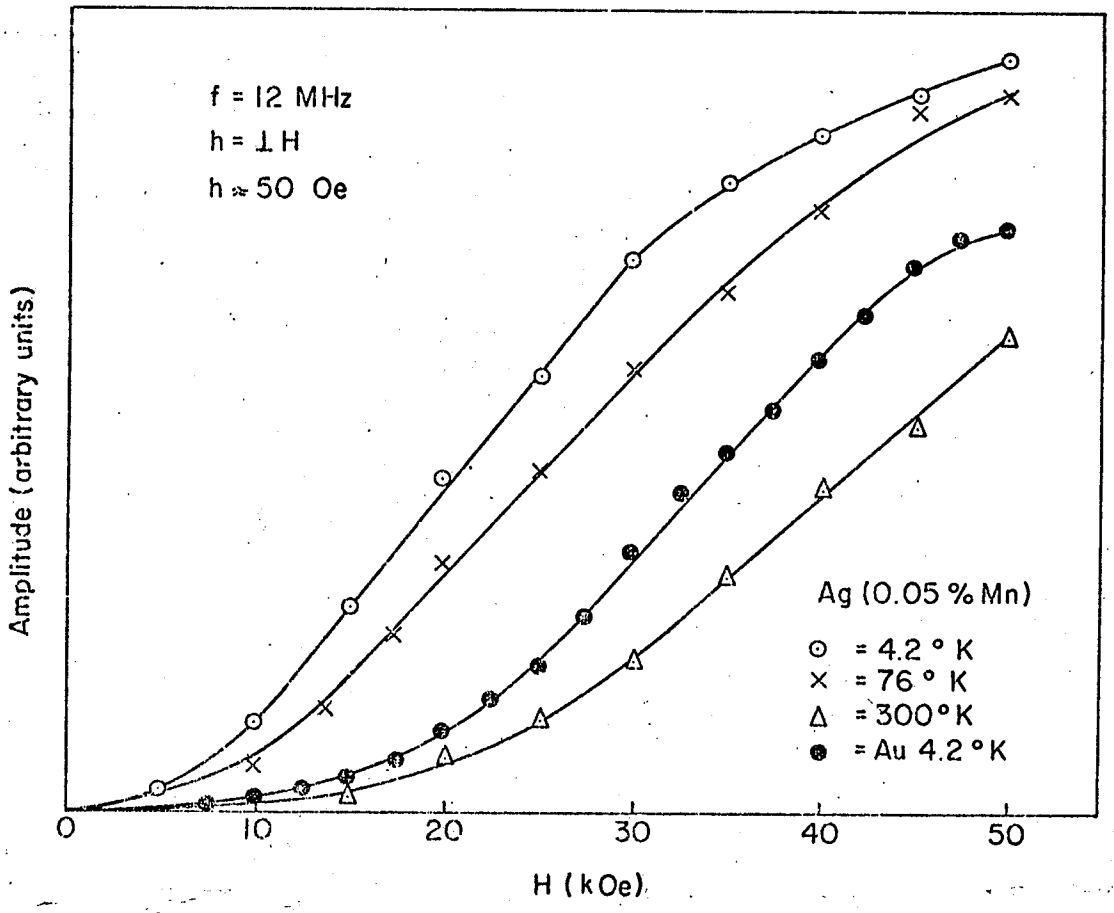

Figure 4.19: Dependence of the Echo Amplitude on H for High Field Intensities.

An echo was also observed at room temperature from Ag Mn for large H.

The nonuniform dependence of E_1 on H can be a consequence of the variation of the material properties with the static magnetic field, H. Therefore, for Al and Cu the direct excitation process was also studied, using the experimental arrangement shown in Figure 4.20. The amplitude of the excited ultrasonic pulse, linear excitation, shows an H^2 dependence for both longitudinal (a) and transversal (b) geometry. (The same coil was used to generate and detect the signal.) The field dependence of the amplitude of such a signal is shown in Figure 4.21 ($\lambda \perp H$).

The amplitude of the echo depends also on the relative orientation of the RF and the static magnetic field (Fig. 4.22) and is maximal for $h \perp H$.

B2 Temperature dependence of the echo

Apart from the Mg sample there is no cut off at a critical temperature, above which the echo suddenly disappears. The echo amplitude increases with H and therefore the temperature interval for the echo observation depends on H and h_1, h_2.

The temperature dependence of the echo from the 150 μm Al particles, for various frequencies is shown in Fig. 4.23a while in Fig. 4.23b this dependence is shown for different sizes of Al powders at a fixed frequency. The echo amplitude as a function of frequency

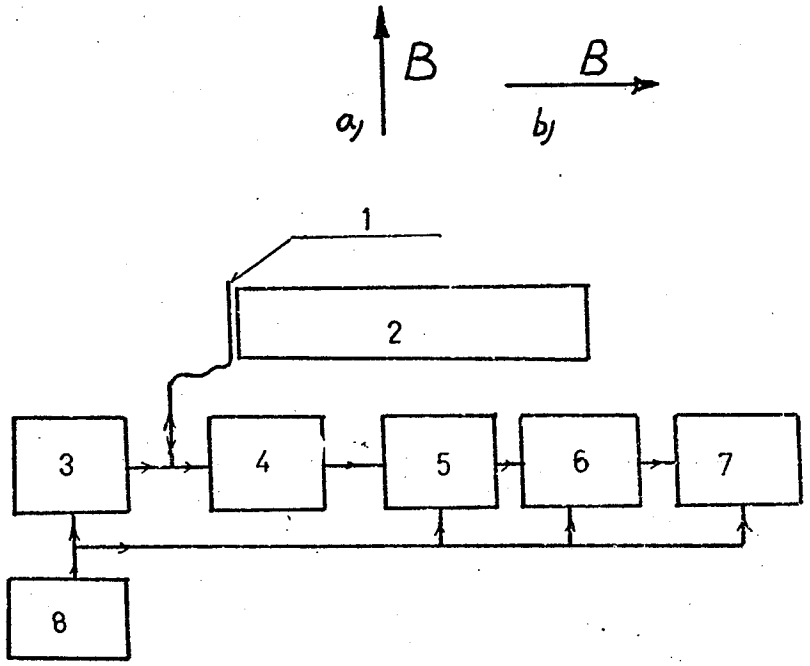

Figure 4.20: Block Diagram of the Direct Excitation of Ultrasonic Waves a, Longitudinal b, Transversal, Excitation. (1 -flat coil, 2 -bulk metal sample, 3 -4 - RF pulse generator and receiver. 5 -box car integrator, 6 -scope, 7 -recorder, 8 -trigger.)

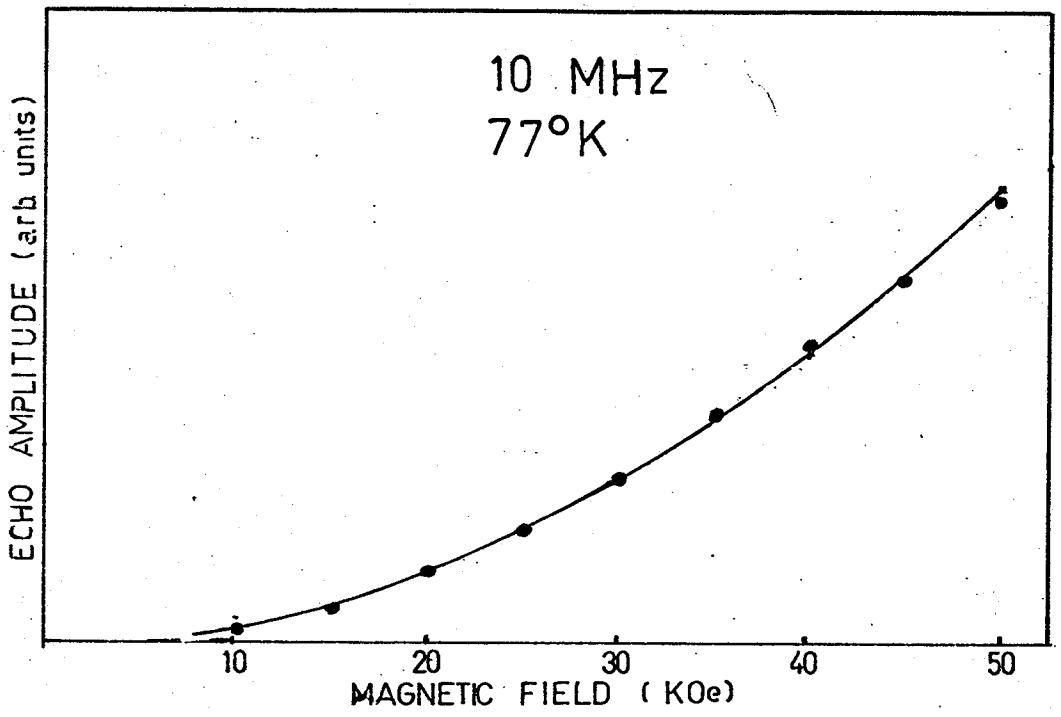

Figure 4.21: Amplitude of the "Direct Excitation" Signal From Al as Function of H (Transveral Wave).

Solid line is the expected H^2 dependence.

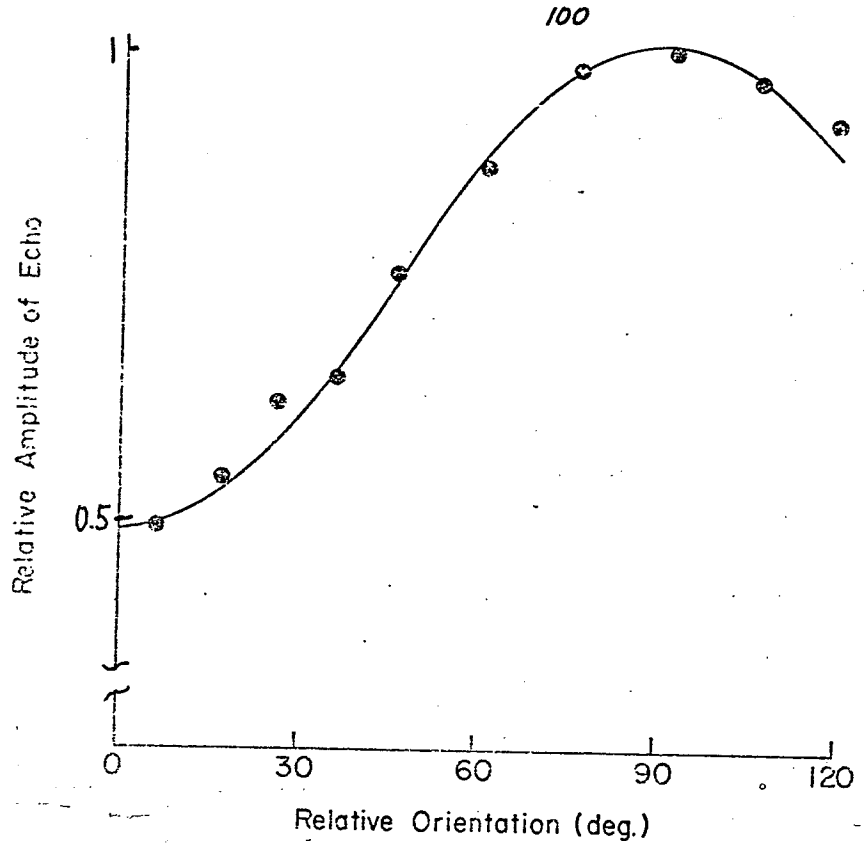

Figure 4.22: Dependence of the Echo Amplitude on the Relative Angle Between h and H.

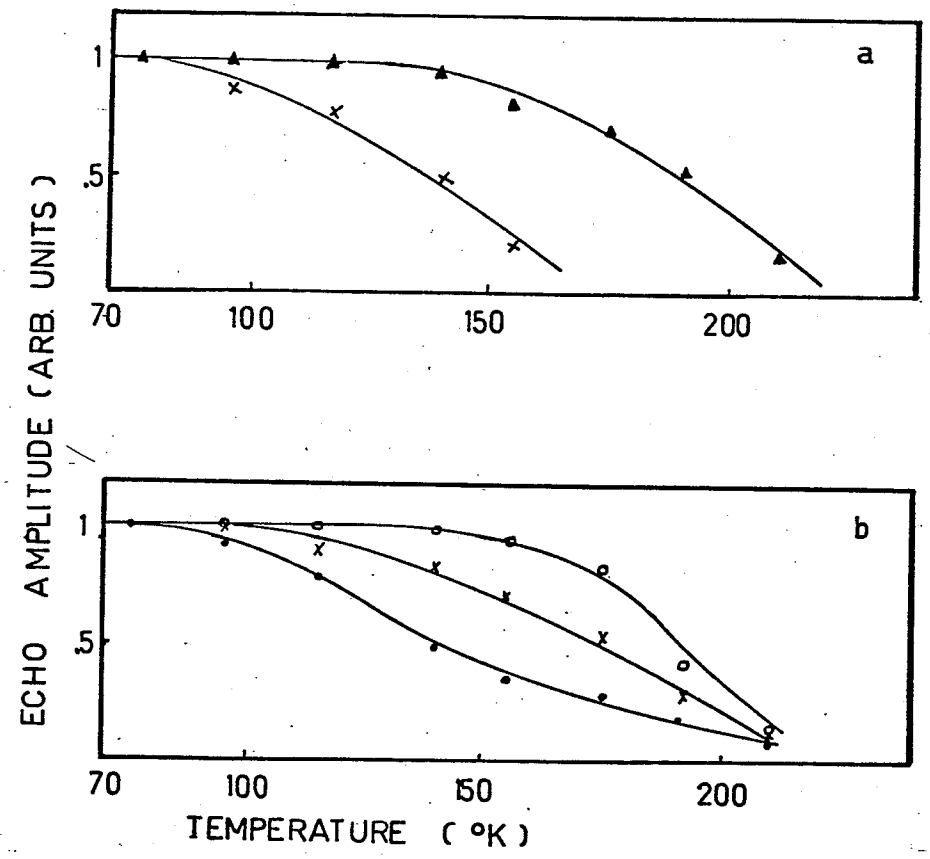

Figure 4.23: The Echo Amplitude as a Function of Temperature for a) Particle Size (▲ ≈ 150 μm, × ≈ 80 μm) (at 20 MHz) b) Frequency (o 40MHz, × 20MHz, ● 10MHZ of 150 μm particles.)(Al, 77°K).

for filings of Al Au and Cu (10MHz, 10KOe) is shown in Fig. 4.24.

The extreme sensitivity of the observed E_1 vs T dependence to the experimental conditions can be seen from Fig's. 4.23 and 4.24 where two different RF coils are used. The temperature interval of the echo observation from Al in these two arrangements is different for different frequencies, size and shape of the powders. (Fig. 4.23 is commercial Al, Fig. 4.24 Filings)

The temperature below which the echo was observed for the particular experimental set up at a field of H = 10 KOe and a frequency of 10MHz from various samples is in Tab 3.1 (filings).

The Mg sample shows a very strong dependence of the echo amplitude on the temperature below $4.2^{o}K$ as can be seen in Fig. 4.25.

B3 The relaxation time of the echo as a function of H.

The relaxation time is similar for all the filings and is fully determined by the shape of the particles. Therefore it does not have any intrinsic physical significance. It also does not depend on the intensity of the magnetic field ($H<10KOe$) or temperature.

The relaxation time of regular particles is much longer and decreases at high field intensity H. Fig. 4.26 shows the relaxation time of the echo from $\approx$ 80 μm size Al regular particles at different frequencies.

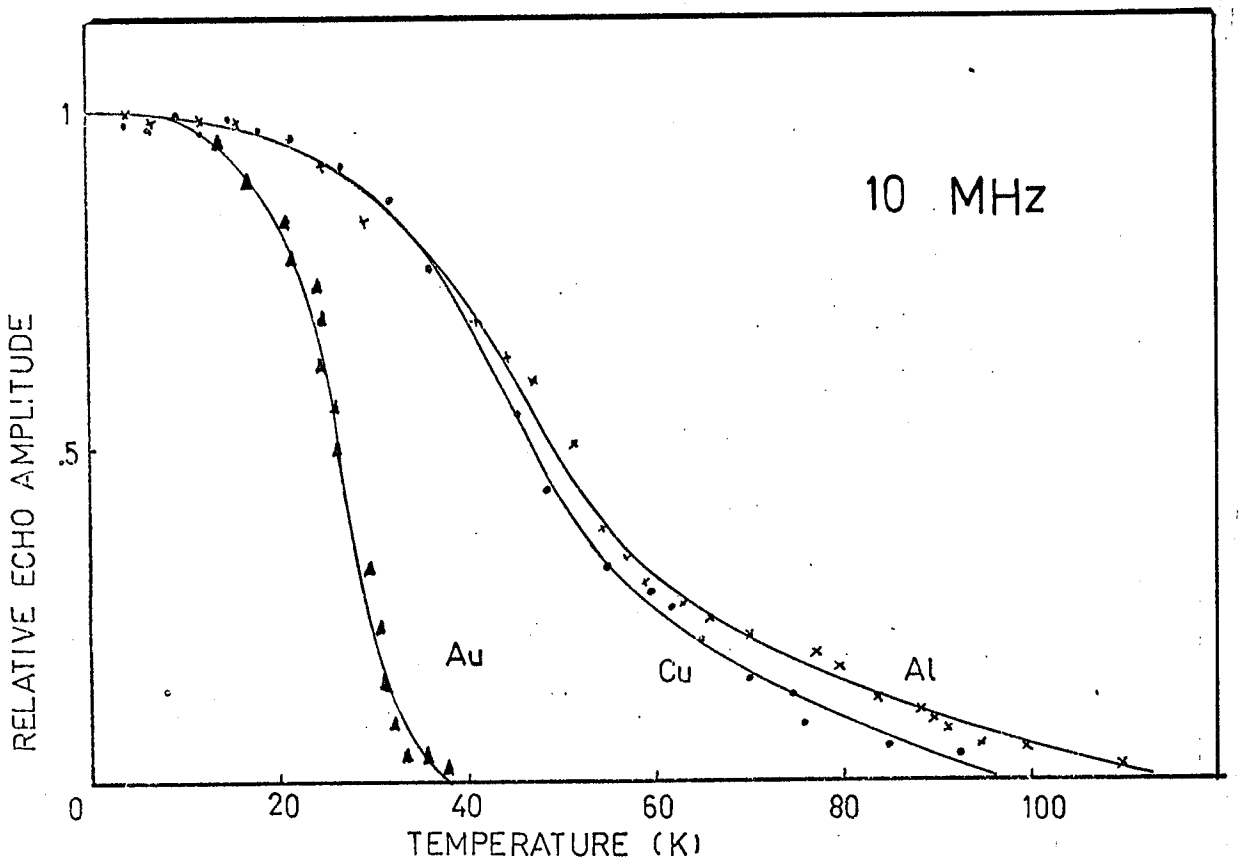

Figure 4.24: Echo Amplitude as a Function of Temperature (Al, Cu, Au)

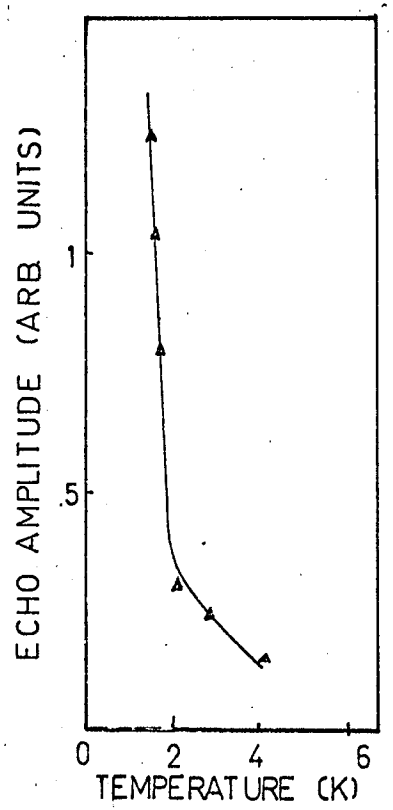

Figure 4.25: Echo Amplitue as a Function of Temperature (Mg) (10 MHz)

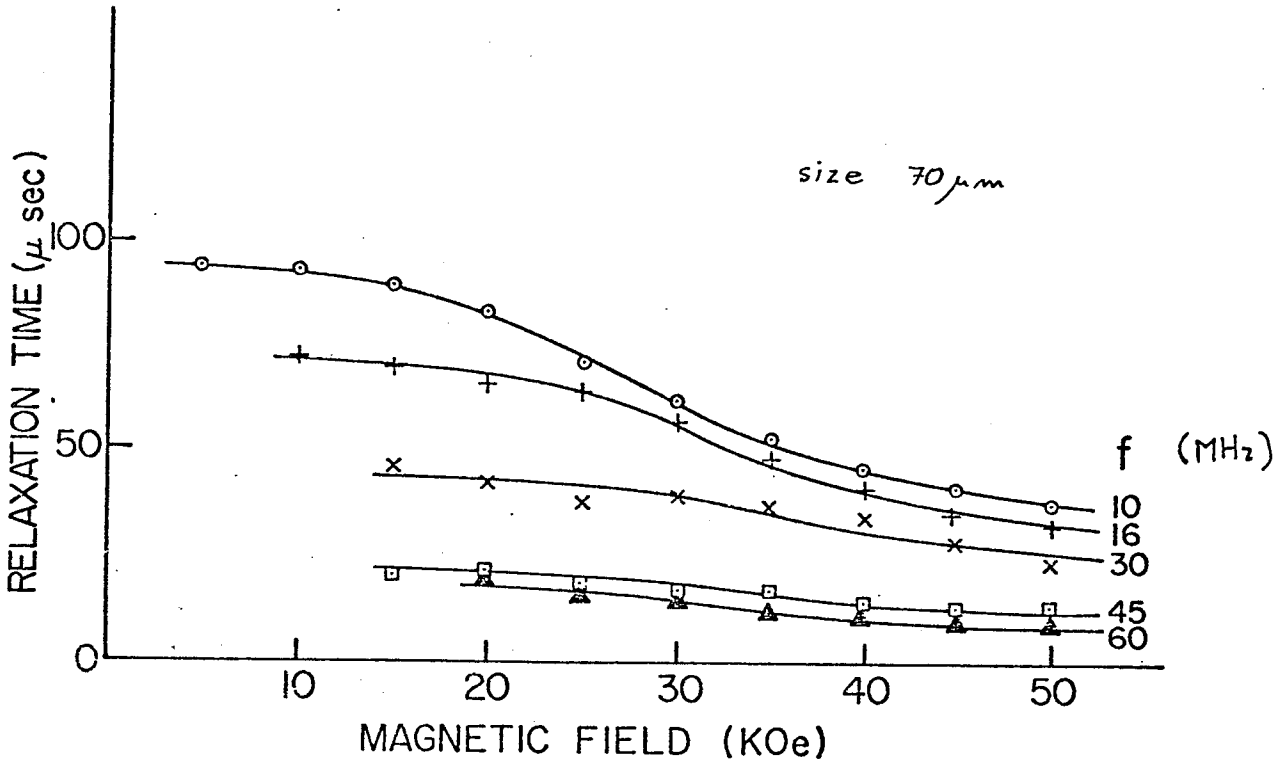

Figure 4.26: Relaxation Time of Echo From Al Powder as a Function of Biasing Magnetic Field. (Frequency is a Parameter.)

B4 Effect of impurities or alloying

As was mentioned in the introduction, Snodgrass did not observe an echo from pure Ag,[20] while a small amount of paramagnetic impurities enhanced the echo. On the other hand, Pacult and coworkers reported a strong echo from pure Ag. In this study no echo was observed from pure Ag at H = 10 KOe for the entire temperature range and only a weak one at H$\gtrsim$ 30KOe. Small amounts of paramagnetic impurities (Mn, Ni) strongly enhanced the echo, making it comparable to that from Al (strongest echo).

This anomalous effect is observed from dilute

Ag Mn (0.01% - 0.1%) alloys.

When the impurities' concentration was higher than 0.1% (estimated from nominal concentrations) the echo disappeared.

The lack of an echo from Ag is in sharp contrast to the observation of a strong echo from Au or Cu, therefore two different "pure" Ag samples were used (5N Alfa Inorganic and Spec Pure from Johnson Matthey and Mallory). To avoid the possibility of the presence of oxygen in the Ag lattice some samples were annealed in H_2 but no sample showed an echo.

Similarly, no echo was observed (H = 10KOe) from Ag doped with less than 1% In, Au, Cu.

No enhancement of the echo amplitude was observed in dilute AuMn (0,05%) or CuMn (0,01; 0.05; 0,1; 0.5%) alloys. Small amounts of impurities (over 0.1%) eliminated the echo, while the presence of impurities had no effect on the relaxation time.

The echo was not observed from filings of metals of technical purity (Cu, Al).

In some alloys the echo amplitude increases with increased ordering. The alloys were prepared by melting in an arc furnace and the echo from filings increased after annealing them. This was observed from Cu Ag (9%, 13%, 20%). An interesting case is demonstrated in Fig. 4.27, where the echo amplitude from Al Mn (1%) is plotted as a function of the annealing

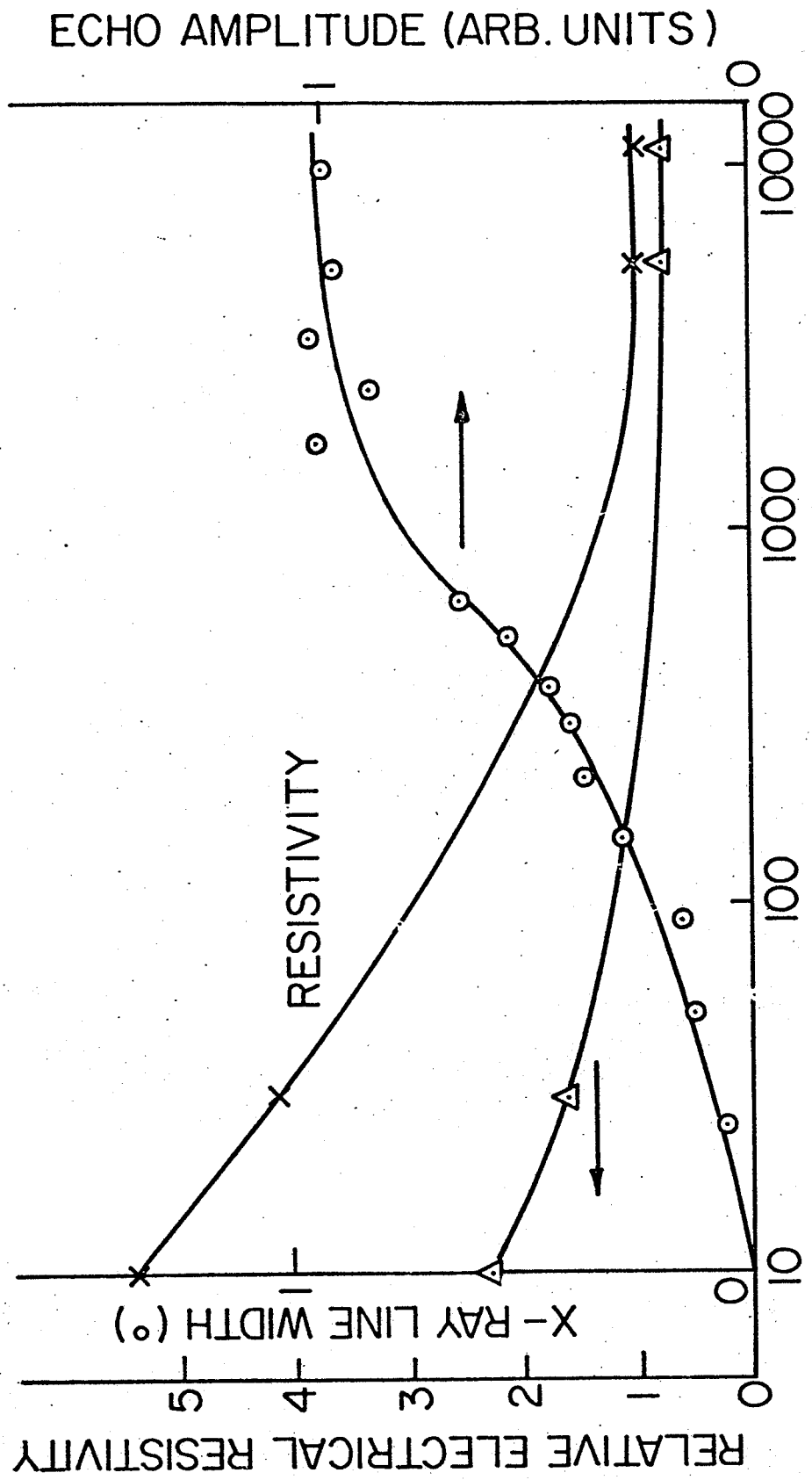

Figure 4.27 Dependence of the Echo Amplitude, X-ray Line Breadth and Electrical Resistivity on Annealing Time for Al Mn (1%).

time ($350^{o}C$) in a vacuum of (10^{-4} torr).

The increase in the echo amplitude corresponds to a decrease in the X-ray diffraction line breadth ({112} line) and a decrease in the electric resistivity. These results are due to an increase in ordering via precipitation of Mn. During the annealing process new diffraction lines gradually appeared from the Mn precipitates.

Apart from Ag, impurities always reduce the echo.

B5 The effect of deformation or thermal treatment.

Quenching or deformation of pure Al powder reduces the echo. This is partially recovered after annealing.

Deformation changes the particles' shape, which naturally leads to a change of the relaxation time. However, in the case of the regular Al powder the relaxation time increased with the subsequent annealing. For example, at $77^{o}K$, a particular sample of deformed Al powder had a T_1 of 56 μ sec and after annealing a T_1 of 62 μ sec.

B6 The effect of temperature on the relaxation time of the echo.

The relaxation time is not dependent on temperature. Small changes are within the experimental error.

B7 The effect of the particles' insulation.

Insulation of the surface of Ag Mn by the solution of Na_2S does not affect the echo. Mixing the Al powder with inactive powder (glass) gradually reduces the echo.

C The echo from ferromagnetic powders.

The coupling between the RF field and the elastic vibration in ferromagnetic materials is stronger than in normal metals and therefore shorter pulses can be used. Typically, the RF pulse duration, tw, is $\approx 5\,\mu$ sec.

The following properties of the echo were common for all ferromagnetic powders used in this study:

C1 The echo amplitude as a function of the biasing magnetic field, H, passes through a maximum

C2 The relaxation time of the echoes is affected by the biasing field. The only exception is the echo from the ferrite powder, where the relaxation time is very short and is fully determined by the low Q of the sintered material.

Qualitatively, the statements above are demonstrated in Fig. 4.28 for Ni powder and two different orientations of H and h. The detailed experimental results are listed below.

C1 Dependence of the echo amplitude on the strength of the biasing field

The relationship of E_1 to H depends on many factors:

a: relative orientation of H and h (Fig. 4.28).

b: macroscopic shape of the powder sample (size of the tube holding the powder).

c: mixing of the powder with inactive substances (glass powder).

d: temperature.

e: thermal and mechanical history of the sample.

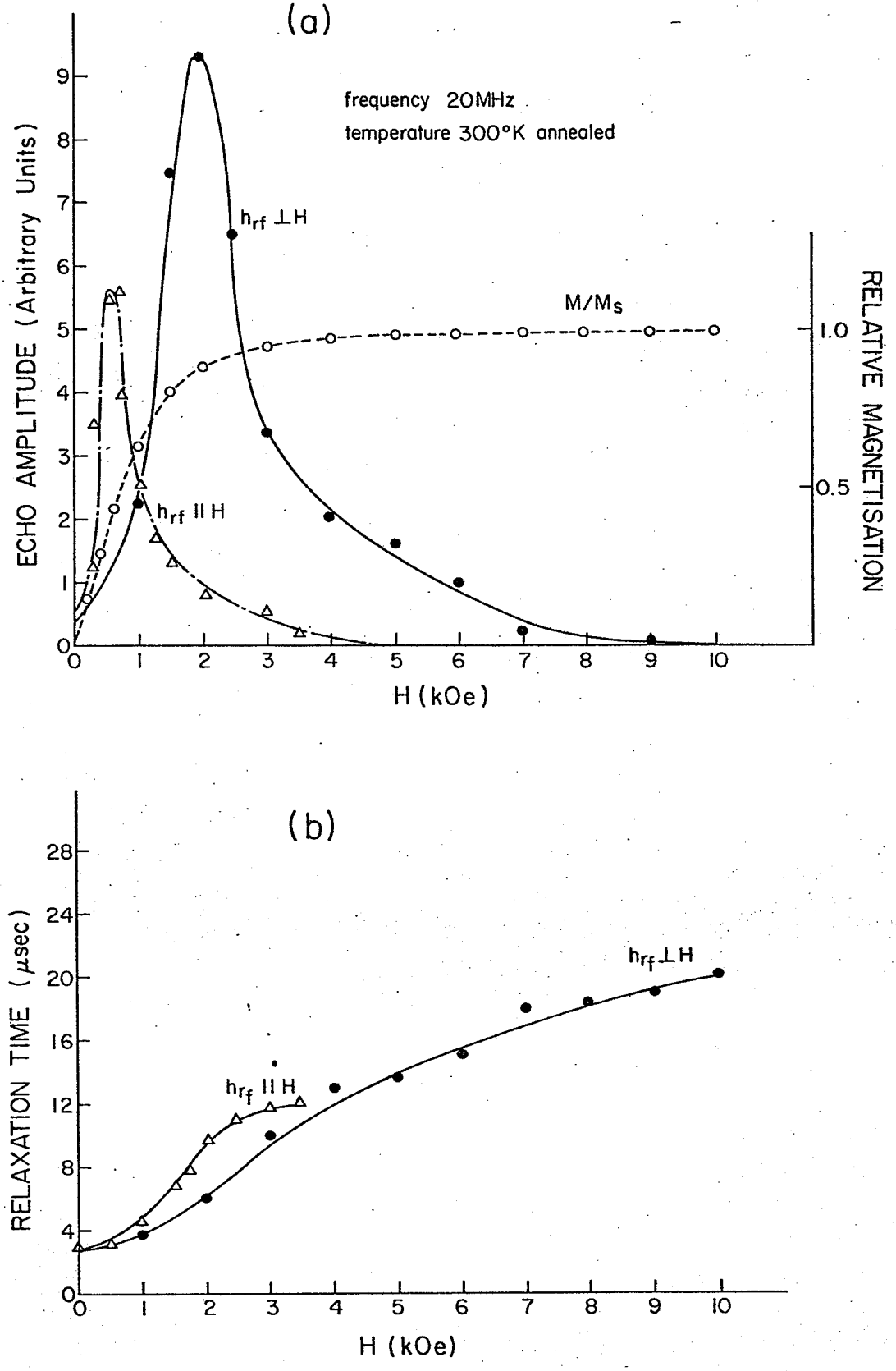

Figure 4.28 Echo Amplitude and Relaxation Time as a Function of Biasing Magnetic Field H (Ni, 20 MHz).

All the observations above indicate that the actual coupling between the RF magnetic field and the elastic vibrations depends on the degree of saturation, which in turn depends on the demagnetization tensor, $\tilde{\mathcal{D}}$, of the sample.

The field#, at which the echo amplitude is maximal for $h \perp H$ is approximately 7 KOe for the RCo_5 compounds, 3-4 KOe for Ni and Fe, 5 KOe for Co, 1 KOe for the powdered ferrite, 300 Oe for the bulk ferrite, and 700 Oe for $\alpha\ Fe_2O_3$.

It is interesting to mention that the same excitation process, which causes the echo in powders, is able to excite an echo in bulk material.(69) Figure 4.30 shows the echo amplitude from bulk and powdered ferrite as a function of biasing field H. The difference in the shapes of the curves (curve a,b) can be explained by the different demagnetization factors of the bulk and powder samples. The macroscopic shapes of the bulk ferrite core and the sample holder for powder samples are similar. Therefore, the difference originates from the fact that the powder is not well characterized by a uniform demagnetization factor. The echo from bulk ferrites was observed from different samples (ferrite cores used for chokes, ferrite antennas) of arbitrary shape. Practically all samples that showed a ringing (induction) signal after one pulse produced an echo

#Footnote: For identical samples with a ratio of diameter to length ≈ 4 leads to $\mathcal{D}_\perp \cong 6$ and $\mathcal{D}_{||} \cong 0.5$

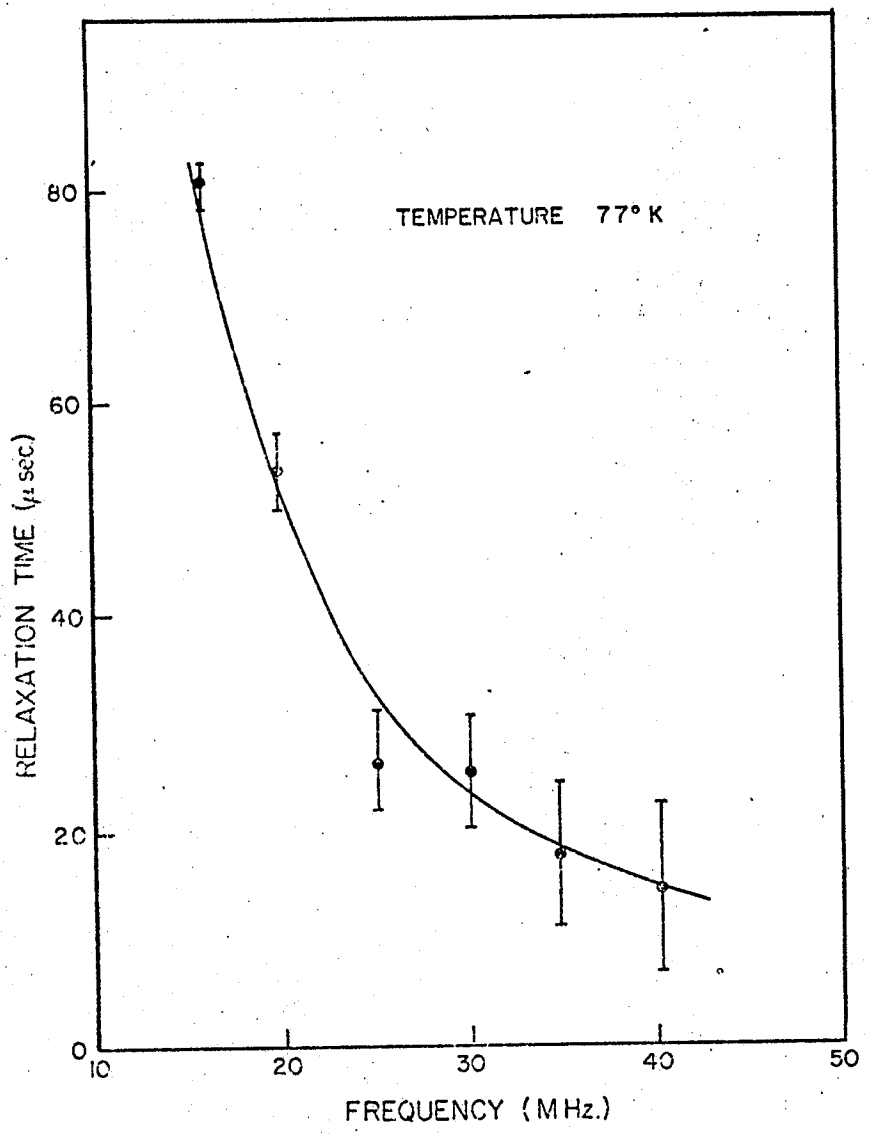

Figure 4.29 Relaxation Time of Echo From Bulk Ferrit as a Function of Frequency ($77^{o}K$)

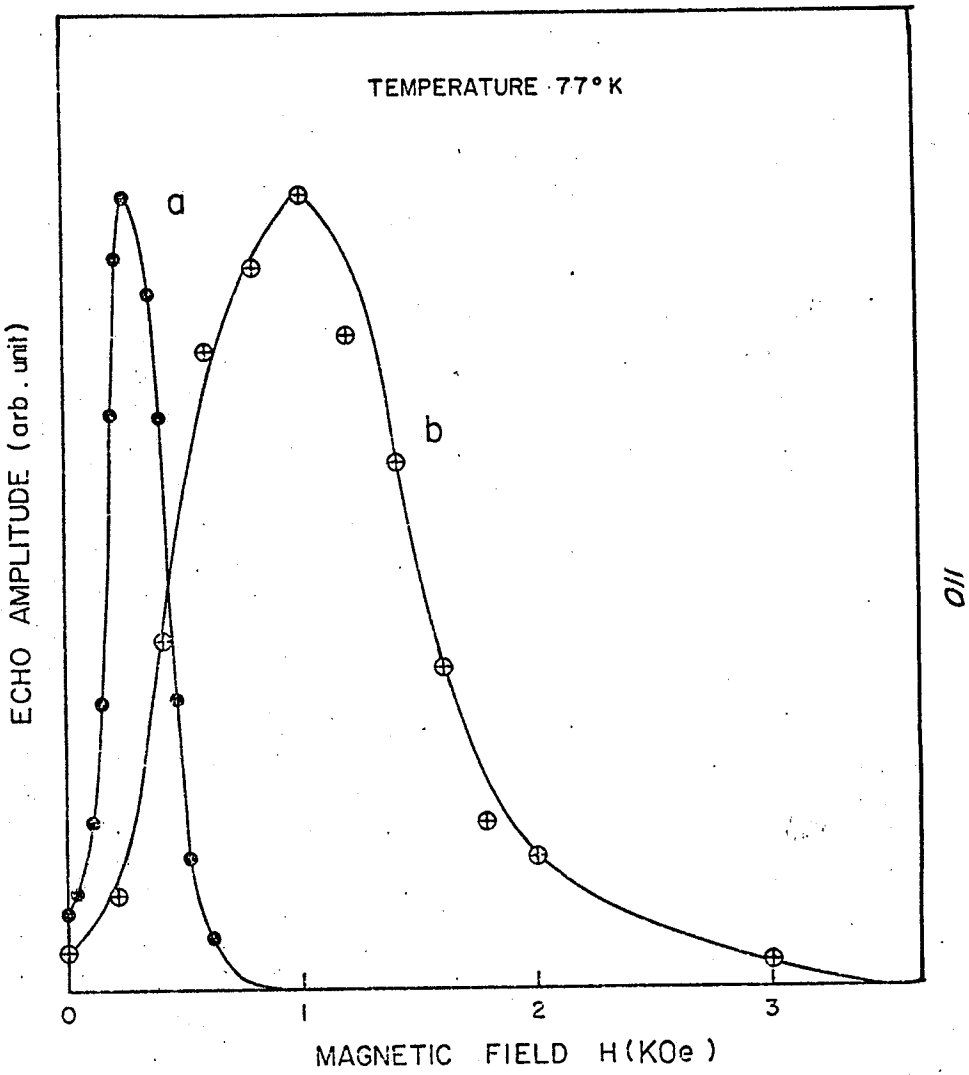

Figure 4.30 Echo Amplitude as a Function of Biasing Field for Bulk (a) and Powdered (b) Ferrite($77^{o}K$)

during a two pulse excitation.

The relaxation time of the echo from bulk and powder samples is different, but in both cases it follows the general hyperbolic decrease with the frequency that was demonstrated in Section A. Figure 4.29) shows the relaxation time from a bulk ferrite sample as a function of frequency. As expected, the bulk ferrite has a longer relaxation time than the corresponding powder (negligible surface losses). Also, the relaxation time is only weakly temperature dependent, but it depends on the experimental arrangement (for example, the geometry of the sample's support or its orientation relative to the biasing magnetic field).

The pulse width required for echo formation is 10 μsec for bulk in comparison to 2-3 μsec for powders. This time is too long to produce travelling waves (the pulse duration is much longer than the time required for sound to travel through the sample), and resonance mode refocussing is probably responsible for the echo in both cases. In powder samples the individual modes are localized in the particles, while in the bulk sample different modes can exist simultaneously. The presence of many modes in the bulk can also be deduced from the complex induction signal, following the RF pulses, which is formed by multimode superposition.

No excitation of the echo from ferromagnetic metals via interaction of the eddy currents with static magnetic field (as in normal metals) is observed at high field intensities, H, and low temperatures.

Experimental observations[70] of the excitation of ultrasonic waves by RF fields in Ni indicates that this direct process does not play a significant role in Ni, but that it is present in other 3d metals at high field intensities. An attempt was made to observe an echo, produced by the direct process, from Co powder in high field intensities (up to 50 KOe) at 4.2°K. The echo amplitude passes through a maximum at 5-6 KOe (magnetostrictive excitation) ($H \perp h$) and disappears at approximately 15 KOe. No further echo is observed at high field intensities (Figure 4.31).

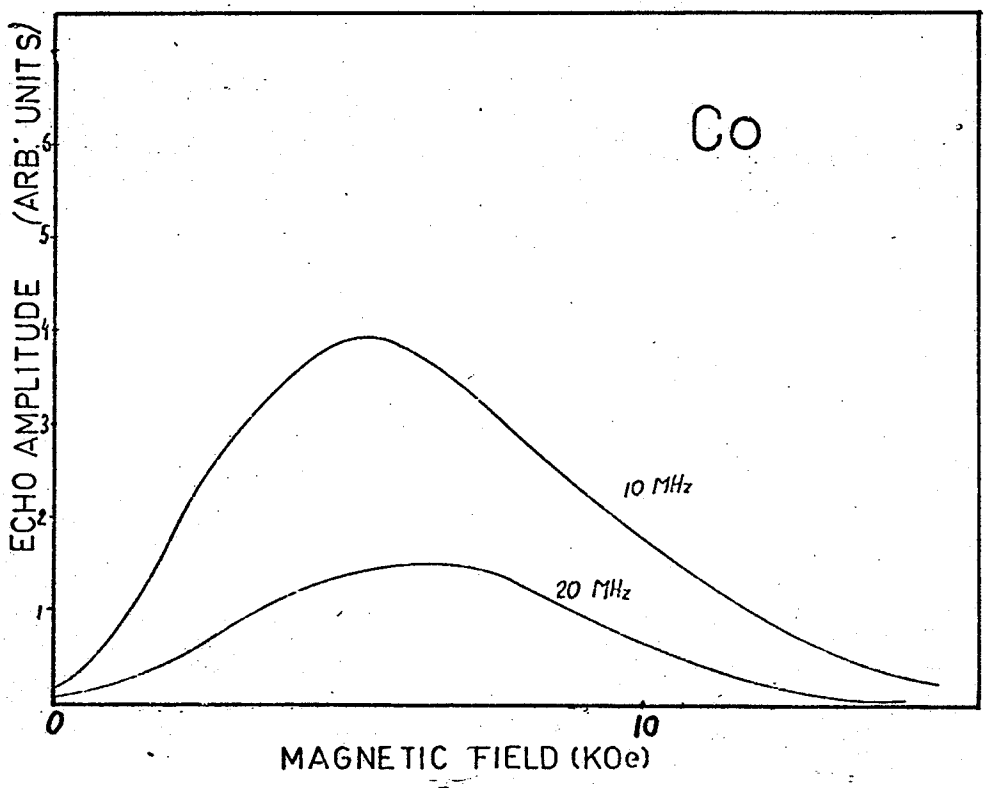

Figure 4.31 Echo Amplitude as a Function of the Biasing Field (4.2°K)

The echo amplitude, as a function of H, is strongly affected by the sample's mechanical or thermal history. Samples filed from bulk material have a reasonably strong echo amplitude, in zero applied magnetic field. After annealing this initial echo amplitude drops to zero. Figure 4.32 shows the echo amplitude for a deformed and an annealed Fe sample. Proper annealing of Ni was not possible, since annealing at 400°C sintered the particles and force was required to separate them. Ni annealed at 350°C for 10 hours still showed a weak echo in zero biasing field. No thermal treatment of RCo_5 materials was performed (except for hydrogen diffusion) These materials are notoriously good gas absorbers and oxidize quickly.

Annealing also reduces the amplitude of the echo for the optimum biasing field. This supports the view that the actual details of magnetization change are responsible for the echo.

A similar effect is observed in both Fe and Ni powders.

Excessive deformation of the powder completely eliminates the echo in all deformable powders.

The dependence of E_1 (H) on the magnetic history can also be seen in Fig. 4.32 where the echo amplitude is traced for the increasing (up), decreasing (down) and opposite polarization of the H (up reverse).

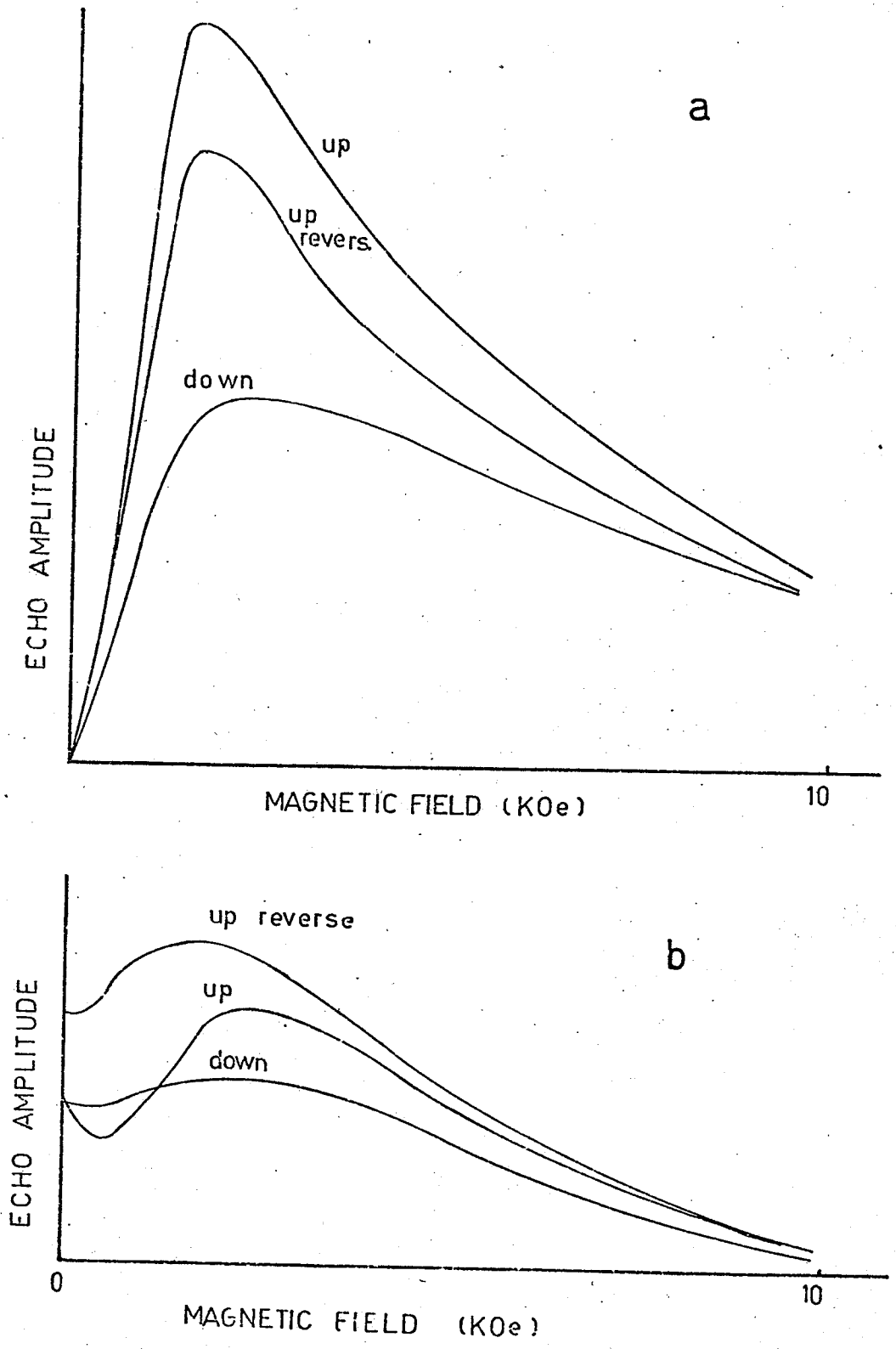

Figure 4.32 Echo Amplitude as a Function of the Biasing Field in Fe ($77^{o}K$) (a) Annealed (b) Deformed (scale of a is magnified 10 x)

The dependence of E, on the biasing field is more pronounced for cubic materials (Fig's. 4.28, 4. , 4.32) than for the hexagonal (Fig's. 4.31, 4.33).

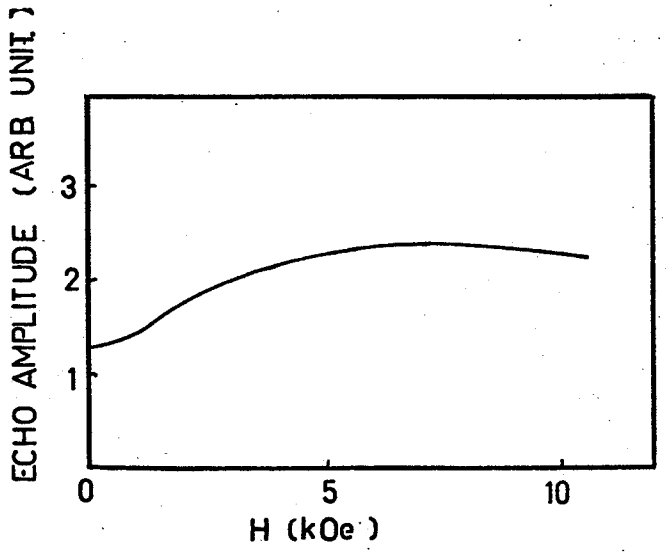

Figure 4.33: Echo Amplitude for YCo_5 as a Function of H (10MHz, 77°K).

C2 The dependence of the relaxation time, T_1 on the biasing field.

T_1 depends on both the temperature and the biasing field. The dependence of T_1 on H for annealed Ni for various temperatures and frequencies is shown in Fig. 4.34. The T_1 vs H dependence is sensitive to the history of the sample. The T_1 vs H for annealed and deformed Ni is shown in Fig. 4.35. The annealed and deformed sample has a coercive field H_c of 33 Oe and 95 Oe respectively.

A similar dependence of T_1 on H is observed in all metals, i.e. the relaxation time is constant at low fields H, increases with increasing H and saturates as a sample approaches its magnetic saturation. T_1

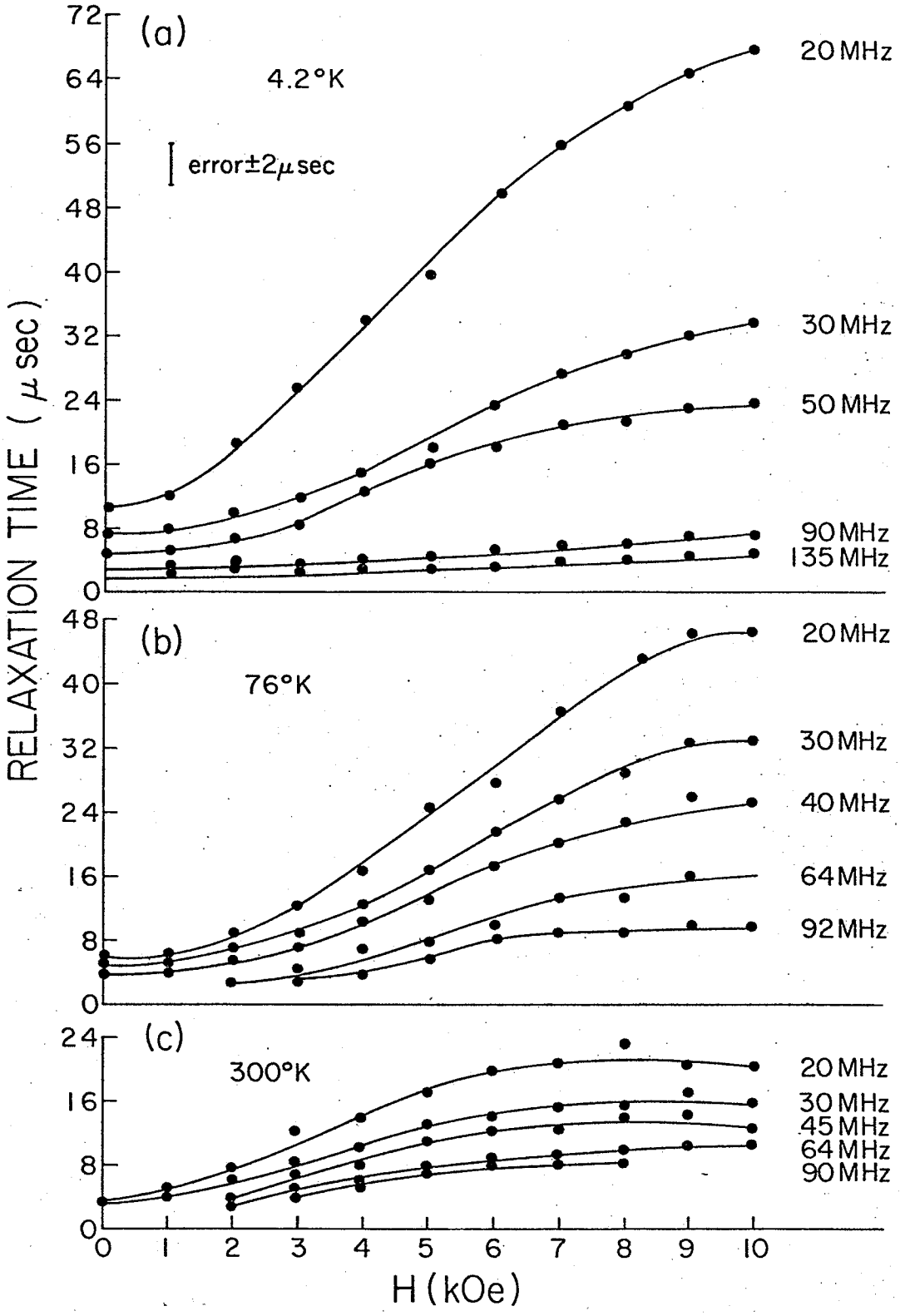

Figure 4.34: Relaxation Time as a Function of Biasing Field (Annealed Ni)

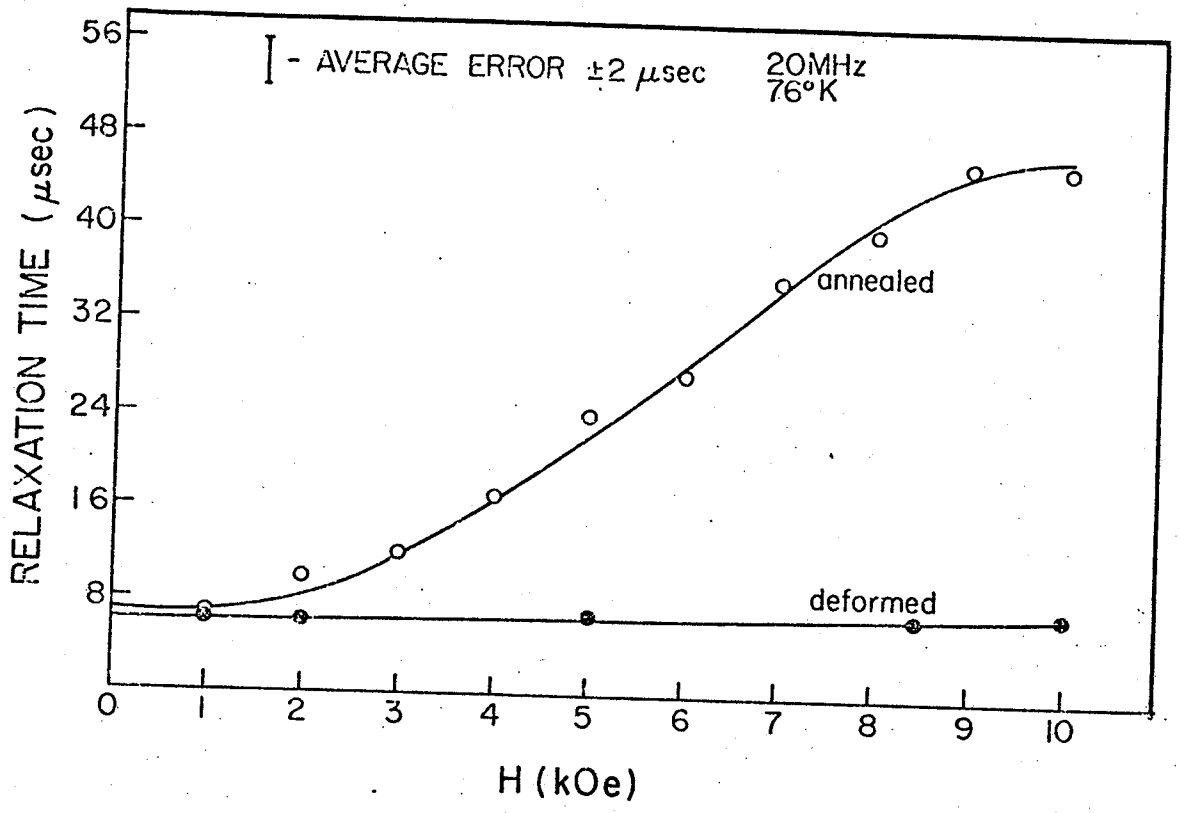

Figure 4.35: Relaxation Time as a Function of the Biasing Field for Deformed and Annealed Ni Powder.

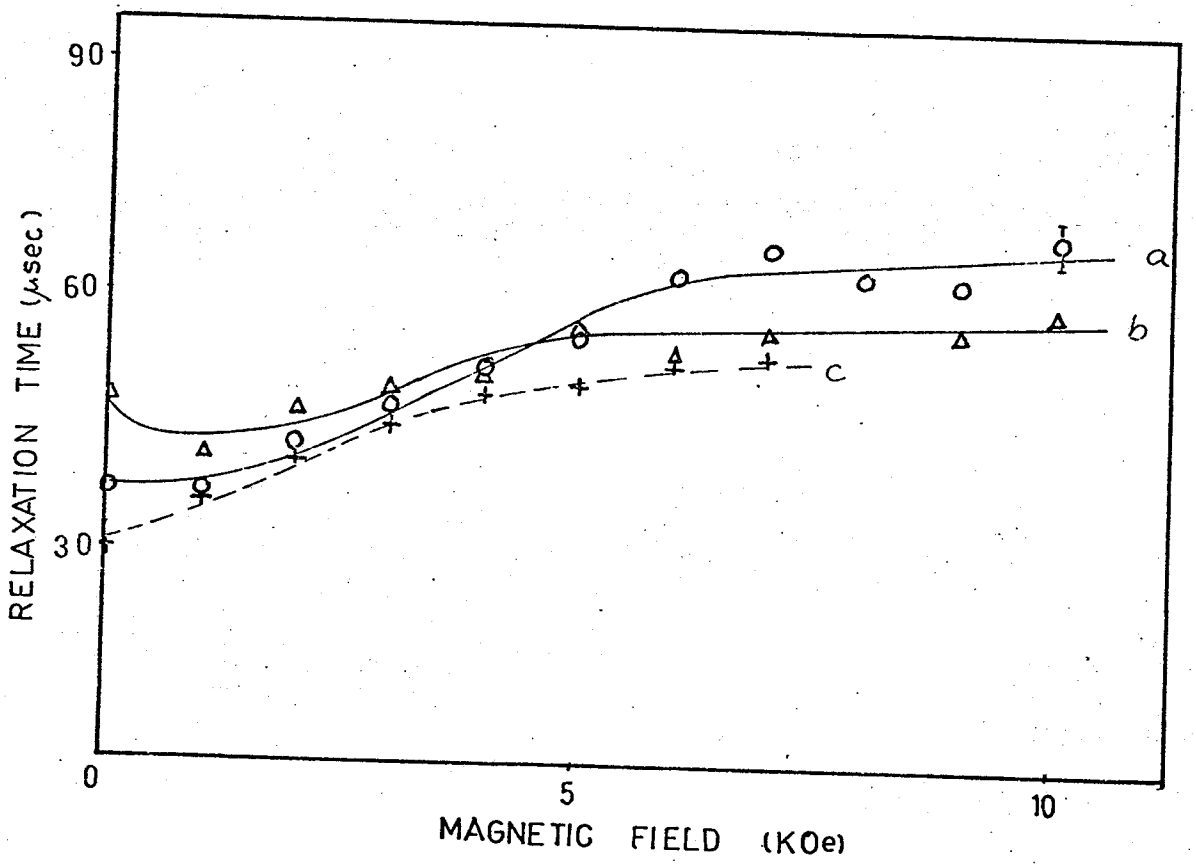

Figure 4.36: Relaxation Time of Fe as a Function of the Biasing Field. (a) 77°K annealed; (b) 77°K deformed; (c) 300°K annealed.

as a function of H for Fe (at 10 MHz) is shown in Fig. 4.36.

Hematite ($\alpha - Fe_2O_3$) also has strong magnetic losses which disappear at saturation.[71,72] The relaxation time of the echo from $\alpha - Fe_2O_3$ powder and also the decay of the induction from the few big particles (≈ 3 mm) excited by one pulse is shown in Fig. 4.37. The echo is observed in a biasing field internal of 400 Oe to 2000 Oe.

Ferrites: All the samples were commercial cores of unknown composition.# They all have a very short relaxation time which is field independent Fig. 4.38.

The relaxation time of all samples is independent of the strength of the RF pulses.

C3 Temperature dependence of the echo

As has already been seen, the echo amplitude depends strongly on the degree of the magnetization of the sample. The same degree of the magnetization at different temperatures requires the presence of a different H. therefore monitoring the echo amplitude as a function

#Footnote: A particular ferrite, data of which are shown in Fig's 4.30, 4.31 and 4.38 has a composition 46% Fe, 18% Ni, 0.12% Co, 0.03% Mn and oxygen as estimated by the electron microprobe analysis (weight %)

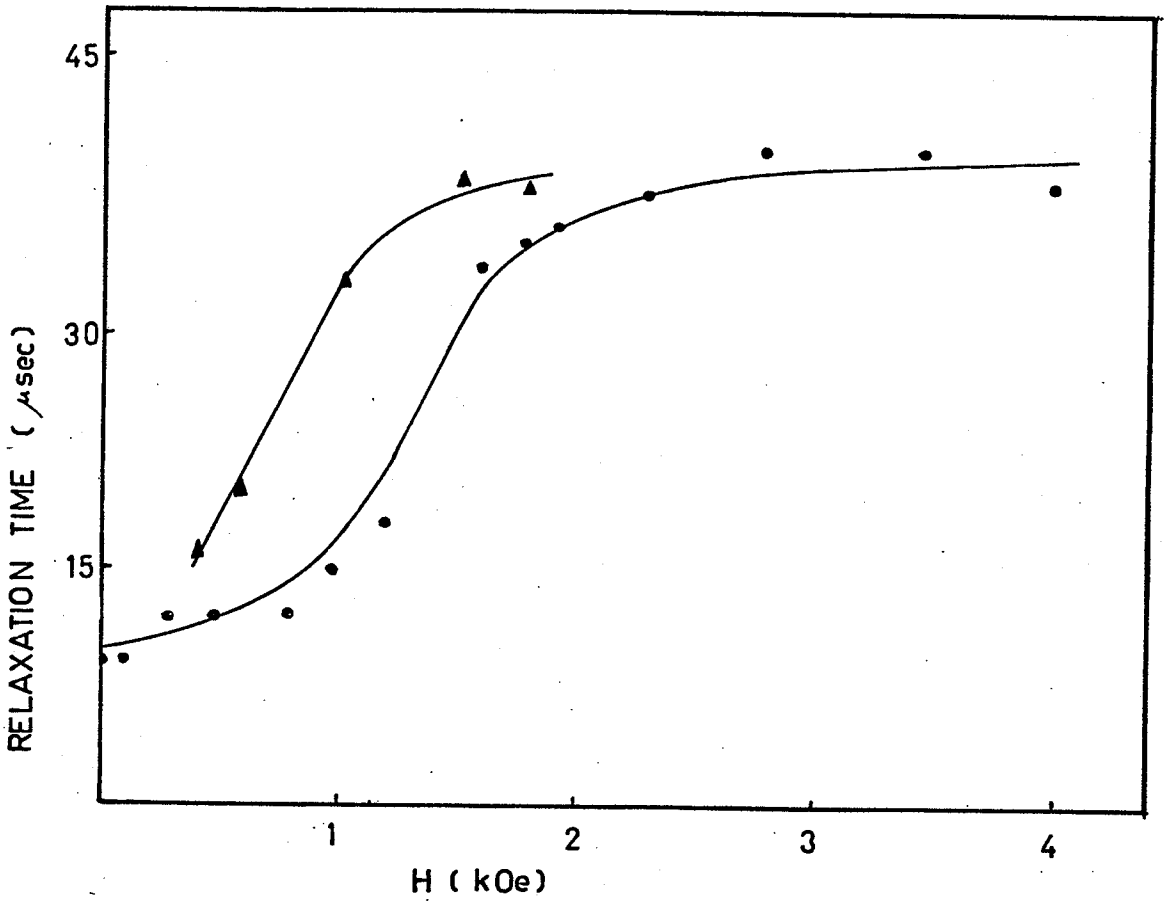

Figure 4.37:- Relaxation Time of the Free Induction (●) and an Echo (▲) as a Function of H for $\alpha - Fe_2O_3$ (10MHz, 293°K).

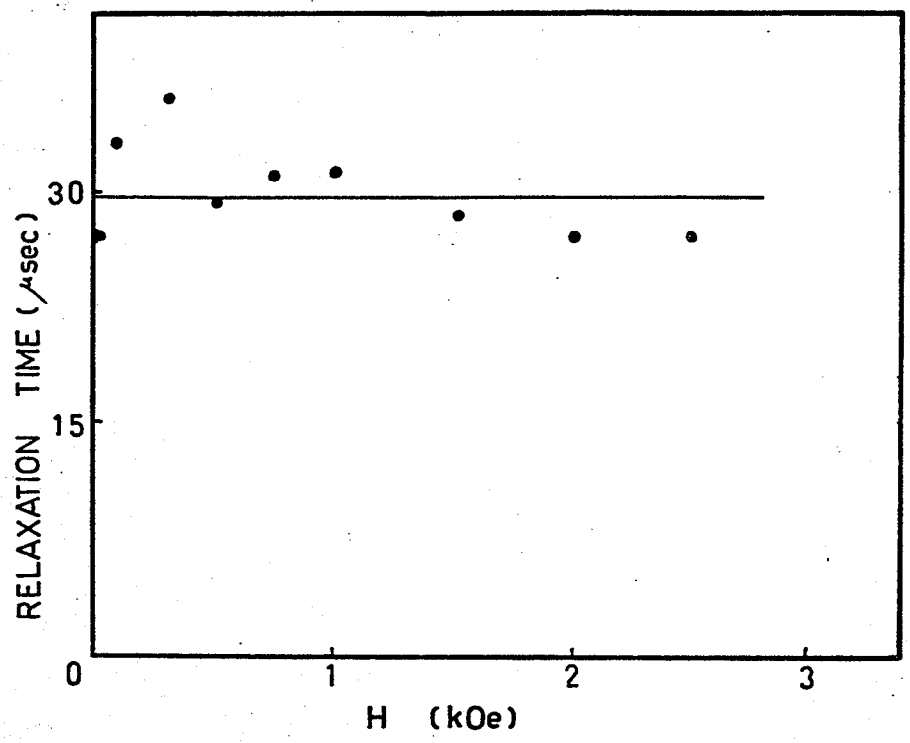

Figure 4.38: Relaxation Time of the Ferrite Powder as a Function of H (77°K, 10 MHz).

of temperature for a constant H has only a qualitative character. However, the echo amplitude decreases strongly with temperature in Co, y Co_5 or ferrite whose magnetic properties are only weakly temperature dependent in the temperature range below room temperature. For example, no echo is observed from Co at room temperature. This is illustrated in Figure 4.39 where the echo amplitude for a constant delay is monitored as the sample is warmed up. At low temperatures no significant change of the echo amplitude is observed. While for ferromagnetic metals the echo increases slightly (in optimal biasing) as the temperature decreases, for ferrites the echo maximum occurs, at 150°K. No change in the range 1.5 - 4.2° K is observed.

C4 RCo_5 Compounds [65,66]

Two samples of Y Co_5 and $NdCo_5$ were prepared by crushing. Both samples showed properties identical with those from ferromagnetic metals, with a relatively weak echo amplitude. In addition, both these samples showed a very strong magnetic aftereffect and some anomalous behavior which will be described in this section.

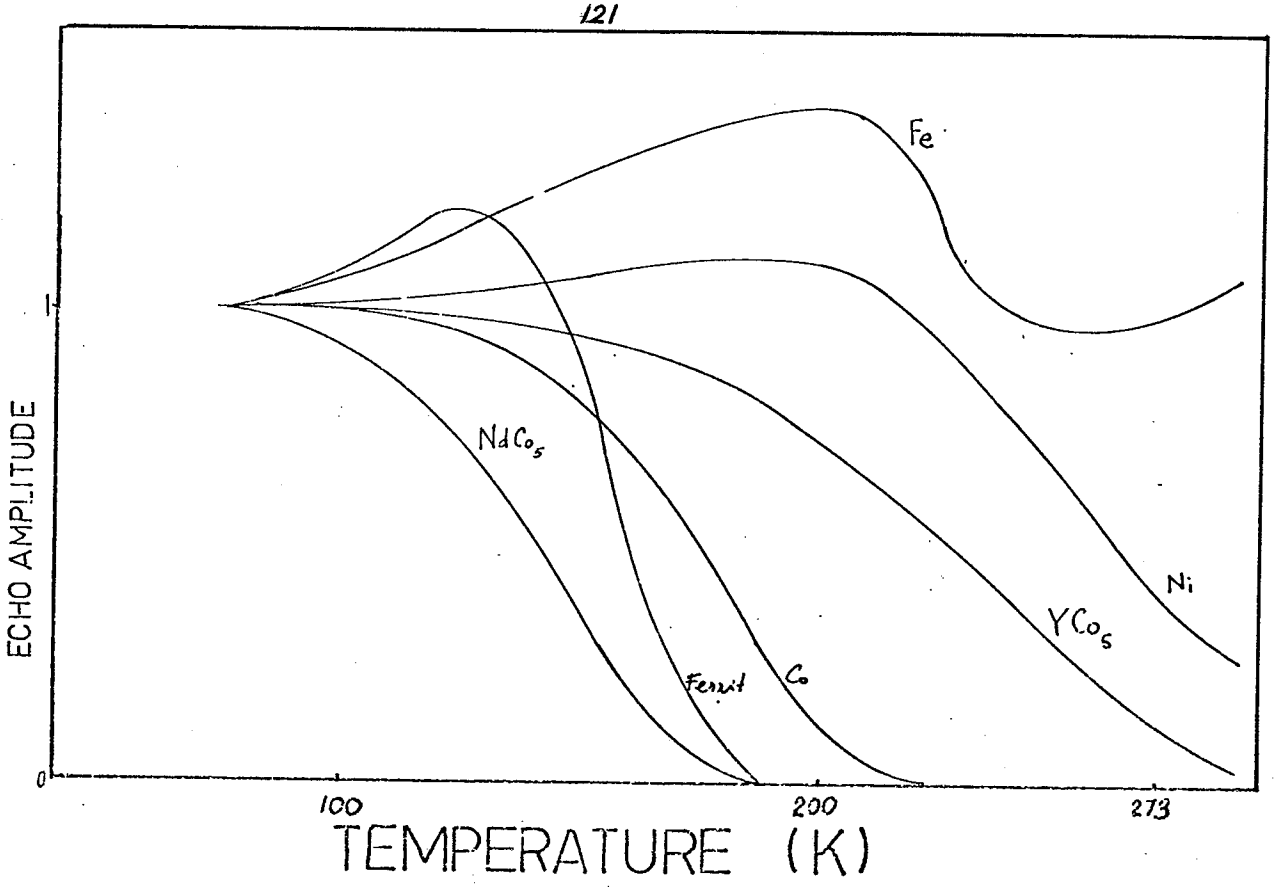

Figure 4.39: Echo Amplitude as a Function of Temperature for Various Materials (10 MHz)

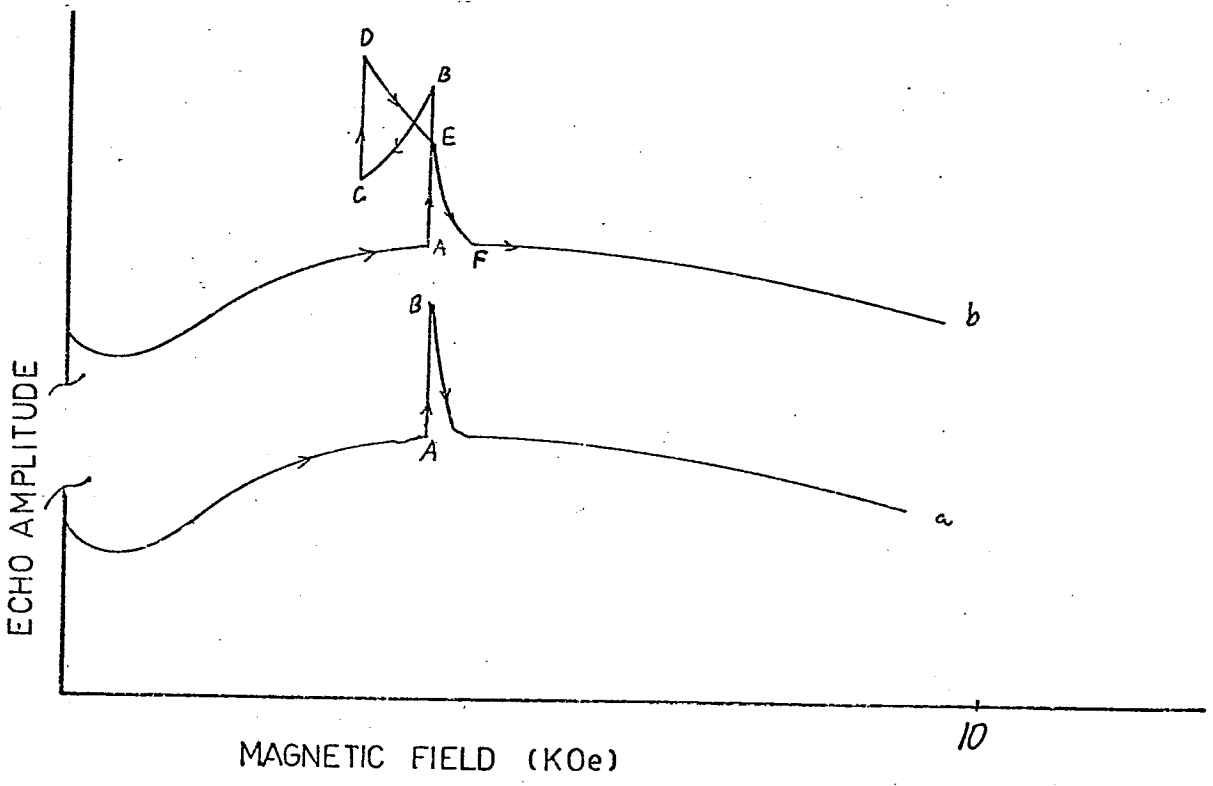

Figure 4.40: Echo Amplitude as a Function of Sweep Speed of Biasing Field (See Text). ($NdCo_5$, 10MHz, 77°K, $\frac{dH}{dt} \approx 33$ Oe/sec)

(a) The amplitude of the echo from both samples at 77°K was dependent on the sweep speed of the biasing magnetic field H(Figure 4.40). Curve a is the echo amplitude for a certain $\frac{dH}{dt}$. When the sweep is stopped (Point A) the echo amplitude increases with time. Continuing the sweep causes the amplitude to drop to its original value.

(b) Memory of the sample (Figure 4.40 curve b). The echo amplitude during subsequent sweeps is larger. Figure 4.40 curve b represents the following sequence of events: sweep forward, stop (A) with an increase of amplitude (A-B), reverse sweep (B-C), stop (C) with an increase of amplitude (C-D), sweep forward (D-E-F).

When the field intensity reaches the initial maximum field (H_B) at E the echo amplitude suddenly drops (E-F) to the initial amplitude.

This effect is closely related to a similar decrease in the AC susceptibility[108] or NMR signal in the presence of a sweeping magnetic field, and can be observed directly on the field dependence of the shape of minor hysteresis loops[109] This effect disappeared after annealing the powder in vacuum.

A partial recovery of the effect is caused by diffusing hydrogen into the sample. (The effect of diffused D_2 on the echo amplitude from Y Co_5 is shown in Figure 4.41)

The observedaftereffect is only weakly temperature dependent as can be seen in Fig. 4.42 where the echo amplitude E, is plotted as a function of the rate of change of the biasing field.

The presence of hydrogen also affects the echo relaxation time. The changes in E_1 or T_1 due to hydrogen presence, are not reproducible. The RCo_5 samples are polycrystaline powders and their elastic properties are determined by the preparation procedure, which is not known. As an illustration of the dependence of $T_1(H)$ on the thermal treatment the $T_1(H)$ of $NdCo_5$ is in Fig. 4.43. Curve a shows the initial powder (probably containing H_2) while b shows the same powder after annealing in a vacuum (300°C 24 hours).

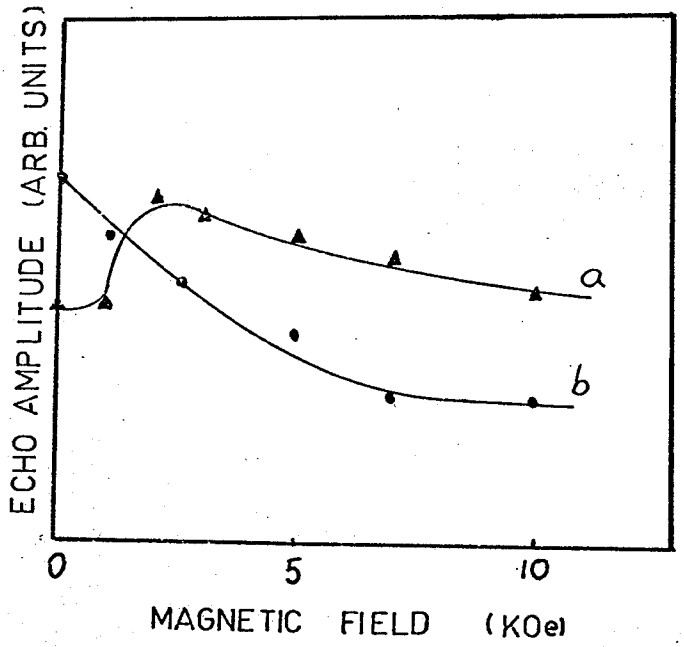

Figure 4.41: Echo Amplitude for Y Co_5 (72°K, 16 MHz) (a) vacuum annealed (b) annealed in D_2

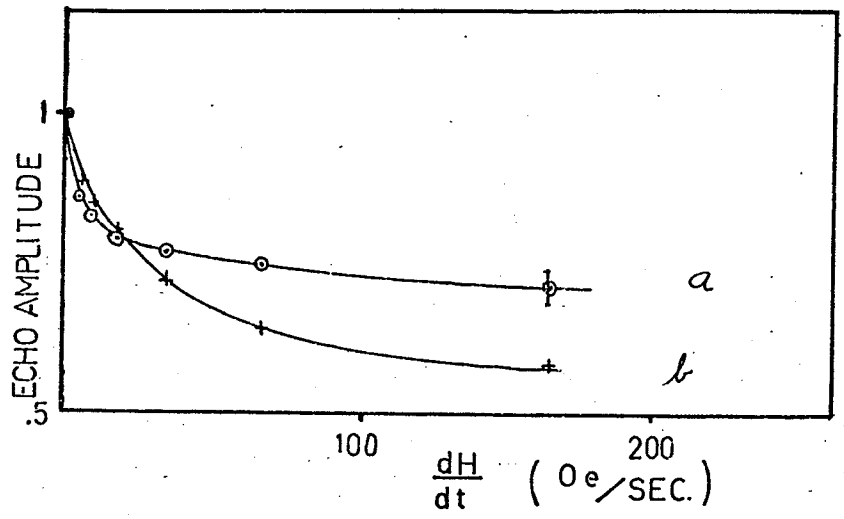

Figure 4.42: Echo Amplitude as a Function of $\frac{dH}{dt}$ (a) $300^{O}K$, (b) $77^{O}K$, (Y Co_5).

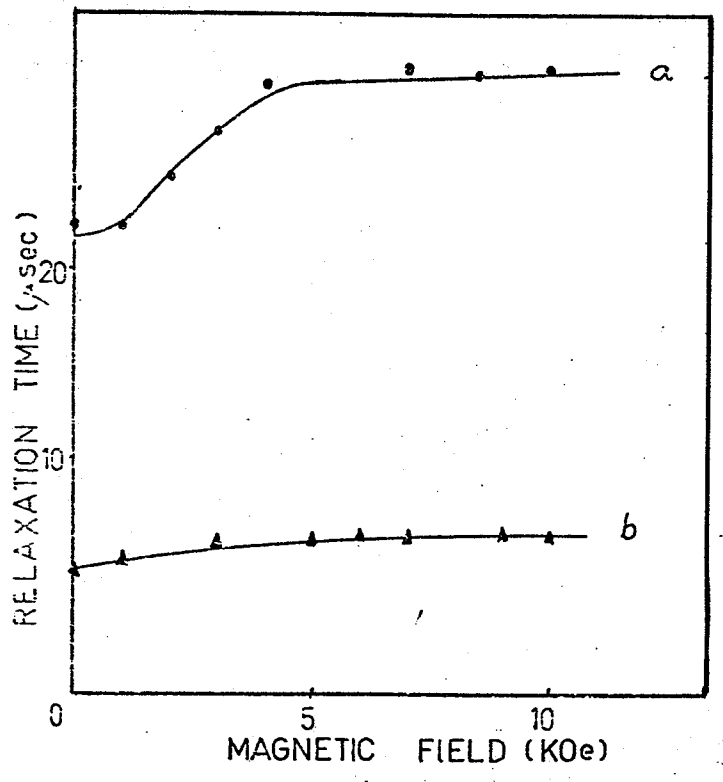

Figure 4.43: Relaxation Time of $NdCo_5$ powder before (a) and after (b) vacuum annealing (12 MHz, $4.2^{O}K$).

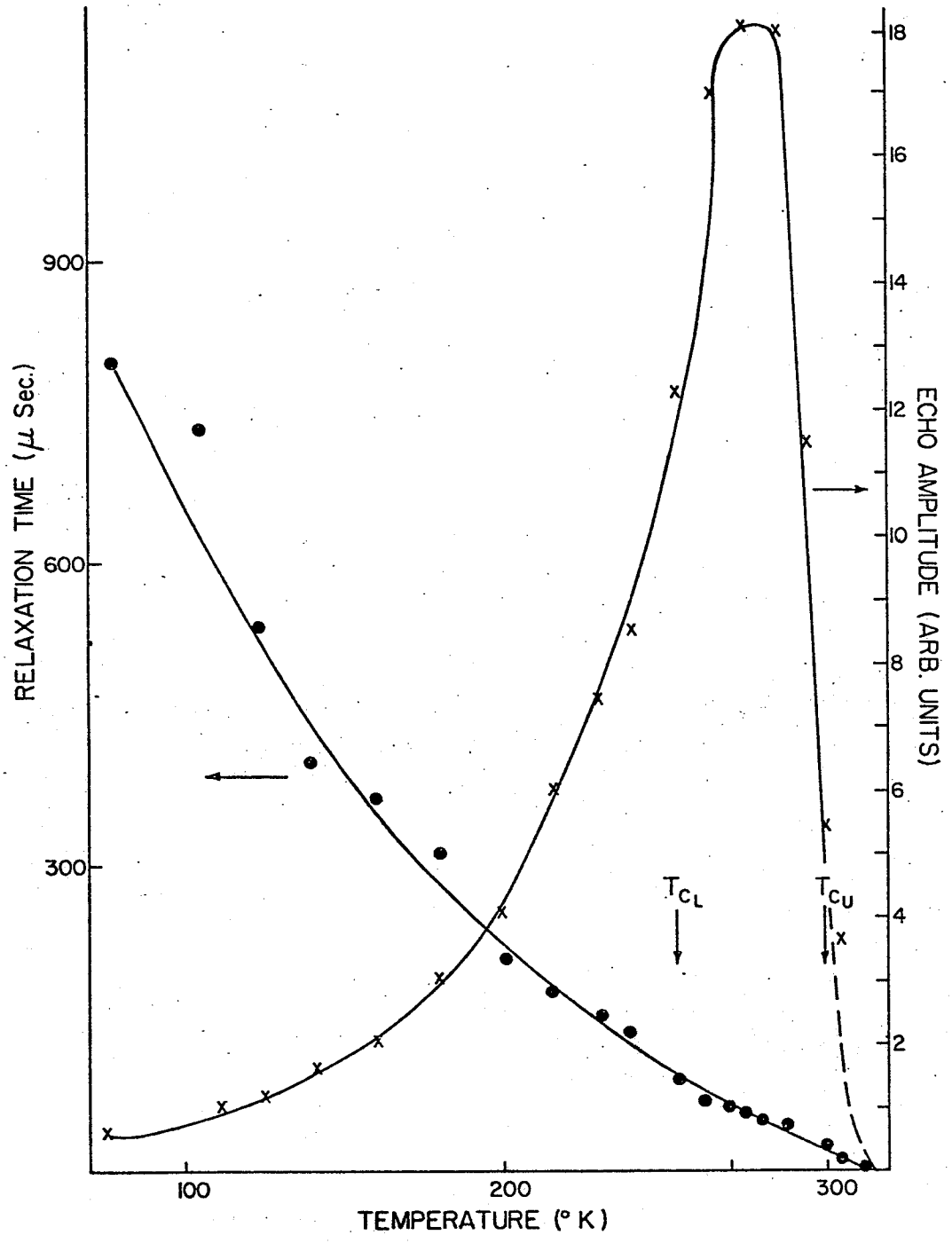

Fig. 4.44: The Amplitude (x) and the Relaxation Time (●) of the First Echo as a Function of Temperature (Rochelle Salt).

T_{CL} and T_{CU} indicate upper and lower Curie point

D The echo from piezoelectric powder:

This "group" contains only one material, Rochelle salt. The echo amplitude as a function of temperature passes through a maximum in the ferroelectric phase, Fig. 4.44. In this figure the relaxation time as a function of temperature is also plotted.[73] At low temperatures it becomes very long the longest of all materials used in this study. The echo does not require the presence of any biasing field and depends only slightly on the biasing field up to 6 kV/cm Fig. 4.45 (above 6 kV/cm during the RF pulses h $\approx$ 2 kV/cm a spark occurred between the capacitor plates).

E Determination of the Elastic Modes:

In order to distinguish between collective and single particle vibrations, the following experiments were performed.

(a) Ferromagnetic particles (Ni) were allowed to fall freely through the spectrometer coil. Ill-defined echoes were observed, clearly demonstrating the single particle character of the observed echo.

The observation of echoes from normal metal powders requires low temperatures and longer RF-pulses, therefore similar experiments using normal metal powders were not attempted.

(b) However, Al powder was mechanically vibrated at 120 Hz in the spectrometer coil, using a low RF pulse repetition rate of 30 Hz. It was expected that the vibrations reducing the coupling between particles would almost completely destroy the echo in the case of collective vibrational modes, but would not alter the echo in the case of single particle modes. Only a slight change of the echo amplitude was observed, thereby strengthening the case for the single particle modes also in normal metals.

(c) Piezoelectric powder (Rochelle salt) excited by an RF-electric field between two parallel plates produced an echo from a single layer of separate particles, demonstrating its single particle origin.

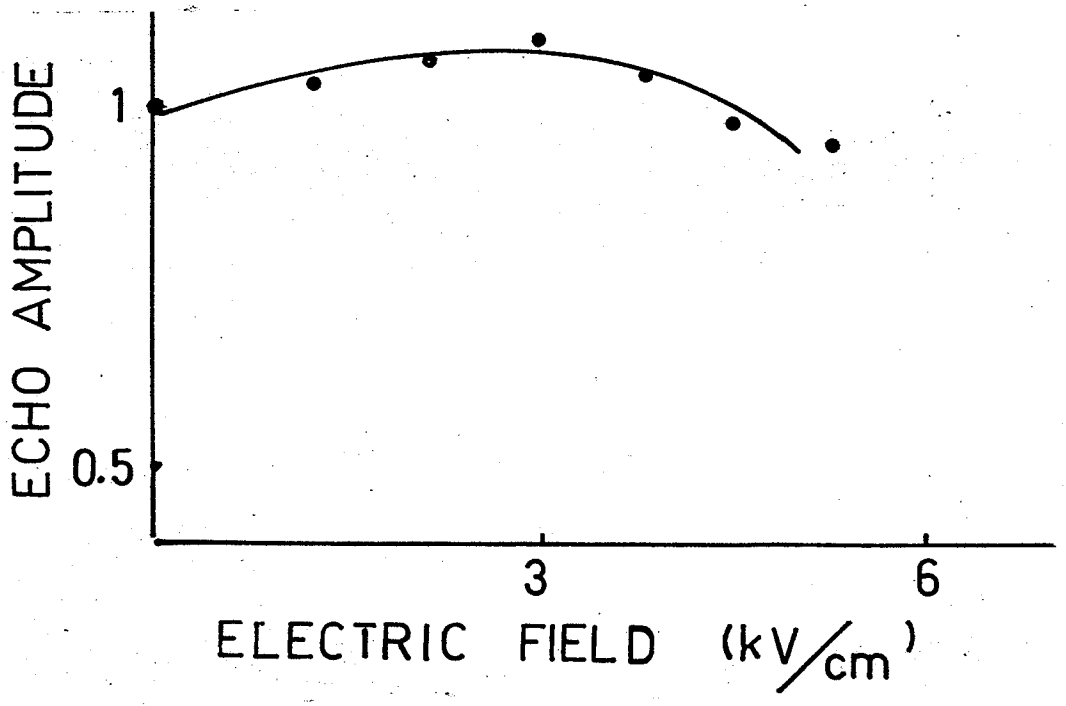

Fig. 4.45: Dependence of the Echo Amplitude, E_1, on the Biasing Electric Field (293°K, Rochelle Salt).

4.3 Discussion of the Experimental Results

It was stated previously, without any proof, that all the echo properties are consistent with the echo formation due to parametric mixing.

The following facts support this model:

α) The echo decays exponentially and the relaxation rate is not amplitude dependent, also in the few cases where a deviation from exponential decay was observed for a short pulse delay, the echoes decay exponentially in the longer time interval.

The amplitude dependent processes were simulated for a simple model of 20 Θ classes, on a computer, assuming different simple power dependences of the frequency or attenuation on the amplitude. The short time required for the echo build-up (to fit the experimental data the echo raise time must be less then 15 μsec) leads to a strong dependence of the resonance frequency W or attenuation T_1 on the amplitude, which resulted in a fast dispersion of the echo for ω(A) and to strong attenuation for T_1(A). Therefore, the assumption that the echo amplitude increases during the short time interval which is not experimentally accessible can not be correlated with the long relaxation time observed.

The independence of the echo envelope (Fig. 4.1b) on the RF pulse strength directly contradicts the amplitude dependent echo formation processes.

β) The relaxation times of the different echoes closely follow the relationship predicted for the parametric process which was derived under the assumption that the lowest possible echo formation process is dominant. i.e. The first and stimulated echoes are formed by the 3-rd and the second echo by the 5-th order processes.

(Processess in which only a few θ -classes are excited can also lead to complex echo pattern, but the relaxation rate of the different echoes is expected to be the same.)

γ) The dependence of the first echo amplitude on the strength of the RF pulses also indicates that the first echo is formed by a third order mixing process. i.e. It increases linearly with the first and quadratically with the second pulse.

Two different 3rd order processes can lead to the first echo.

a: Field dependent elastic constants (Eq. 2.24) and (Eq. 2.92) leading to an echo of the form

$$E_1 \propto dN\varepsilon x_1 h_2^2 t_{w2} \propto d^2 N \varepsilon h_1 h_2^2 t_{w1} t_{w2} \qquad (4.4)$$

where $x_1 \propto d h_1 t_{w1}$ is the amplitude of the elastic vibration due to pulse 1, d coupling between the RF field and the force acting on the particle and ε is the strength of the nonlinear term leading to the echo.

b: Amplitude dependent driving force, leading to an echo of the form (Eq. 2.33) and (Eq. 2.92).

$$E_1 \propto dN\varepsilon x_1 x_2^2 \propto d^4 N\varepsilon h_1 h_2^2 t_{w_1} t_{w_2}^2 \qquad (4.5)$$

Both lead to an identical dependence of E_1 on h_1 and h_2, but they differ in their dependence on the pulse length and on the coupling coefficient d.

The expressions above were obtained (Chapter II) under the assumption, that both the elastic amplitude x and h vary as $e^{i\omega t}$. A presence of harmonics in x or h can lead to different dependencies of E_1 on h_1 and h_2.

The experimental results are compared with the conclusions of this model with the aim of selecting between the above two possibilities and determining the physical origin of the mixing process.

Before discussing the experimental results it is worthwhile to point out the simplifications used in the derivations of the expressions above. α) the frequency difference between the elastic modes and the RF field is neglected during the RF pulses. β) The mixing term is assumed to be weak ($\varepsilon \ll 1$), γ) The amplitude of the elastic modes is assumed to be proportional to the RF pulse duration ($x \propto dh t_w$).

δ) The second pulse is assumed to be so short that the decay of the amplitude due to pulse I is negligible during the second pulse.

It is clear that a better agreement between the model and the experimental results can be expected for short RF pulses. The pulse length required for the echo formation varied for different materials, being 2-3 μsec for the ferromagnetics and piezoelectrics and $\approx$ 10 μsec for most of the normal metals.

A Common properties of the powders:

The free induction following one RF pulse (A1) is the linear response which points out α) presence of the resonance modes at the given frequency. β) presence of a coupling mechanism between the RF field and the elastic vibrations.

Free induction is not expected if the elastic mode distribution $n(\omega)$ is constant. The signal following the RF excitation is present, if $n(\omega)$ is nonuniform. The disappearance of the free induction from the smaller particles (which still show the echo) indicates that discontinuities in the mode density distribution, which is more pronounced for the large particles, is responsible for the free induction. The resonance frequencies of the particles depend on their boundary conditions.

A redistribtuion of the particles changes the fine structure of this induction signal.#

It should be pointed out that not all powder having a strong induction signal exhibited an echo under the two pulse excitation.

The exponential decay (described in part A2) of the echo is a direct consequence of its origin due to a parametric mixing. The deviations from this exponential decay at short pulse delay cannot originate from the distribution of the particles' relaxation times, because experimentaly $\frac{\partial^2 \ln E_1}{\partial t^2} < 0$ while from the distribution of relaxation times one expects $\frac{\partial^2 \ln E_1}{\partial t^2} > 0$. Possible origins of this effect are

a) Presence of higher order processes contributing to the echo.

b) Saturation of the amplitude.

c) Superposition of the echo with the free induction.

The presence of more than one echo after a two pulse excitation clearly indicates that at least 5-th and 7-th order mixing processes must also be present, and can affect the echo decay. For example, 5-th order processes; of the form $a_1 a_1^{*2} a_2^2$ or $a_1^* a_2^3 a_2^*$ contribute to the first echo and,

#Footnote: Irregularly shaped solids have a very complex mode structure as was, for example, observed by Lyall and Cochran (49).

depending on their phases, they will add or subtract to/from the basic $a_1^* a_2$ echo process. The contribution to the first echo by the process ($a_1 a_1^{*2} a_2^2$) relaxes as $T_1' = T_1/2$ and therefore it is significant only for short pulse delays.

Another physical process which can lead to a reduced efficiency for echo formation is amplitude saturation. If the first pulse is long enough for a particle to reach its saturation amplitude, the effect of the second pulse will depend on the degree of relaxation of the amplitudes of vibrations due to pulse I. This case can be present only if the echo is formed by the amplitude dependent driving force.

The change of the mechanical quality factor automatically affects the echo characteristics (A3), clearly proving that the elastic vibrations of the particles are necessary for the echo formation.

Fixing of the particles' surface (A3β,γ) eliminates the echo.

The quality factor depends on both the shape of the particles and also on the environment. For example. the echo from all filings has a relaxation time which is much shorter then from regular particles of identical materials. The relaxation time also depends on the particle size and generally decreases with decreasing size of the particles (Fig. 4.4).

The echo pattern and the ratio of the relaxation times (Tab. 4.1) is in good agreement with the expected

values $T_2/T_1 = 3/4$, $T_3/T_1 = 1/2$ (Eqs. 2.47 and 2.48).

However, the ratio of the intensities of the first and second echo is surprising. The second echo originates from higher order approximations in the solutions of the equation of motion (Eq's 2.15, 2.16) or from the independent existence of the higher order mixing terms in the system's hamiltonian. For example x^3/h^3 or x^5/h.

In the first case the higher order approximations are of higher power of ε, therefore a strong second echo would indicate that ε is not small.

In the second case it is hard to understand the same ratio between the amplitudes $E_2/E_1 \approx 0.1$ for all of the different samples.

The estimation of the order of magnitude of the parameter ε is crucial for the selecting of the echo process. A direct estimation is difficult, because of large unknown factors related to the number and amplitude of elastic modes involved in the echo formation.

It is theoretically possible to estimate ε from a direct comparison of the induction signal following one RF pulse, immediately after the end of the RF pulse with the echo amplitude. This could not be performed on our apparatus, due to the dead time of the receiver.

The lower limit on ε is $\varepsilon > 10^{-6}$ because no free induction from a few (1-10) particles is observed and a sample consisting of $\approx 10^6 - 10^7$ particles shows a strong echo.

The hyperbolical decay of T_1 with the frequency f, is a consequence of the constant Q of the particles From Eq. (2.38)

$$T_1 = \frac{Q}{\pi f}$$

In some cases T_1 decreases with f faster than expected from Eq.(2.38). This is due to the fact that at higher frequencies smaller particles resonate which have smaller Q's (Fig. 4.4)

Note on 3 Pulse Excitation :

It was mentioned in Chapter II that, for a 3 pulse excitation, the stimulated echo can be produced by two different mechanisms relaxing with different rates.

(a) phase memory (Mode a_1 and a_2 are mixed with a_3 at the time of the third pulse.)

(b) energy memory (Mode a_2 and a_2 are mixed at the time of the second pulse to form a DC mode which, after mixing with the third pulse, will contribute to an echo.)

For the phase memory process $T_s = T_1/2$, while for the energy memory process no such relation can be established and because the energy scattering process can take place only through multiphonon scattering (energy dissipation) the relaxation time in this case, can become very long at low temperatures. This is observable from bulk samples.[12] In the powder samples $T_s \simeq T_1/2$ is well satisfied in the entire temperature range $1.5^{\circ}K$ - $300^{\circ}K$ and therefore, the energy process does not play any significant role in powders.

Dependence of the Echo on the Pulse Length:

The dependence of the echo shape (A6) on the length of the RF pulses is complex.

The echo amplitude does not increase with pulse duration for pulses $\geq 10\mu$sec for any sample. This is clearly a consequence of the finite Q of the particles and indicates a limitation of the model.

For very short pulse lengths, the variation of their length also varies their amplitude (no square pulse) and therefore it is impossible to select between the two possibilities of the echo formation described by Eq. 4.4, 4.5).

The complex echo pattern (Fig. 4.8) is probably due to excitation by transients at the beginning and the end of the RF pulse which acts as additional RF pulses with a wide band width. Fig. 4.46.

Variation of the echo amplitude with pulse separation (Fig.4.10) is a consequence of the nonuniform distribution of the phases of the particles' vibrations at the time of the second pulse. The noncoherent pulse generator starts each pulse with the same phase, therefore a slow increase of the pulse delay varies the relative phase between the RF pulses. Particles coherently excited by pulse I will be fully defocussed at the time $t_0 \geq Q/f$

$$t_0 \approx \frac{10^4}{10^7} \approx 10^{-3}\,sec$$

For $t < t_0$ the oscillators phases are nonuniformly distributed and therefore echo formation depends on the relative phase of pulse I and II.

A weak echo is excited by a long first and a short second pulse which suggests an amplitude dependent force is responsible for the echo origin.

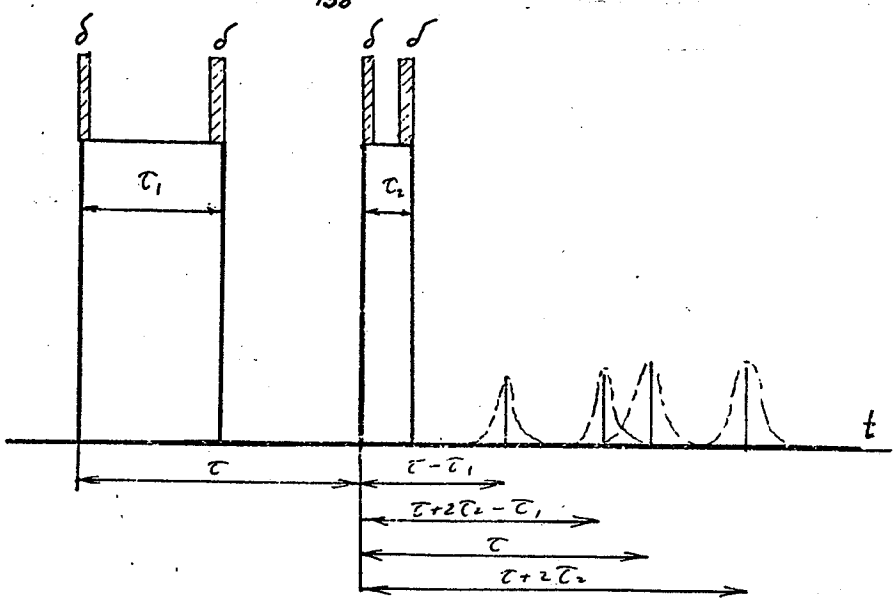

Figure 4.46 Modulation of the Echo Shape by the Transients.

The first pulse saturates the oscillators and therefore the response to the second pulse is limited.

In the case of the echo formation of the field dependent elastic constants, saturation would not affect the interaction between the RF field and elastic vibrations.#

The variation of the echo amplitude with the strength of the RF magnetic or electric pulses (A6) corresponds to the expected dependence for the third order mixing process. ($h_1 h_2^2$) at low intensities.

In the large intensity range the variation is much more complex and cannot be described by a simple power dependence $h_1^\alpha h_2^\beta$ (α, β constants). The linear dependence between the echo amplitude and the intensities of the RF pulses for $h_1 = h_2$ (Fig. 4.13) does not agree with any known echo model.

#Footnote: This however is not a convincing proof, because the length of RF pulses affects the number of oscillators excited.

The echo spectrum shows a relationship between the particle size and the frequencies range in which it can be observed (Fig. 4.15)

As can be seen in Fig. 3.2 no definitive limits can be put on the particles' size in any sample. Regular Ni particles, Fig.3.2b show an echo at 14MHz and very weak one at 10MHz. The size of these particles is $\approx$ 50 ± 20 μm., this leads to the estimation for the velocity of sound (1.4 ± 0.6) x 10^5 cm/sec, which is far less than for bulk Ni which is 3.10^5 cm/sec for the shear and 5.10^5 cm/sec for longitudinal vibrations. The observations above indicate that the elastic constants of the particles are reduced or that more than one particle is involved in the elastic vibrations. The latter contradicts the experimental evidence described in section E.

No dependence of the echo amplitude on the repetition rate was observed in this study. The origin of the inital increase of E_1 from a fresh sample is probably due to aligning of the particles in the sample in such a way that a maximum number of particles can resonate. Once the echo is established its amplitude is independent of the repetition rate.

Pacult et al (16) reported the disappearance of the echo for a repetition rate less than $\approx$ 1 Hz and suggested that this is a consequence of collective

vibrations and that a certain minimum repetition rate is required to maintain them in the sample. However, the repetition rate 1Hz still represents an "infinite" internal between the pulse sequence, because the relaxation times of the echoes are in the order of $10 - 10^2$ μsec.

B The echo from normal metals:

The driving force in metals Eq.(2.94) is proportional to both the intensity of the RF-magnetic field, h, and the static magnetic field, H,. Therefore it is not surprising that the presence of a static magnetic field is necessary for the excitations of the free induction and the echo.

The coupling coefficient, d , in this case is proportional to H, therefore from the dependence of E_1, on H one can distinguish between the two possible echo mechanisms.

The modulation of the elastic constants by h leads to an (Eq. 4.4)

$$E_1 \propto \varepsilon d^2 h_1 h_2^2 \propto \varepsilon H^2 h_1 h_2^2 \tag{4.6}$$

while the amplitude dependent force leads to (Eq. 4.5)

$$E_1 \propto \varepsilon d^4 h_1 h_2^2 \propto \varepsilon H^4 h_1 h_2^2 \tag{4.7}$$

where it is assumed that the coefficient, ε , describing the echo process is independent of H.

The second echo is expected to vary with H as

$$E_2 \propto h_1^2 h_2^3 H^6 \tag{4.8}$$

for the amplitude dependent force and

$$E_2 \propto h_1^2 h_2^3 H^3 \tag{4.9}$$

for the field dependent elastic constants.

The experimental evidence is inconclusive. As can be seen on Figs. 4.17 and 4.19 the dependence of the echo amplitude on H depends on the relative intensity h_1 and h_2 as well as on the magnitude of H. and for a constant ratio h_1/h_2 it also depends on the material (Fig.4.18). At low field intensity the observed dependence of $E_1(H)$ is $E_1 \propto H^4$. As was mentioned earlier for $h_1 = h_2$ the $E_1 \propto h$. From this empirical relationship it follows that $E_1 \propto h H^2$ this is the dependence reported by the aforementioned authors (Refs. 14, 16,20)#

#Footnote: All previously reported experiments used $h_1 = h_2$.

The free induction follows the H^2 dependence as expected ($\alpha^2 h \propto H^2 h$).

A clear experimental distinction between these two possible forms of the parametric interaction leading to either $E_1 \propto H^2$ or H^4 could be made with an experimental arrangement where the second RF pulse is applied without the presence of the DC field (H). In such a case only a mixing due to the field dependent elastic constants can lead to an echo.

The temperature dependence of the echo amplitude:

The amplitude of the vibrations excited by the volume force

$$\vec{F} = \frac{1}{c} \vec{\delta} \times \vec{H}$$

depends on the distribution of the eddy currents and therefore depends on the electrical resistivity ρ, of the powders. The actual relationship between the amplitude x and ρ is very complex. Generally the amplitude decreases with increasing ρ. In the macroscopic approximation the excitation process depends on the material only through its resistivity and therefore is identical for all good conductors and depends on a/Δ where a is the size of particles and Δ the skin depth.

The variation of ρ with temperature in all metals is similar. It can be expressed by a universal curve $F\,(T/T_D)$ on a reduced temperature scale T/T_D, where

T_D is a characteristic constant for a given material closely related to the Debye temperature (Bloch — Gruneisen Law[74]),

i.e.

$$\rho(T/T_D) = F(T/T_D) \qquad (4.10)$$

No one material exactly follows this relationship. To fit the experimental data of $\rho(T)$ to $F\ (T/T_D)$ it is necessary for T_D to be temperature dependent.

However, the observed deviations are small. Tab. 4.2 shows the Debye temperature for the samples used in this study.

Because the Lorentz force depends, for similarly shaped particles, on their electrical resistivity only, the vibrational amplitude for all metals is expected to behave identically on the reduced scale T/T_D. Thus the measurement of E_1 as a function of the temperature can reveal information about ε.

Table 4.2: Debye Temperature of the Normal Metal Samples

Material	T_D(°K)	Material	T_D(°K)
Ag	225	Cu	343
Al	428	Mg	400
Au	165	Mn	410
Cd	209	Zn	327
Cr	630		

Namely, if ε has a purely geometrical origin, i.e. it originates in the particle vibration and is material independent, then the echo should be observed from powders of all good conductors and the temperature dependence on the reduced scale T/T_0, will be the same. This is not the experimental case.

The samples used can be divided into two groups: one, containing Al, Cu, Zn in which the echo amplitude decreases gradually with increasing temperature. And Mg, Cr in which the echo decreases very fast at low temperatures. A special case is Ag, which does not show an echo at H = 10 KOe for any temperature.

In the first group, the echo amplitude is constant at low temperatues, where the resistivity of the metal is constant (residual resistivity) and then gradually decreases with increase in temperature. The actual dependence is size and frequency dependent, as expected. (both factors change the a/Δ ratio, where a is the particle size)

The faster decrease of E_1 with temperature for Au then for Cu or Al in Fig. (4.24) can be understood from their different T_D (Tab. 4.2). $\rho(T)$ for Au relative to Cu should be scaled by a factor of 2 in temperature.

Assuming that the thermal component of the resistivity is dominant, one can calculate the skin depth Δ as a function of temperature. This is done in Fig. 4.47 for Au and Cu (at 10 MHz) using the resistivity measurements by White and Woods.[76] The thermal component of the resistivity is dominant at higher temperatures.

The temperature dependence of the echo from alloys is similar to that from pure metals. i.e. Al Mn behaves like Al. The echo from Ag Mn varies with temperature in the same manner as that from Al or Cu.

Contrary to expectations, Mg showed an anomalous strongly temperature dependent echo amplitude at temperatures below 4.2°K (Figure 4.25).

The temperature dependence of the echo from various samples leads to the conclusion, that ℓ (Eq. (4.4, 4.5)) is material dependent. Ag is the only sample in which the echo is enhanced by the addition of impurities. In addition, the temperature dependence of the echo from Ag Mn 0.05% is similar to other pure metals (Al, Cu). Therefore, it was natural to assume that for some reason the "pure" Ag is not pure but has a large resistivity, This does not seem to be the experimental case.

The lack of an echo from Ag cannot be explained by accidental impurities (for example, oxygen) since the Ag samples were highly pure and some were also annealed in H_2 gas (400°C). This rules out a simple explanation that impurities (Mn) enhance the echo in Ag by purification of the host through internal oxidation. In the entire temperature range no echo was observed (H = 10 KOe) from Ag doped with less than 1% In, Au, Cu. However, Ni and Mn both enhanced the echo. All our results agree with those reported by Snodgrass[20] who observed an echo at a fixed frequency of 4MHz. In addition, the relaxation time is independent of impurity concentration since it is completely dominated by surface losses and decreases with frequency. Increasing the amount of impurities gradually reduces the echo, which disappears for c > 0.15% Mn in Ag (c is the percentage of Mn actually put in the alloy). No chemical analysis was performed on the samples. This cut-off arises because of the increase in resistivity with impurity concentration ($\Delta\rho/c \approx 7 \mu\Omega cm/\%$)[77] in the alloy.

The echo enhancement cannot be correlated with any other properties of Ag Mn alloys and is contradictory to the impurity effects in the other materials.

The following properties of dilute Ag Mn alloy are reported: Mn in Ag has a magnetic moment corresponding to S = 5/2,[78] and

it orders (anti ferromagnetically) at low temperatures [79]. (Due to the RKKY interaction). The spin dependent resistivity shows a Kondo behavior[80] with $T_K \approx 0.1^oK$[78] and there is no reason to expect anomalous properties for high temperatures ($T > 20^oK$).

Many authors, however, have observed anomalies in thermal conductivity[81], magnetic properties[82], or NMR line breadth.[83] This has been claimed to be the result of internal oxidation[83] or impurity clustering.[82]

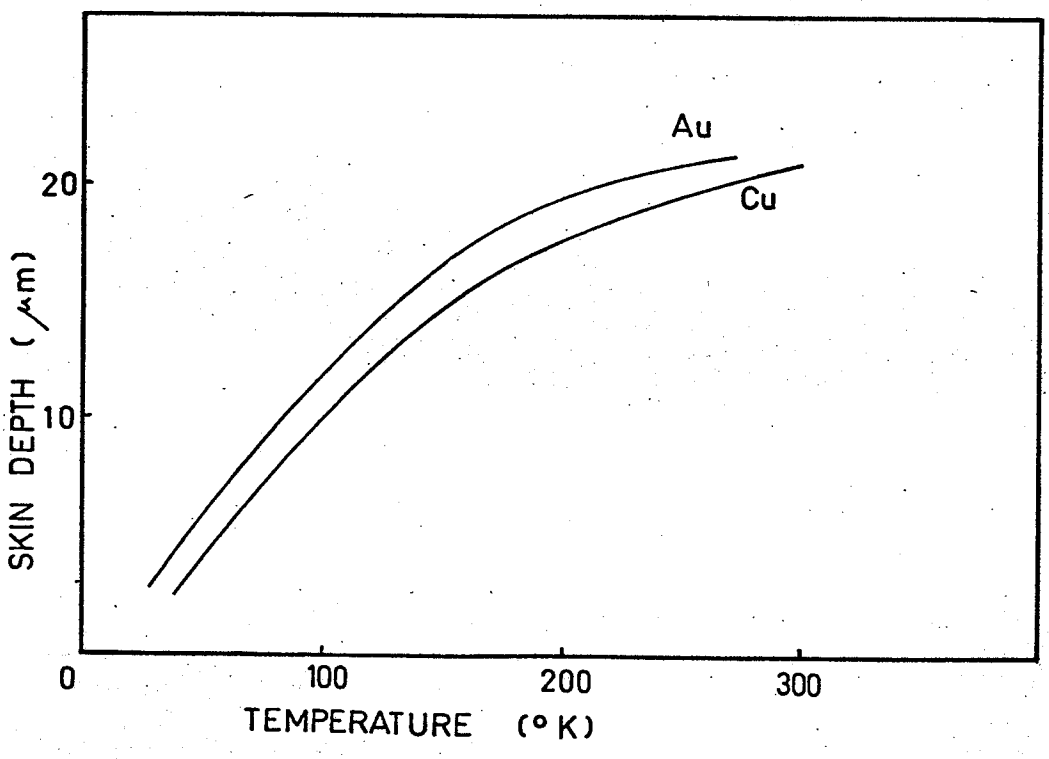

Figure 4.47: Skin Depth Δ as a Function of Temperature (10MHz).

The reduction of the echo amplitude with alloying or deformation in other materials is equivalent to a change of the temperature, i.e. it reduces the echo through an increase of the resistivity.

The gradual increase of the echo amplitude with annealing time for Al Mn (Fig. 4.27) can be explained the same way. Substituted Mn has a strong effect on aluminum's electrical resistivity [86] ($\Delta\rho/c \approx 3\mu\Omega cm/\%$) and therefore the strong variation of resistivity is related to the aging process.

The slight increase of the relaxation time T_1 after annealing in Al powder can be explained by an increase of the Q factor by annealing due to the removal of the dislocations introduced by deformation.

T_1 in other samples is fully determined by the irregular shape and does not reflect any intrinsic property.

The reduction of the relaxation time at large H is a consequence of the losses by induced eddy currents.

The vibration of a particle in the presence of H is equivalent to a stationary particle in a variable field $\mathcal{H}$ (in normal metals $B \cong H$)

$$\mathcal{H} = \mathcal{H}_o e^{iwt} \propto Hu(t) = Hu_o e^{iwt} \qquad (5.9)$$

where u(t) is a surface displacement.

The proportionality factor in Eq. (5.9) depends on the shape and vibrational mode of the particle and the geometry of the experiment.

The induced eddy currents, j, in the particle are proportional to $\mathcal{H}_0$. The dissipated energy E_D is proportional to j^2 and hence $\mathcal{H}_0^2$ #.

The logarithmic decrement δ is defined by (Eq. 2.39) as the ratio of the energy dissipated per cycle ($\approx j^2 \propto \mu_0^2$) to the total energy ($\approx \mu_0^2$) therefore the logaritmic decrement δ_H is amplitude independent. The relaxation time of the oscillators is

$$T_0 = \frac{1}{f(\delta + \delta_H)} = \frac{1}{f(\delta + kH^2)} \qquad (4.12)$$

δ_H is expected to decrease with increasing a/Δ ratio. This can be seen in Fig. 4.48 where

$$\frac{1}{f}\left(\frac{1}{T_{1\,H=50\,Oe}} - \frac{1}{T_{H=0}}\right) \qquad (4.13)$$

is plotted for different frequencies(Fig 4.26)

For illustration, the relative energy loss for a spherical particle as a function of a/Δ is shown in Fig. 4.49 (Normalized to 1 for $a/\Delta = 10$).

The angular dependence of the echo amplitude shows that the maximal amplitude of the echo occurs

#Footnote: For simple shapes the problem can be solved exactly (85).

when H ⊥ h. In this geometry the transversal vibrations are preferably excited.

Origin of the echo:

For large amplitudes of vibration almost any system can produce some nonlinearity which can lead to an echo. The similar properties of the echo from all metals suggest that the echo has the same origin in all samples.

In the macroscopic approximation the driving force can be modulated only through the modulation of the eddy currents (or mass density, which is unlikely).

This can be due to particle deformation (affecting the path of the eddy currents) or due to modulation of the specific resistivity of the material by vibrations.

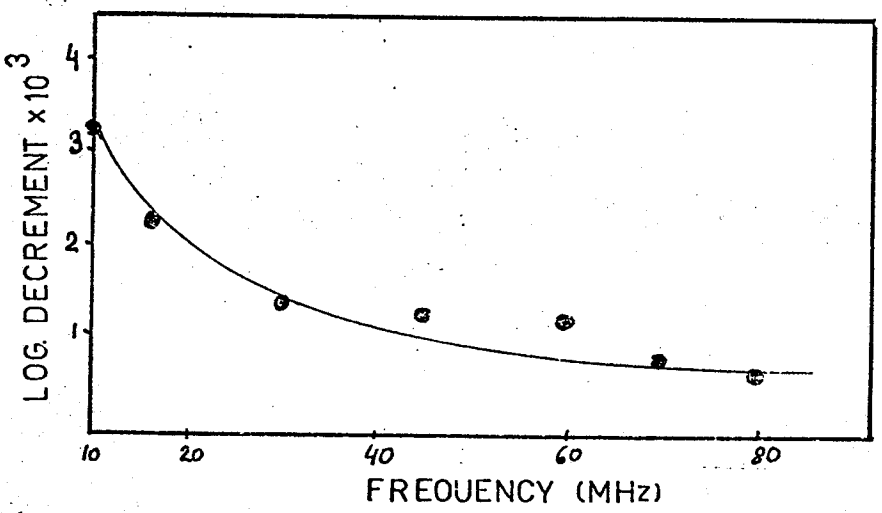

Figure 4.48 Magnetic Contribution to the Loss for Al Powder as a Function of Frequency.

$$(\delta_E = \frac{1}{f}\left(\frac{1}{T_{1H=50KOe}} - \frac{1}{T_{1H=0}}\right)$$

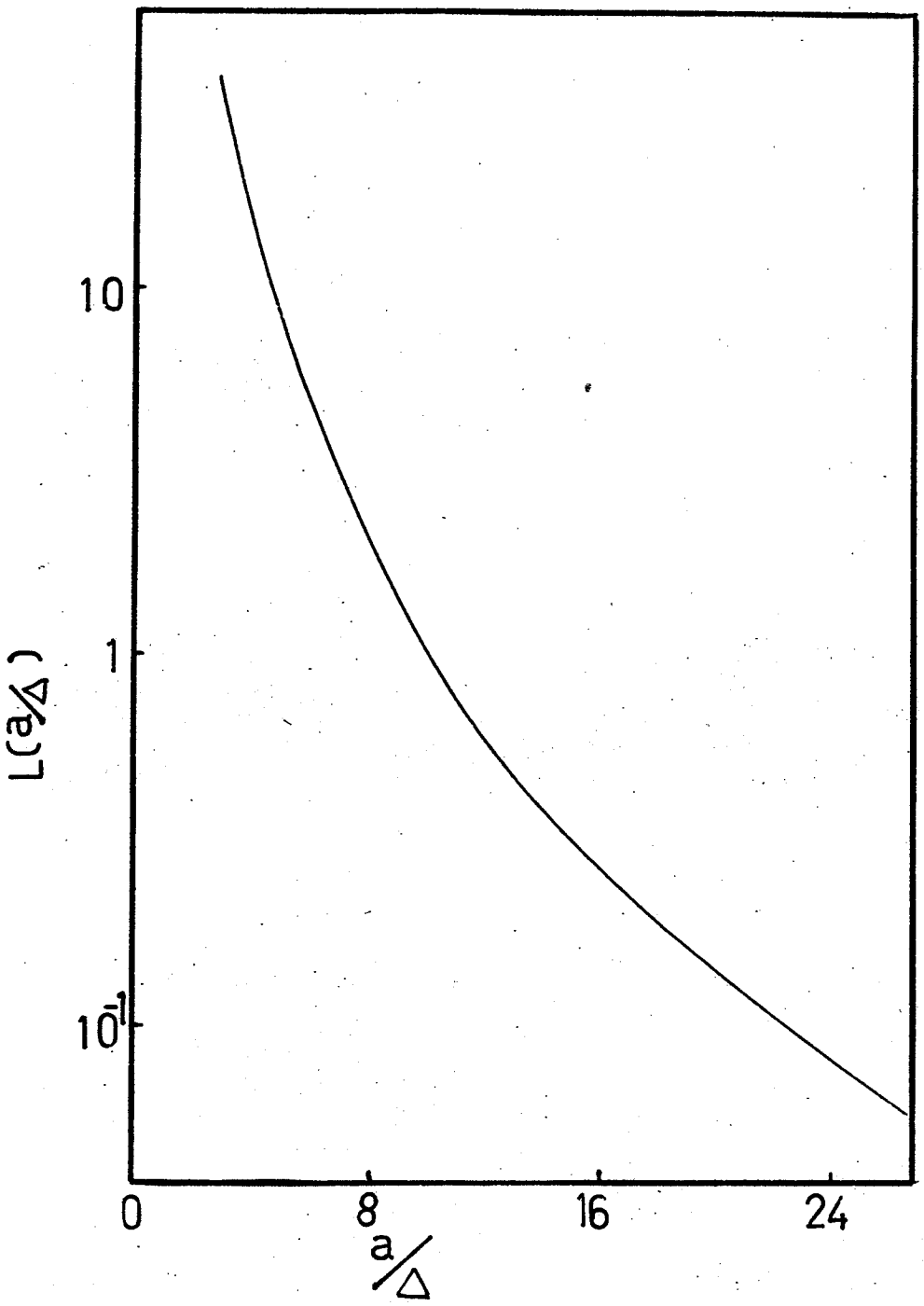

Figure 4.49 Plot of Losses $L(a/\Delta)$ For Spherical Particle.

Modulation of the elastic constants by the Rf field can also lead to an echo. The first and last processes are not sensitive to the material, apart from its resistivity and therefore, if they are responsible for an echo, it should be present in all good conductors.

The second process, i.e. modulation of the specific resistivity by the deformation, can be sensitive to the material. Tab. 4.3 lists the stress dependent coefficient of the resistivity for the noble metal groups,[86] $\frac{1}{\rho_0}\frac{\partial \rho}{\partial \sigma}$. The specific resistivity can be written in form

$$\tilde{\rho}(\tilde{\sigma}) = \tilde{\rho}_0\left(1 + \frac{1}{\rho_0}\frac{\partial \rho}{\partial \tilde{\sigma}}\tilde{\sigma} + \frac{1}{2}\frac{\partial^2 \rho}{\partial \tilde{\sigma}\partial \tilde{\sigma}}\tilde{\sigma}\tilde{\sigma} + \cdots\right) =$$

$$= \tilde{\rho}_0\left(1 + \tilde{\rho}_1\tilde{\sigma} + \tilde{\rho}_2\tilde{\sigma}\tilde{\sigma} + \cdots\right) \qquad (4.14)$$

The specific resistivity is a tensor, but for cubic materials it is a scalar and ρ_1 has only two independent components $\rho_{1,\parallel}$ and $\rho_{1,\perp}$ index indicates relative direction of the current and elastic stress.

Table 4.3

Piezoresistivity Coefficients For Noble Metals[86]

Material	Inverse Elastic Modulus $1/E_M$ ($cm^2/dyne$)	$\left(\frac{1}{\rho_0}\frac{\partial \rho}{\partial \sigma}\right)_{\parallel} \cdot 10^{10}$	$\left(\frac{1}{\rho_0}\frac{\partial \rho}{\partial \sigma}\right)_{\perp} \cdot 10^{10}$
Au	$0.81\ 10^{-10}$	1.25	-2.4
Ag	$1.26\ 10^{-10}$	2.86	-0.04
Cu	$1.25\ 10^{-10}$	3.87	-4.8

Instead of the stress dependent resistivity it is convenient to introduce the strain dependent resistivity $\varrho(e)$. In the simple one dimensional case.

$$\varrho_1(e) = E_M \varrho_1(\sigma) \tag{4.15}$$

From Tab. 4.3 one can see that $\varrho_1(e)$ differs strongly for $\perp$ and $\parallel$ directions and $\varrho_1(e)$ is of the order of unity for Au and Cu and two orders magnitude less for Ag.

The equation of motion has the form

$$\ddot{e} + \omega^2 e \propto \vec{F}(e,t) \propto \frac{\vec{j}(e) \times \vec{B}}{c} \tag{4.16}$$

where $j = j_0(e)\,(e^{i\omega t} + c.c)$.

The relationship between the resistivity $\varrho(e)$ and force $\vec{F}(e,t)$ is not clear, because j is distributed through the volume of the particles and therefore the relationship between $\vec{F}(e,t)$ and the Lorentz force $\frac{1}{c}\vec{j} \times \vec{B}$ is not known.

The modulation of j by the shape variation leads to the same echo as a modulation of the specific resistivity.

Note: The echo can be formed only if the right side of equation (4.16) contains a term in $j_0(e)$ varying as $e^{i2\omega t}$. For example, if $j_0(e)$ contains a component proportional to e^2, or $\varrho_1(e) = \varrho_1(-e)$ as in the case of transversal vibrations.

The modulation of the elastic constants, C by the RF field is described by

$$C = C_0(1 + \varepsilon h^2) \tag{4.17}$$

therefore the equation of motion has the form

$$\ddot{e} + \omega^2(1 + \varepsilon h^2) = F(h) \propto dh \tag{4.18}$$

The force on the right side does not contribute to the echo and therefore Eq. (4.18) is identical to Eq. (2.15).

None of the mechanisms described above can definitely be selected as responsible for an echo. The resistivity variation in the higher order approximations is not known.

The modulation of the eddy currents by the variation of shape of the particles is expected to be similar for particles of the similar shape and the same is true about the variation of the elastic constants. Thus the experimental evidence suggests, that modulation of some internal variable cause the echo in most cases.

As far as the magnitude of the different effects is concerned the $\varsigma_1(e)$ is of the order of unity (Tab 4.3). i.e.

$$\varsigma(e) = \varsigma_0(1 + e) \tag{4.19}$$

the same is true about the change of the surface resistivity due to change of the shape.

$\varsigma_2(e)$ or higher terms are not known. The variation of the elastic constant is approximately $C - C_0 \approx 10^{-6}$ [53] at $h \approx 10^4$ Oe . i.e. ε in Eq. (4.18) is of the order of 10^{-14}. All these effects are too weak to lead to the strong echo experimentaly observed.

Probably the origin of the echo must be sought in a microscopic model for the excitation of acoustic waves. However, the microscopic model has not been solved for a real material and therefore a further discussion of possible nonlinearities is premature.

Properties of the members of the noble metal group are similar, and it is doubtful that a simple model can distinguish between its various members.

Torque acting on the particles (Eq. 2.93) was recently proposed as the excitation mechanisms in connection with the collective modes of the vibrations.[16] The authors proposed collective modes to explain the echo from particles smaller then the critical size ($a < \frac{v}{\lambda}$, where v is the velocity of sound and λ is the acoustic wavelength and a is the radius of the particles). Interaction between particles is necessary for the introduction of the restoring force to maintain the vibrations.

For the collective vibrations one expects that

a) The increasing regularity of the particles' shape will reduce the echo amplitude (less interaction). The opposite is true.

b) Rigid motion of the particles is insensitive to their intrinsic properties, that is, in the case of

the collective vibrations the relaxation time cannot reveal any information about the volume energy loss of the particles. This point is inconclusive. Filings have short relaxation time and no really regular particles were used in this study. The small differences in the relaxation time for annealed and deformed Al are just outside of the experimental error.

In extremely pure materials, in the anomalous skin effect region, the elastic vibrations can be excited in the absence of an external field H, because phonons can be generated by surface scattering of the electrons.[87,88] It is possible that in this region an echo can also be observed without presence of H. Echoes similar to these reported here were observed from superconducting powders in a magnetic field[9] ($H < H_{c_2}$). This echo was discussed in terms of the vibrational modes of fluxoids. This echo can also be explained through processes analogous to those in other normal metal powders. In materials with a large resistivity in the normal state, direct echo excitation is weak but it suddenly increases as the material becomes superconductive. Since the AC conductivity of a superconductor is finite but large, the transition suddenly enhances the excitation process.

C The echo from ferromagnetic materials:

As in normal metals both echo processess described by Eq's (4.4) and (4.5) are possible. The RF field is coupled to the particles by the piezomagnetic coefficient, d, which is highly nonlinear and depends on the microscopic distributions and pinning of ferromagnetic domains and domain walls.

The dependence of the elastic modulus, E_M, on the external magnetic field (ΔE_M effect) is also closely related to the domain dynamics. $\Delta E_M = E_M(H) - E_M(0)$ typically is of the order of 10^{-2}-10^{-1}.[56] Therefore the frequency shift is considerable and probably different particles are tuned into resonance at different stages of magnetization.

Formally the force, produced by the interaction of h on the particle is expressed through the stress, σ, which follows from the dependence of the free energy of the particles V on the strain e and magnetization M. V can be expandended in a Taylor series of the form

$$V = V_0 + \frac{\partial V}{\partial \tilde{e}}\bigg|_0 \tilde{e} + \frac{1}{2}\frac{\partial^2 V}{\partial \tilde{e}\,\partial \tilde{e}}\bigg|_0 \tilde{e}\,\tilde{e} + \cdots \qquad (4.20)$$

where the coefficients of the expansion can be written in the form.

$$\underbrace{\frac{\partial^n V}{\partial \tilde{e}\cdots\partial \tilde{e}}}_{n}\bigg|_0 = \tilde{B}_{M2}\vec{M}\vec{M} + \tilde{B}_{M4}\vec{M}\vec{M}\vec{M}\vec{M} + \ldots \qquad (4.21)$$

i.e.

$$V = V_0 + (\tilde{B}_{12}\tilde{e} + \tilde{B}_{22}\tilde{e}\tilde{e} + \cdots)\vec{M}\vec{M} + (M^4) \qquad (4.22)$$

The magnetization, M can be expandent in powers of the external field h.

$$\vec{M} = \vec{M}_o + \tilde{\chi}_1 \vec{h} + \tilde{\chi}_2 \vec{h}\,\vec{h} + \ldots \qquad (4.23)$$

where $\tilde{\chi}_1$ is the susceptibility tensor and $\chi_2 \ldots \chi_m$ are higher order susceptibility tensors. Assuming $h = h_o e^{i\omega t}$ and substituting Eq. (4.23) into Eq. (4.22) leads to

$$V = V_o + (\tilde{B}_{12} e + \tilde{B}_{22} \tilde{e}\,\tilde{e} + \ldots)(\vec{M}_o \vec{M}_o + 2\tilde{\chi}_1 \vec{M}_o \vec{h} e^{i\omega t} + (2\vec{M}_o \tilde{\chi}_2 + \tilde{\chi}_1 \tilde{\chi}_1) h_o^2 e^{2i\omega t} + \ldots) + \qquad (4.24)$$

The stress $\tilde{\sigma}$ is obtained from Eq. (4.23) as

$$\tilde{\sigma} = \frac{\partial V}{\partial \tilde{e}}$$

This derivation illustrates, that even if one includes only the lowest term i.e.

$$\tilde{\sigma} = \frac{\partial V}{\partial \tilde{e}}\Big|_{i_o} = \tilde{B}_{12}(\vec{M}_o \vec{M}_o + 2\chi_1 M_o h_o e^{i\omega t} + \ldots \; e^{2i\omega t} + \ldots) + \ldots$$

the stress and therefore force acting on particles contains many harmonics.

Excitation of higher harmonics by the RF field in ferromagnetic substances is observed experimentally.(89) The derivation above has only a formal value, because none of the $\tilde{\chi}$ are known; they depend on the shape, size and history of the particles.

An illustration of the strong dependence of the coupling between the RF field, h, and the produced stress, σ, on the intensity of h is shown in Fig. 4.50.(90)

The dependence of the echo amplitude on the biasing field H is qualitatively similar to that of coupling constant, d.#

Ferromagnetic materials consist of fully saturated domains, each having a deformation ℓ_s. In the fully demagnetized state, since there is a random distribution of domains, the average deformation is $\ell = \frac{1}{3} \ell_s$ (cubic case). A redistribution of the domains leads to a change in the value of ℓ and in the saturated state $\ell = \ell_s$. Displacement of 90° or 71° domain walls leads to a net change in the deformation, while that of 180° walls has no effect. In polycrystalline materials different types of domains, initially equally distributed, disappear at different degrees of saturation M/M_s (M_s is the saturation magnetization) as can be seen from Table 4.4.

#Footnote: d is an 3-order tensor, $\tilde{d}$, relating $\tilde{\ell}$ to $\vec{h}$ but because the whole discussion is only qualitative, it is assumed that d is scalar.

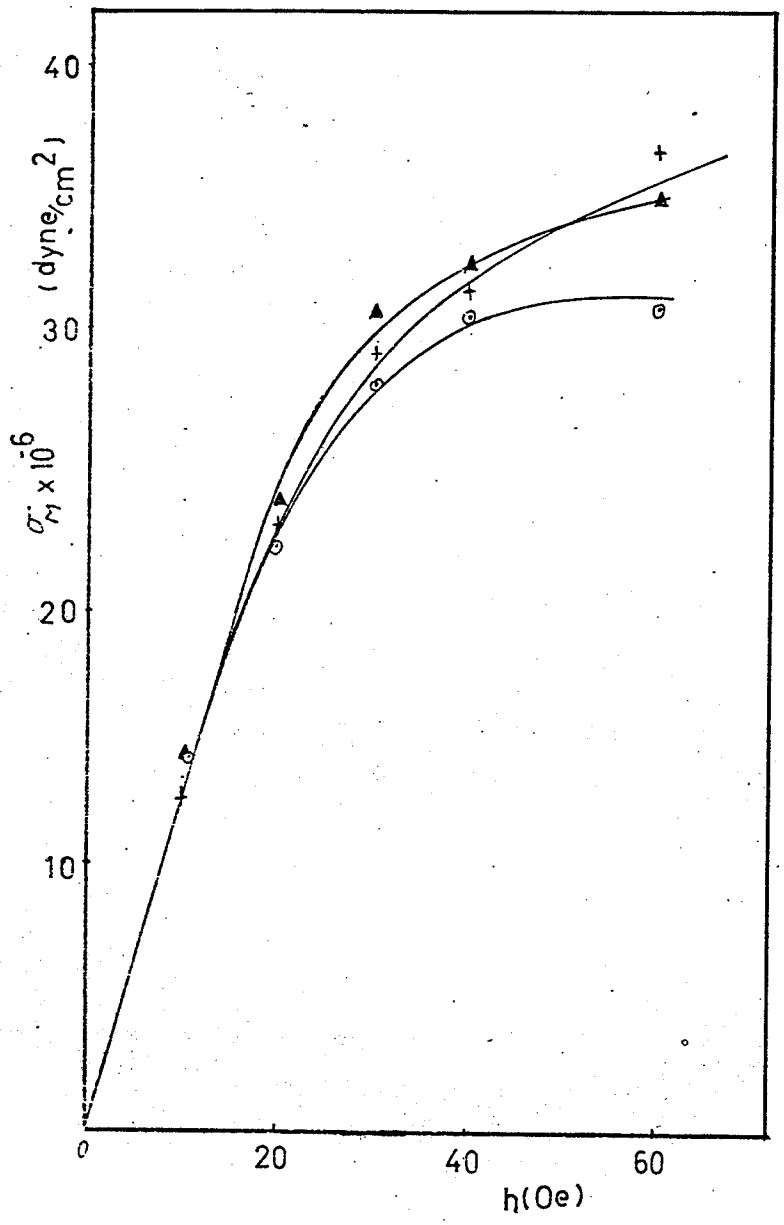

Figure 4.50 Magnetostrictive Stress Amplitude σ_M as a Function of RF Field for Different Biasing Induction B (after (90)) (o 2KG, x 3KG, ▲ 4KG)

Table 4.4[57]

M/M_s Values for Disappearance of Different Types of Domains (For Polycrystalline Cubic Material <111> Easy Axis)

Angle of Wall	M/M_s
180	0.5
109	0.79
90	0.85
71	0.91

d is related to the differential magnetostriction, therefore, one expects the excitation to be weakest at low induction and strongest close to saturation (0.7 - 0.9 of M_s) where all 180° domains are removed and the magnetization process continues through magnetization rotation and/or displacement of other walls and ℓ varies strongly with H.

For example, d(Eq.2.102) for domain rotation is

$$d = \frac{3\lambda M_s}{K_1} \qquad (4.26)$$

where λ is the magnetostrictive constant and K_1 is an anisotropy constant.

The variation of strain with H is discussed by Chikazumi.[57] The dependence of d on H varies with domain arrangement in that d is small in the demagnetized state, peaks close to saturation, and drops to zero if all domain walls are removed. If the external RF-field, h, is perpendicular to H then excitation is possible, beyond saturation, by magnetization rotation. and decreases as $\frac{h}{H}$.

The field dependence of the echo amplitude is less pronounced fromthe uniaxial materials (Co, YCo_5) Figs. 4.31 and 4.33 than for the cubic materials (Ni, Fe, Ferrite Fig's 4.28, 4.32 and 4.30.). In uniaxial materials only magnetization rotation leads to net magnetostriction; in cubic materials both the magnetization rotation and domain wall motion lead to the elastic excitations. Direct comparison of the degree of magnetic saturation with the echo amplitude, Fig. 4.28, indicates that magnetization rotation is dominant also in cubic materials.

In order of strength, the echo was strongest from Ni followed by ferrites, Fe, Co, RCo_5 (at optimal bias H and at $77^{O}K$).

α-Fe_2O_3 produced an echo only in the ferromagnetic region (above $260^{\circ}K$).

A strong echo from Ni can be expected because Ni has a large λ and small K_1 (Eq. 4.26). YCo_5 on the other hand has a large K_1. The echo amplitude as a function of H for Ni, Fig. 4.28, can be compared with the field dependence of the electromechanical coupling coefficient k, Fig. 4.51 which is defined as a ratio of the magnetoelastic energy to the geometrical mean of the magnetic and elastic energy

$$k = \frac{\tilde{d}\tilde{\sigma}\vec{H}}{((\frac{1}{2}\tilde{s}\tilde{\sigma}\tilde{\sigma})(\frac{1}{2}\tilde{\mu}\vec{H}\vec{H}))^{1/2}} \qquad (4.27)$$

where $\tilde{s}$ is the elastic constant and $\tilde{\mu}$ the magnetic permeability.

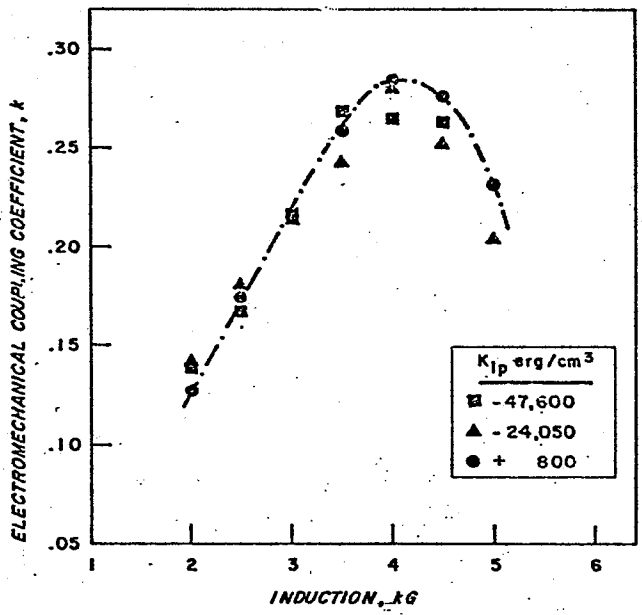

Figure 4.51 Electromechanical Coupling Coefficient k as a Function of Induction for Ni Ring (After Huston et al.(77))

The formation of an echo from a bulk sample (Fig. 4.29) is interesting. When we reported this effect originally[69] we proposed that bulk elastic modes (very high harmonics) are responsible for the echo. This conclusion was based on the fact that the echo depended on the boundary conditions of the bulk sample. A subsequent search for an echo in other bulk materials, single crystals of α-Fe_2O_3, manganese ferrite or Rochelle salt did not show an echo from bulk, while all these materials produced an echo in powder form.

This leads to the conclusion that the presence of an echo in sintered ferrite is related to its grain structure and that the echo originates from the excitation and refocussing of modes localized in the individual grains of polycrystal material. This is unexpected, because the echo relaxation time is approximately 60 μsec (at 15MHz), suggesting the Q factor is of the order 3×10^3, which means that individual grains are effectively decoupled at this frequency

A very large Q related to the high frequency resonance modes in bulk materials was reported previously from CW experiments on piezoelectric materials.[91]

The variation of E(H) with orientation is due to the large demagnetization factor of the sample.

The internal field is $\vec{H}' = \vec{H} - \vec{M}\tilde{\mathcal{D}}$, where $\tilde{\mathcal{D}}$ is the demagnetization factor and is dependent on the shape of the sample. This contributes to the different behavior of the samples for H ∥ h and H ⊥ h. For bulk samples, since the ratio of the sample's diameter to its length is approximately 4, the demagnetization factors are

$$\mathcal{D}_{\perp} \approx 6 \qquad \mathcal{D}_{\parallel} \approx 0.5$$

Loosely packed powder samples have a demagnetization factor which depends only on particle shape[56], and therefore $\mathcal{D}$ for inhomogeous samples is not well defined.

The temperature dependence of the echo:

The variation of d with temperature is very complex. The anisotropy constant K, saturation magnetostriction λ_s, and domain walls mobility affects d.

In Ni, where λ_s is constant for $T < 300^{\circ}K$, K_1 linearly decreases with temperature and the coercive field H_c is very small, one would expect the echo amplitude to increase with increasing temperature. This is not experimentally observed.

The strong variation of the echo amplitude with temperature in YC_{o_5} or C_o is not understood. The magnetostriction constant is temperature independent, K decreases with temperature and therefore the

magnetostrictive excitation is again expected to increase with temperature. The echo decreases with temperature, thus the experimental results indicate that the coefficient $\mathcal{E}$, describing the echo process must be temperature dependent.

Again it is necessary to point out, that the excitation in magnetic conductors is limited to the skin depth, which varies with temperature and the biasing field ($\mu_r \gg 1$).

Rubinstein and Stauss[15] reported that the initial echo amplitude from lithium ferrite is temperature independent. (4.2 - 300°K).

All of the metal samples show a dependence of the relaxation time on the biasing field. The variation of T_1 with H in all samples has the same behavior and varies very little at low H and than increases with an increase in magnetization and saturates at large magnetization.

The fact that the attenuation is maximal at H = 0 and decreases with increasing H indicates that the variation of T_1 with H is due to microeddy currents. As can be seen from Eq. (2.106) this process has a relaxation character with the characteristic frequency f_c given by Eq. (2.105).

At room temperature bulk polycrystaline Ni has a characteristic frequency (f_c of 10^5 Hz [59] (due to domain rotation)) which corresponds to domains of a size of ξ = 50-200 μm. Since the 30-70 μm particles used here are multidomains particles, a smaller ξ and hence a higher characteristic frequency can be expected.

The relaxation time in the saturated state increases with decreasing temperature. (Fig. 4.35) This can be caused either by a reduction in eddy current losses (increased conductivity) or by a reduction of the losses due to magnetization modulation. This process was studied by Simon ;[92] an acoustic wave travelling through a magnetically saturated crystal causes a small variation of the magnetization, which relaxes through eddy currents. An experimental verification of the presence of this process in Ni is given by Sakuray.[93] This process can also be viewed as a relaxation process with the characteristic frequency.[92]

$$f = \mu_r \sigma_e v \cdot 2 \cdot 10^{-3} \qquad (4.28)$$

where v is a sound velocity (cm/sec). In the saturated state $\mu_r = 1$ and for $\sigma_e \approx 10^3 - 10^6$ Ωcm this frequency is 10^5 - 10^8 Hz.

One can calculate the magnetic contribution to the logarithmic decreament from the relaxation time $\delta_M = \frac{1}{f}\left(\frac{1}{T_{1\,H=0}} - \frac{1}{T_{1\,H\,saturation}}\right)$. a plot of δ_M vs frequency should approximate the broad relaxation peak described by Eq. (2.106). In Figure 4.52 δ_M is shown as a function of f for Ni at various temperatures.#1 At room temperature the peak is at a frequency of approximately 10 MHz. From Eq. (2.105) this leads to a domain size $\xi \approx 5\mu m$ which is far less than that for bulk materials. However this estimation agrees in order of magnitude, with the estimation made from the equilibrium spacing of planar domains in a sphere [57] assuming that the total energy of a sphere consists of magnetostatic, V_s, and domain wall energy, V_w. The equilibrium spacing of the domains is given by #2

$$\frac{\partial}{\partial \xi}(V_s + V_w) = 0 \qquad (4.29)$$

with the result

$$\xi = 1.2\left(\frac{a\gamma}{M_s^2}\right)^{1/2} \qquad (4.30)$$

#1Footnote: The data at 10 MHz and 20 MHz are taken from different measurements on large particles. At 20 MHz T_1 coincides with the measurement in Fig.(4.34)
#2Footnote: The model above assumes uniaxial material.

where γ is the domain wall energy (erg/cm^2). For Ni $\gamma \approx$ 0.5 erg/c,^{2} [94] and M_s = 450 G. For particles of size a = 50μm this leads to $\xi \approx 10^{-4}$cm(1μm). The increase in electrical conductivity with decreasing temperature reduces f_c and the maximum in $\delta_M(f)$ is shifted toward lower frequencies (curves for 77°K and 4.2°K in Figure 4.52).

Deformation greatly reduces the relaxation time and also its dependence on the biasing field. This effect cannot be explained on the basis of magnetic structure (for example by domain wall pinning) because it is independent of H (Fig. 4.35). A similar reduction of T_1 by deformation can be seen in Figure 4.36. This reduction in the relaxation time is probably caused by deformation induced losses as in other normal metals.

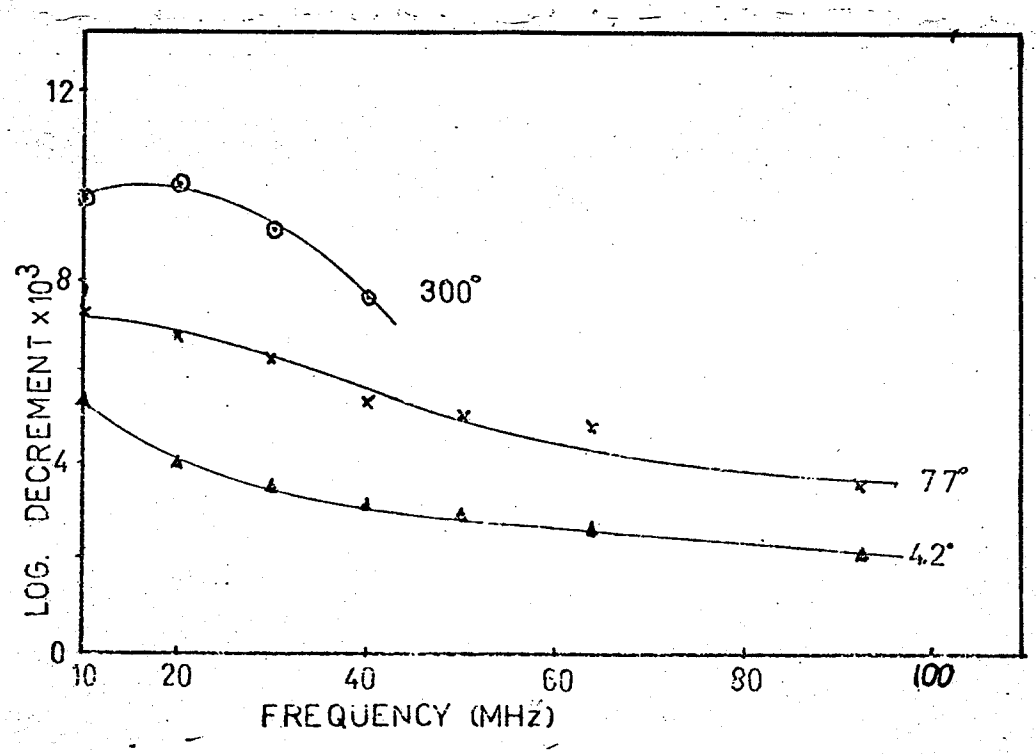

Figure 4.52: Magnetic Contribution to the Logarithmic Decrement of Ni Sample at Various Temperatures.

The relaxation time in all samples was independent of the echo amplitude. Since hysteresis losses increase sharply at deformations of the order 10^{-6} - 10^{-5}(95) a vibrational amplitude, ℓ, less that 10^{-5} is proposed.

The strong acoustic attenuation in hematite (α-Fe_2O_3) was reported previously. It originates from relaxation processes related to the motion of other than 180° domain walls.(71, 72)

In the ferromagnetic region (above 260°K) the magnetic moment lies in the plane with a very small anisotropy and any direction in the plane is possible, therefore a random orientation of magnetic domains is possible.

In pure hematite the domains are removed by a small field ($H < 1000e$) in the plane. This field can sharply increase if some domain pinning process is present. Two types of domains can be observed(96) in hematite (free and pinned), this, together with the random orientation of particles, causes a relatively wide interval for an echo observation. The magnetic moment is in the plane $\perp$ to the c-axis. When the c-axis is $\parallel$ to H the effective field in the plane is zero.

The relaxation time of the echo from α-Fe_2O_3 is the same as the decay of the free induction from a few big pieces (Fig. 4.37), indicating that $T_1 = T_0$. This supports the previous conclusion that the first echo is due to the third order process. (Eq. 2.44)

The elimination of the echo by deformation is a consequence of the increase of the coercive field, H_c which reduces the mobility of the domains and domain walls. Annealing, on the other hand, reduces the hysteresis of the echo amplitude (Fig. 4.32) as a consequence of the reduction of H_c.

The reduction of the echo amplitude by annealing (Fig. 4.32) supports the amplitude dependent force as an echo origin. The reduction of the pinning of magnetization by annealing makes the linear response between the elastic stress σ and RF magnetic field h dominant, reducing the echo formation process.

Let us assume a domain wall at equilibrium. The pressure due to the external field, Ph, and the elastic strain Pe, acting on the domain wall is balanced by a pressure associated with the wall displacement

$$P_e + P_h = \frac{\partial V_w}{\partial x} = R(x) \qquad (4.31)$$

or $\chi = R^{-1}(P_e + P_h)$

where R(x) is some function relating the pressure and displacement i.e. Pe and Ph are mixed by the nonlinear response of the domain wall. It can be mentioned, that for an infinitessimal displacement

$$\left.\frac{\partial V_w}{\partial x}\right|_{x_0+x} = \left.\frac{\partial V_w}{\partial x}\right|_{x_0} + \left.\frac{\partial^2 V_w}{\partial x^2}\right|_{x_0} x + \text{const.} \qquad (4.32)$$

and $\chi \propto P_h + P_e$ - the response (χ) is linear and no parametric mixing occurs. Similar mixing appears when both the elastic strain and external RF field produce torques acting on magnetic domains simultaneously (domain rotation).

The Echo Origin :

As shown in Eq. (4.24), the magnetic energy contains terms by the form $e^{\alpha} h^{\beta}$, α, β integers, which can lead to an echo.

Unlike normal metals, ferromagnetic substances do not have a universal relationship between the variation of elastic constants and the magnetic field. E_M (elastic modulus) as a function of h or H depends on size and shape of particles, as well as on mechanical thermal or magnetic history of the sample.

The equation of motion has the form (one dimensional case)

$$\ddot{e} + \omega^2(e,h)e \propto \sigma(e,h) \tag{4.33}$$

where both terms $\omega^2(e,h)$ or $\sigma(e,h)$ can lead to an echo. In the lowest order suitable terms are (Eq. 4.24).

$$\tilde{B}_{22}(\vec{M}_0 \tilde{\chi}_2 + \tilde{\chi}_1\tilde{\chi}_1)\tilde{e}\tilde{e}\vec{h}\vec{h} \tag{4.34}$$

or

$$\tilde{B}_{32}(\vec{M}_0\tilde{\chi}_1)\tilde{e}\tilde{e}\tilde{e}\vec{h} \tag{4.35}$$

The term (4.34) can be visualized as a field dependent elastic constant, while the term (4.35) as a deformation dependent driving force.

The echo formation is related to the character of the magnetization change with the RF magnetic field.

For a given H the magnetization has some equilibrium value M(H). The change of M with h and therefore d depends on the shape of the energy well. For other than a parabolic well the change in M is nonlinearly related to h (Eq. 4.31) and therefore a simultaneous variation of M by the RF field and deformation can lead to their parametric mixing

The presence of harmonics in x or h automatically leads to an echo. This trivial echo process would lead to an identical echo pattern in all materials, as well as to the same E_2/E_1 ratio. The presence of harmonics in e is certain, and therefore it is desirable to study the spectrum of the sample response to one pulse.

From the experimental evidence it is not possible to determine between the echo formation processes in Eq. 4.4 and 4.5 because d as a function of H is not known and therefore one cannot determine if $E_1 \propto d^2$ or d^4.

As was already seen for the echo from normal metals, the dependence

$$E_1 \propto d^{\beta}$$

is elusive since β varies practically with all parameters.

Torque on Particles:

The direct torque on particles by the RF field should also be considered as a possible excitation process[16] since, unlike normal metals, ferromagnetic particles in a static magnetic field experience a torque $\vec{M}^* \times \vec{H}$ ($\vec{M}^*$ is a particle's total magnetic moment) which can be considered as a restoring force. The equation of motion has the form

$$M^* H \sin\varphi = -J\ddot{\varphi} \qquad (4.36)$$

where J is the moment of inertia of the particle. The resonant frequency of the system is

$$f = \frac{1}{2\pi}\sqrt{\frac{M^{*}H}{J}} \qquad (4.37)$$

Small particles of radius 50μm in a field of 5 KOe have a resonant frequency of 2×10^{4} Hz. Since echo excitation does not require the presence of static magnetic fields, this effect can be neglected.

Rare Earth Materials:

The anomalous aftereffect in RCo_5 materials is not directly related to the echo but is reflected on the echo amplitude.

As can be seen in Figs. 4.40 and 4.42 the echo amplitude increases with decreasing sweep speed of H, or when the sweep stops. This indicates that the coupling coefficient, d, and therefore the domains or domain walls' mobility increases with time once the sample is brought into a given stage of magnetization.

This behavior is opposite to the behavior of the majority of other materials, where the mobility of domains or domain walls decreases with time.

Formally, this effect can be described as an "inverse pinning" process, where the concentration of obstacles pinning the domain wall is a decreasing function of time.

The equilibrium position of the wall is given by

$\frac{dV}{dx} = 0$ where V = V magnetic + V domain wall.

V magnetic = -MHx

V domain wall = $V_D(x)$ (4.38)

The above condition leads to

$$2MH = \frac{dV_D}{dx} \qquad (4.39)$$

If the application of a small field h leads to a wall deviation, χ a Taylor expansion of $\frac{dV_D}{dx}$ is given by

$$2M(H + h) = \frac{\partial V_D}{\partial x}\bigg|_{x=x_o} + \frac{\partial^2 V_D}{\partial x^2}\bigg|_{x=x_o} \chi \qquad (4.40)$$

Using (4.39), equation (4.40) reduces to

$$2Mh = \frac{\partial^2 V_D}{\partial x^2}\bigg|_{x = x_o} \chi \qquad (4.41)$$

and the domain displacement is given by

$$\chi = \frac{2Hh}{\frac{\partial^2 V_D}{\partial x^2}}\bigg|_{x = x_o} \qquad (4.42)$$

Let V_D be time dependent; the V_D can be divided into a time independent V_{DO} and a time dependent part V_{DT},

using $\frac{\partial^2 V_{DO}}{\partial x^2}\bigg|_{x_o} = \alpha$, $\frac{\partial^2 V_{DT}}{\partial x^2}\bigg|_{x_o} = \beta(t)$

Eq. (4.42) can be written. $\chi = \frac{2Mh}{\alpha + \beta(t)}$ (4.43)

For most materials $\beta(t)$ is an increasing function of time, leading to a time decrease of χ and hence to a decrease in the magnetic susceptibility. A common form for $\beta(t)$ is

$$\beta(t) = \beta_o (1 - e^{-t/\tau}) \tag{4.44}$$

which usually originate from thermally activated motion of walls through defects. In these cases

$$\tau = \tau_o e^{Q^x/kT} \tag{4.45}$$

where Q^x is dependent on H. The simplest form for Q is

$$Q^x = Q^x_o - MHx \tag{4.46}$$

Since in rare earth -cobalt compounds $\beta(t)$ must be time decreasing, one can write, in analogy to Eq. (4.44)

$$\beta(t) = \beta_o e^{-t/\tau} \tag{4.47}$$

introducing $\chi(t = \infty) = \chi_o$ then from Eq. (4.43)

$$\chi(t) = \frac{\chi_o \alpha}{\alpha + \beta(t)} \tag{4.48}$$

and $$\ln\left(\frac{\chi_o}{\chi(t)} - 1\right) = -t/\tau + \ln\frac{\beta_o}{\alpha} \tag{4.49}$$

Experimentally, however, a relation similar to (4.45) does not hold and the dependence of the echo amplitude on $\frac{dH}{dt}$ is the same at 77^oK and 300^oK (Jordan aftereffect). See Figure 4.42

Moving Wall :

A simple model, for this moving wall, can be introduced by making $\beta(t)$ velocity dependent. This can be accomplished, for example, by assuming that the concentration of pinning defects inside the domain wall decreases at a constant rate. In the time interval Δt, the concentration of defects decreases to $C_o e^{-\Delta t/\tau}$ and the domain wall travels a distance $\sim \Delta t$.

The average concentration of pinning sites is then given by

$$\bar{c} = \frac{1}{d}\int_0^d c(x)dx = \frac{c_o \nu \tau}{d}\left(1 - e^{-\frac{d}{\nu\tau}}\right) \qquad (4.50)$$

where d is the domain wall width. If $\beta(t)$ is proportional to $\bar{c}$ then $(\beta(t) = \alpha\beta'\bar{c})$

$$\chi(t) = \frac{\chi_o}{1 + \beta'\bar{c}} \qquad (4.51)$$

ie. $$\left(\frac{\chi_o}{\chi} - 1\right) \propto y(1 - e^{-1/y}), \quad y = \frac{\nu\tau}{d} \qquad (4.52)$$

Let $E_1 \propto \chi$ and $E_{10} \propto \chi_o$.

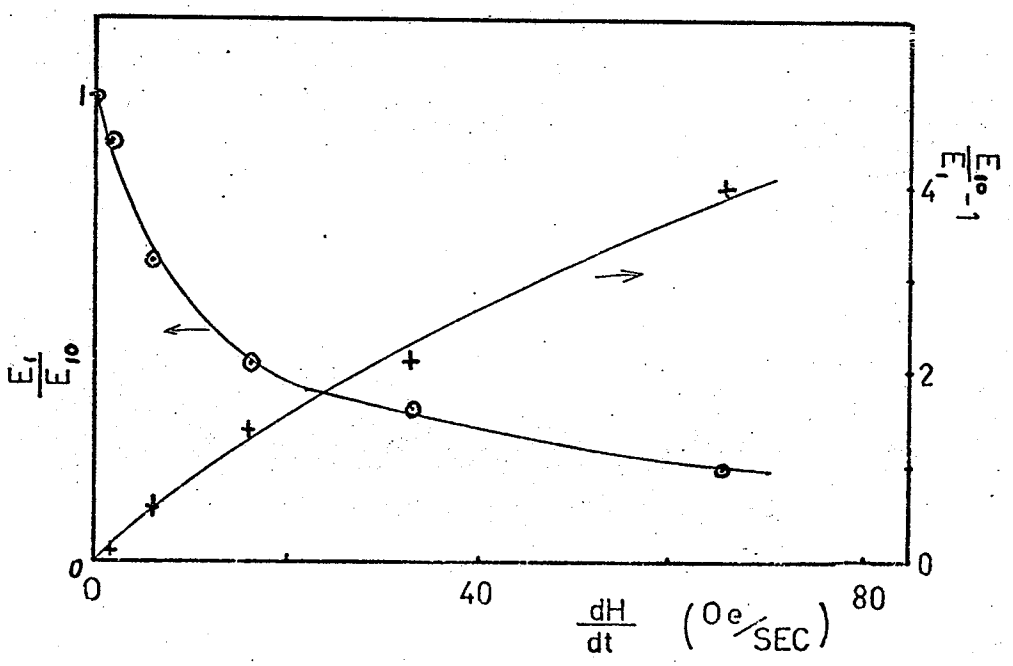

Figure 4.53: Dependence of the Echo Amplitude on the Speed of Sweep of the Biasing Field (Y Co_5, 77°K 16 MHz)

The experimental points and plot of $\frac{E_0}{E_1} - 1$, Eq. (4.52), for the Y Co_5 sample are on Figure 4.53. Equation (4.48) can be compared to any quantity which is linearly related to domain wall displacement. The echo amplitude (at least theoretically) is related to higher powers of the domain or domain wall displacement. However, the experiments already described show that for equal pulses intensities the echo is linearly related to the strength of the driving force. The velocity of the domain walls is related to the rate of change of the mangetization and hence to the sweeping field. The rate of change of the magnetization is given by

$$\frac{\partial M}{\partial t} \approx 2 m A v M_s \qquad (4.53)$$

where m is the number of domain walls, A their area and v their velocity. For a rough estimation let the domains walls have a spacing (ξ) of 1 μm and a width d of 10^{-3} μm and let the particle size (a) be 50 μm, then for a sweep field ($\frac{dH}{dt}$) of 60 Oe/sec, the corresponding magnetization change ($\frac{dM}{dt}$) is $\frac{M \text{ saturation}}{H \text{ saturation}} \frac{dH}{dt} \approx 0.6$ Gauss/cc sec and the wall velocity (v) $\approx 3 \times 10^{-4}$ cm/sec. From Figure 4.53 the corresponding value of y (Eq. 4.52) is approximately 0.5 and τ is of the order of 10 sec.

The model presented above shows that the assumption of a time decreasing concentration of pinning defects can explain the observed effect. One physical possibility is that oscillatory domain wall vibrations push defects (hydrogen intersticials) out of the region swept by the wall (diffusion aftereffect); the other possibility is that the hydrogen atoms are forced into positions where their interactions with domain walls are weak (orientation aftereffect).

It is necessary to remember that an echo excitation requires large RF-pulse intensities ($h \approx 100$ Oe) and therefore Q^* in Eq. (4.46) cannot be considered to be constant but

$$Q^* = Q^*_o - M(H(t) + h(t)) \; x(t) \qquad (4.53)$$

and instead of thermal activation the work is performed by the RF-field which leads to a measured relaxation time, which is temperature independent.

As can be seen the echo amplitude is sensitive to intrinsic properties associated with the domain wall mobility which is consistent with the magnetostrictive excitations of the elastic vibrations.

D Echo from piezoelectric powders:

As in the previous cases, both mechanisms of the echo formation Eq.'s (4.4) and (4.5) are possible, C and d depend on e and h. Both C(h) and d(e) depend on the temperature, biasing or RF electric field, as well as the history of the sample.[97,98] Therefore, from the experimental evidence one cannot distinguish between the two possibilities.

Qualitatively, the temperature dependence of the echo E_1 (Fig. 4.44) follows the variation of d(T)[98] (Fig.4.54). Quantitatively, however, the comparison with theory is poor. d(T) shown in Fig. 4.54 changes the same order of magnitude as the echo while according to the theory $E_1 \propto d^2$ or d^4 depending on the echo process.

The d(T) depends strongly on the intensity of the RF field. The intensity used for the echo excitation is $h \approx 1000\ V/cm$, which is more than the intensity required for the removal of the domains, and therefore a direct comparison of the echo amplitude $E_1(T)$ with published values of d(T) is impossible. In addition, the particles are oriented randomly relative to the direction of the RF field and therefore they are excited differently.

Both the field variation of the elastic constants C(h) and the amplitude variation of the coupling d(e) are expected to be much stronger in the ferroelectric phase, where the presence of ferroelectric domains has a large effect.[99] (removal of the domains is analogous to the ΔE_M effect in the ferromagnetics).

The C(h) in the ferroelectric phase is strongly dependent on the biasing electric field [100, 101], while the echo varies only slightly (Fig. 4.45)

The relaxation time of Rochelle salt is strongly temperature dependent and at low temperatures is the largest from all samples used in this study.

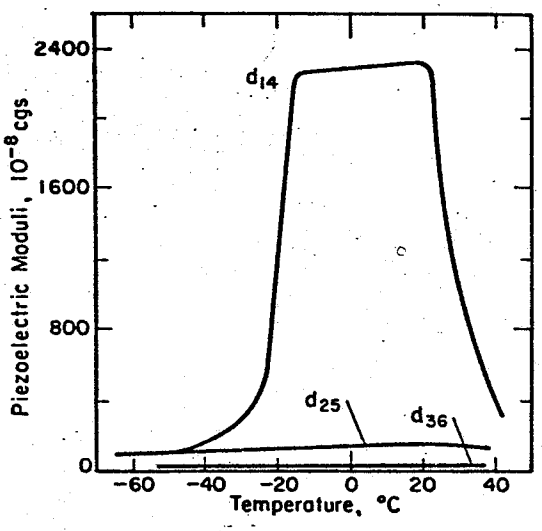

Fig. 4.54: Temperature dependence of the various components of the d tensor for Rochelle Salt.

E Character of the elastic modes:

The presence of an echo in a situation when particles do not mutually interact clearly points out its single particle origin (Section E a & c) in ferromagnetic or piezoelectric powders. In normal metals the long relaxation time of the echo from regular particles also indicates the single particle origin of the echo.

The experiments described in section Eb (echo observed during the vibrations of the sample) also reveal that interaction between particles is not required for the echo formation.

4.4 Conclusion :

Experimentally, the properties of the echo from different types of powders behave similarly, as can be seen from the experiments described in group A.

The echo patterns following the RF pulse excitation in all powders (metals, ferromagnetics, piezoelectrics) are similar; the dependence of the echo amplitudes on intensities of the driving pulses are identical; and the ratios of the relaxation times of different echoes are the same.

This leads to the conclusion that the echo in all cases has a similar origin and the differences between different materials are due to different driving forces.

Comparison of the experimental data with the various echo models in Chapter II selects the parametric mode mixing as the dominant echo process.

The ratio of the relaxation times of different echoes, as well as comparison of the echo relaxation with the relaxation of the induction following the pulse (Fig. 4.37), indicates that the lowest order mixing processes for given echoes are dominant (3rd for the first, 5-th for the second etc). The shape of the echo is determined by the width of the RF pulse and the echo is modulated by transient responses at onset and offset of the RF pulses.

The echo width is not simply related to the RF pulses width and does not reveal any conclusion about the mixing process described by Eqs. (2.25) and (2.29).

The best shaped echoes are obtained by RF pulses of the same width. This is expected because in these cases the Fourier transform of both pulses is the same.

Two different 3rd -order processes are possible. One process, derived from a term in the hamiltonian of the form $\ell_1^2 h_2^2$, can be visualized as a modulation of elastic constants during the second pulse.

$$C = C_0(1 + \varepsilon h^2) \tag{4.54}$$

The second process, derived from a term in the hamiltonian of the form $\ell_1^2 h_2$, can be visualized as a modulation of the coupling coefficient between the force acting on the particle and the external RF field of the form

$$d = d_0(1 + \varepsilon \ell^2) \tag{4.55}$$

For echoes due to higher than 3-rd order process the division into C(h) and d(e) is completely artificial and in all real materials both d(e) and C(h) exist simultaneously.

The echo from normal metals increases with H and does not saturate at H = 50 KOe and h = 100 Oe. It is extremely sensitive to the material's resistivity and impurity content. Most properties of the echo are similar for all normal metals. The echo amplitude for small values of h_1 and h_2 can be described in terms of the driving pulses by a power dependence of the type

$$E \propto h_1^m h_2^n H^{m+n+1} \qquad (4.56)$$

The first echo, m = 1, n = 2, is formed by a third order process and at low intensities of h_1 and h_2 its amplitude varies as $E_1 \propto H^\beta$ with $\beta = 2.5 - 4$ for all metals, Nonlinearities described by Eq. (4.54 leads to $E_1 \propto H^2$ while Eq.(4.55) leads to $E_1 \propto H^4$. Thus dependence $E_1 \propto H^\beta$ with $\beta > 2$ supports the d(e) as a dominant echo process.

For normal metals the echo in all samples, except Ag, was strongest for the pure samples. There is no agreement between the experimental results of different observers[14,20] as far as the echo from Ag is concerned. In this study no echo was observed from pure Ag at H = 10 KOe which agress with Snodgras [20]. Because C(h) is insensitive to the material the absence of the echo from Ag again supports d(e) as an echo process.

Purely geometrical effects, which could explain the close relation between the sample's resistivity and echo amplitude as well as its dependence on H and h, cannot explain the anomalous low temperature behavior for some samples (Mg) or the impurity enhancement in Ag.

On the other hand, the modulation of some internal variable can be sensitive to the material and be reflected on the echo properties.

In the macroscopic description of the driving force through eddy currents the only possible variable is the resistivity.

The description of the driving force through eddy currents is an over-simplification of the actual microscopic process. Speculation about the modulation of microscopic quantities, involved in microscopic theories of generation of acoustic waves in metals would be premature at this time.

Generally, the comparison of experimental results with the consequences of the echo model is poor. For equal RF pulses intensities the echo $E_1 \propto H^2 h$. This relationship contrasts with the dependence of E_1 on h_1 and h_2. The same is true about the constant ratio of E_2/E_1 which is constant instead of having an H^2h^2 or Hh^2 dependence.

The echo formation from normal metals requires long RF pulses $t_w \approx 5-10$ μsec whose duration is

comparable with the relaxation time T_1 of the first echo from filings. ($T_1 \approx 20-30\mu$sec). T_1 of the filings is determined by the extrinsic losses and does not reflect any intrinsic losses, which in normal metals are small. For the regular particles T_1 is limited by the losses due to induced eddy currents, which are proportional to H^2. This principal limitation of T_1 leaves little hope that the echo in normal metals can be used to monitor their intrinsic losses.

The echo amplitude in ferromagnetic metals as a function of H qualitatively follows the expected dependence, while its temperature variation is unexpected, the echo decreases fast in the region where the magnetic properties change is very small. This requires the factor $\mathcal{E}$ describing the echo formation to be temperature dependent.

One possibility is that the domains or the domain walls are moving under the influence of the RF field and the elastic deformation. Pinning at low temperatures causes this motion to be highly nonlinear and therefore leads to an echo. Pinning is reduced by increasing the temperature (thermal activation) and the echo decreases. Annealing also reduces the pinning and therefore reduces the echo. The process above can affect both, d, or E_M. The dependence of d, on the biasing field, H, is complex and not known in detail, therefore E_1 (H)

cannot be compared with expected d^2 or d^4 dependencies following from Eq's. (4.54) and (4.55) for the different processes of the echo formation.

As in the normal metals, the echo amplitude, E_1, as a function of h_1 and h_2 varies with the magnitudes of h_1, h_2 or H. For $h_1 = h_2$ the and ratio E_2/E_1 is constant which disagrees with the model presented. The dependence $E_1 \propto d^{\beta}$ must therefore be taken with caution, because β depends on h_1, h_2 or H for $h_1 = h_2$ one expects in analogy with normal metals that $E_1 \propto d^2$.

The relaxation time of ferromagnetic conductors is determined by microeddy currents, and the echo relaxation can be used to monitor these losses.

From polycrystaline ferrites an echo was also observed from bulk samples, which behaved similarly as the echoes from powders.

The echo from the ferromagnetic powders is typically stronger, less temperature dependent and requires shorter RF pulses than the echo from normal metals. The coupling coefficient d is 1-2 orders of magnitudes stronger in ferromagnetics and also the field dependence of the elastic constants is more pronounced.[55] The coupling coefficient $d(h)$ and elastic constants C(h) are sensitive to the domain structure and therefore to the history of the sample.

In view of the present observations, one can identify the strong variation of relaxation time with temperature in lithium ferrite reported by Rubinstein and Stauss[15] as having an intrinsic origin. The ferrites have strongly temperature dependent losses, which are probably caused by transition of the transition metal. ions between the two states with different valency[102]

The echo from piezoelastic powder does not differ from the previous two. The echo properties are identical in both the ferro and piezoelectric phases, indicating that the echo formation is independent of the domain structure. Popov and Krainik [11] reported an echo from bulk SbSi (ferroelectric) and proposed the excitation and refocussing of the oscillations of ferroelectric domains as the mechanism responsible for the echo. This process is not important in the powder of Rochelle salt.

The presence of a strong second echo in all materials, with the amplitude $E_2/E_1 \approx 0.1$ is interesting. The large ratio E_2/E_1 indicates either that the nonlinearity causing the echo is not samll, or that the higher order terms in the hamiltonian are present. The dependence of E_2 on h_1, h_2 and H is complex. For $h_2 = \frac{1}{2} h_1$, $E_2 \propto H^{4-5}$ for normal metals. While for $h_1 = h_2$ $E_2 \propto H^2 h$ and the E_2/E_1 ratio is independent of H or h for all powders.

The presence of harmonics in ℓ for the amplitude dependent coupling coefficient Eq.(4.55) can lead to an observed echo pattern.

As can be seen, the experimental evidence is inconclusive as to the selection between the echo formation by the amplitude dependent force or the field dependent elastic constants. However, the first is preferred.

Crucial information required for a better understanding of the echo is an estimation of the echo intensity with respect to the amplitude of the vibration i.e. E_1/E_0. A comparison of the initial amplitude of the free induction during or immediately after the RF pulse would be very valuable. The lowest limit, $E_1/E_0 > 10^{-5}$, is based on the fact that no induction was observed from a few particles and an echo was observed from a sample containing $\approx 10^6 - 10^7$ particles.

The goal of the experiments related to the echo excitation from large Rochelle salt crystals was to compare the echo amplitude with the free induction from one particle. As was pointed out in section A, no echo was observed from large particles of Rochelle salt. This suggests that only the basic, or low harmonics, vibrational modes of the particles are responsible for an echo.

CHAPTER V

CONCLUSION AND SUGGESTIONS FOR FURTHER STUDY

The problem associated with echo generation has 3 parts.

(a) Establishing the coupling mechanisms between the RF field and the elastic vibration of the particles.

(b) Determining the vibrational modes.

(c) Selecting the physical nonlinearity responsible for an echo.

From the foregoing discussion, the answers for a - c are:

(a) the coupling mechanism is due to direct excitation of sound in normal metals, via the Lorentz force in the skin depth, magnetostrictive excitation of sound in ferromagnetic metals (Chapter IV. B, C, D) and piezoelectric excitation in piezo or ferroelectrics;

(b) in all powders single particle vibrational modes are responsible for an echo (Chapter IV) and probably the transversal component of the modes is dominant;

(c) the nonlinearity of the coupling originates from the simultaneous effects of elastic deformations and RF fields on some internal variable of the material (domain distribution in ferromagnetics and electron structure in normal metals).

The model introduced in Chapter II is general and can be used to describe the echo from various multioscillator systems.

Due to the multimode origin of the echo the echo process is not sensitive to the detailed description of the coupling. For example, in ferromagnetic powders the echo from cubic and uniaxial materials behaves

similarly. In the former, both wall displacement and domain rotation cause excitation of elastic vibrations, while in the latter only domain rotation can contribute to the excitation process. Echoes from different normal metals also behave similarly, while their crystallographic and electronic structure is very different.

To generate an echo, large vibrational amplitudes are necessary. This requires a large driving force; therefore, good electrical conductivity in normal metals and low coercivity in ferromagnets are necessary.

The relaxation time of the echo reflects both the extrinsic and intrinsic losses in the system. In normal metals the extrinsic losses dominate in most cases. In ferromagnetic metals the relaxation time is determined by microeddy losses.

Apart from the study of particle kinetics the observation of the relaxation time can reveal some information about the loss mechanisms in materials which cannot be studied in bulk or have losses too large to be studied by the standard ultrasonic technique.#

The sensitivity of the echo method is limited by the Q of the powder sample. The Q's for the different samples estimated from the present experiments are in Table V.I.

#Footnote: The relaxation time of the first echo, T_1, is related to the attenuation coefficient, A, obtained in travelling wave experiments by

$$A = \frac{1}{v\, T_1} \qquad [\text{Np/cm}]$$

where v is the velocity of sound in the material (cm/sec).

TABLE V.I

Quality Factor for Different Samples

Material	T_1 (μsec) at f = 10 MHz	$Q = T_1 \times \pi \times f$
Sintered Powders (Ferrite)	20	600
Sintered Bulk Ferrite	60	1800
Polycrystaline Metals		
Regular Shape	160	5000
Filings	50	1800
Single Crystal Powders		
Rochelle Salt	800	25000
Lithium Ferrite*	1500	40000

* Reference 15

No dependence of the echo relaxation time on pulse amplitude was observed, therefore the relaxation time of the first echo can be used to measure the acoustic losses in powder samples even if the specific mixing process responsible for the echo is not known.

The method is especially useful for powders with a large internal loss since these losses will dominate and no great care has to be taken in powder preparation.

One sample can be used to measure the attenuation in a wide frequency range. In this work the application of the method was demonstrated for Ni powder.

There is potentially a large group of materials in which an echo can be excited, therefore this method can have a wide application.

A quantitative estimation of the magnitude of the nonlinearity,

ε', responsible for echo, is difficult. The large uncertainity arises in the estimation of: a) the number of particles involved in the echo formation (those which have a resonance frequency in the bandwidth of the RF-pulse), and b) the magnitude of the effective coupling between the elastic vibration and the RF-field.

A direct estimation could be made from a comparison of the echo amplitude to the vibrational amplitudes of the particles (Initial amplitude of the "free induction"). This could not be done on the apparatus used in this study (See Chapter III).

The uncertainty in the coupling could be reduced by comparing the echo amplitudes with the amplitude of vibrations from bulk samples, where a simple geometry allows one to estimate the coupling coefficient.

Lu and Fedders[33] estimated that nonlinear term in the hamiltonian for bulk ferroelectrics to be of the order of 10^{-7} times the total energy, but this estimation is very crude. It would be desirable to obtain some knowledge about the mixing term from some direct experiments. A comparison of the free induction and echo from the same volume of bulk and powdered Rochelle salt excited by one or two RF pulses of the same intensity and duration indicates $E_1/E_o \simeq 0.1$. This direct comparison yields to an upper bound, which is probably several orders of magnitude off, because the vibrations in these two cases are different.

For the majority of the samples, the variation of the echo amplitude with the experimental conditions can be qualitatively explained as being due to a change of the amplitudes of elastic vibrations, which are linearly related to the RF-field, i.e. they do not reflect the

specific properties of the mixing process. However, there are exceptions, which rule out an extrinsic origin of the echo. In all the experiments described here the amplitude of the RF-field cannot be considered to be small, and therefore, higher order terms in the coupling between RF field and elastic vibrations are always present.

The quantum mechanical treatment of the problem (Appendix II) is included more for its formal elegance than practical value. The dependence of the echo on a large number of external parameters makes this formalism of little value at this time.

It was experimentally demonstrated that similar echoes can be excited in bulk materials by the same coupling mechanism[101]. There is at present a large interest in the study of material properties through the echo method[12, 97, 103-107]. This is especially true for the stimulated echo in bulk materials, because the energy dependent process of echo formation can relax only through multiphonon scattering. Echo observation from powders indicates the possibility of producing a similar echo in bulk normal metals. It was not possible to observe an echo from bulk Al at 4.2°K and 10 KOe. A stronger biasing field is probably necessary.

Mode excitation in bulk solids does not need to be spatially localized. Interesting effects may be observed from the study of interactions between elastic waves travelling in different directions, or having different polarization.

The echoes described here are a subgroup of elastic echoes from solids. Generally, an echo can be formed only under coherent excitation. In the case of RF excitation this is well

satisfied because the sample is usually much smaller than the RF wavelength and it would be interesting to try to form an echo by different means.

All of the discussions of the echo properties are only qualitative and are based on a one-dimensional analogy. In reality the particles are 3-dimensional, the vibrational amplitude is the strain i.e. a tensor quantity and terms like e^3h or e^2h^2 are described by a 7-th or 6-th rank tensor.

The echo formation process points out the presence of nonlinear responses in the materials which are otherwise hidden behind a large linear response. Because the echo is insensitive to the physical processes causing the nonlinearities, they must be studied by different methods.

Quantitative understanding of the echo formation process requires simultaneous information about the linear as well as the nonlinear response. Therefore a further study of the echo phenomenon should go toward a microscopic understanding of the process. This requires a sensitive measurement of the material properties for example, the effect of the uniaxial deformation in bulk normal metals on the direct generation of ultrasound.

The specification of the elastic modes could also lead to a better understanding of the echo process.

It would be worthwhile to study an echo spectrum of a sample of regular, almost identical, simply-shaped particles (spheres) for which a mode spectrum is known.

It is desirable to extend the measurements to lower frequencies.

The relaxation time, T_1, is inversely proportional to the frequency and longer relaxation times lead to smaller experimental error, therefore, small changes in T_1, as a result of the different treatment of powders, could be measured.

Most important of all is the estimation of the magnitudes of the nonlinearity causing the echo. The simplest way of arriving at this would be to make a comparison of the amplitude of the free induction with that of the echo.

In the observations presented it is impossible to distinguish between the two processes of echo formation (C(h) or d(e)). Feasible experiments which could be conducted to discriminate between the two possibilities could be performed on normal metals by using a pulsed electromagnet as opposed to the steady current electromagnet. Then a DC magnetic field could be applied only during the first RF pulse. If the second RF pulse applied without the DC field, excited an echo, then the field dependent elastic constants would be responsible for the echo; if not, then the nonlinear driving force would be responsible.

A problem of some interest is the strong temperature dependence of the relaxation time. Rubinstein and Stauss[15] reported a strong decrease of the relaxation time of lithium ferrite with temperature. A similar decrease is observed in this study from Rochelle salt or saturated Ni powder.

The Rochelle salt and Ni powders are the only samples which do not have a relaxation time limited by the irregular shape and which produce an echo in a wide temperature range. Therefore it would be

interesting to know whether this reduction of the relaxation time with temperature is a universal relationship or whether it is the specific property of selected samples.

APPENDIX I

NORMAL MODES FORMULATION[110,111]

Let us consider a lossless system with hamiltonian $H(p,q)$. The equations of motion for the canonical coordinates have the form

$$\dot{q} = \frac{\partial H}{\partial p}, \quad \dot{p} = -\frac{\partial H}{\partial q} \tag{I.1}$$

Define $a = Ap + iBq$

$$a^* = Ap - iBq \tag{I.2}$$

then H can be written as $H(a, a^+)$ and (I.1) has the form

$$\dot{a} = i2A\,B\,\frac{\partial H}{\partial a^*}$$

$$\dot{a}^* = -i2AB\,\frac{\partial H}{\partial a} \tag{I.3}$$

For a harmonic oscillator $H = aa^*$ and $2AB = \omega$ (I.3) has the form

$$\dot{a} = i\omega a \qquad \dot{a}^* = -i\omega a^* \tag{I.4}$$

with solutions

$$a = a(o)e^{i\omega t} \qquad a^* = a^*(o)e^{-i\omega t}$$

For a many modes system

$$H = \sum_i H_i = \sum_i a_i a_i^* \tag{I.5}$$

where a_i, a_i^* represent normal modes rotating in opposite directions.

Let us assume that the system supports two different kinds of modes a_i and b_i.

Then the parametric coupling between a and b can be introduced by the interaction hamiltonian H_{int} containing the products of a_i, a_j^*, b_k and b_ℓ^*.

$$H_{int} = \sum_{\substack{ijk\ell \\ rsmn}} a_i^r a_j^{*s} b_k^m b_\ell^{*n} \tag{I.6}$$

where r, s, m, n are integers.

The echo formation can be formulated as follows:

Let b_i have the form

$$b_i = b_o e^{i\omega_i(t - \tau)} \tag{I.7}$$

and

$$a_i = a_o e^{i\omega_i t}$$

then H_{int} of the form

$$H_{int} = \sum_i a_i^{*2} b_i^2 \quad \text{or} \quad \sum a_i a_i^{*2} b_i \tag{I.8}$$

can lead to an echo.

The hamiltonian of the system has the form

$$H = \sum_i a_i a_i^* + \sum_i b_i b_i^* + H_{int} \tag{I.9}$$

Solving (I.3) with (I.9) for a_i and summing through all i-s lead to an echo.

In powders modes a represent the elastic vibrations following the

pulse I and b the RF field during the second pulse. Although this formulation does not introduce any new physics, its advantage is the easy recognition of the terms leading to an echo.

A similar approach can be used for travelling waves.

The generation of the modes is introduced by including the interaction with the external force in the hamiltonian.

Unfortunately, the hamiltonian of the real system is not known; therefore this direct approach has little value. However, the terms of H_{int} in II.8 are the lowest order processes leading to an echo and are independent of the actual hamiltonian.

APPENDIX II

QUANTUM MECHANICAL FORMULATION

Replace a, a^* in Appendix I by the annihilation and creation of boson operators (a, a^+) where

$$[a, a^+] = 1 \tag{II.1}$$

The hamiltonian has the form

$$H_{int} = H_{i\ \ell}^{rsmn}\, a_i^r\, a_j^s\, a_k^{+m}\, a_l^{+n} + \text{complex conjugate} \tag{II.2}$$

For the harmonic oscillator.

$$H_o = \hbar\omega\,(a^+a + \tfrac{1}{2}) \tag{II.3}$$

The expectation value $a(t)$ is

$$\langle a(t) \rangle = \mathrm{Tr}\,(\rho(t)\, a(o)) \tag{II.4}$$

where $\rho(t)$ is the density matrix

$$\rho(t) = L\,\rho(o)\,L^{-1} \tag{II.5}$$

$$L = e^{-i/\hbar\, Ht} \tag{II.6}$$

Rearranging (II.4) and using (II.5)

$$\langle a_i(t) \rangle = \mathrm{Tr}(\rho(o)\, L^{-1} a_i(o) L) \tag{II.7}$$

The echo process is formulated as follows:

$$< a(t) > = \sum_i < a_i(t) > \qquad \text{(II.8)}$$

and $L = K_3 K_2 K_1$ with $L_1 = e^{-i/\hbar\, H_o \tau}$

$$L_2 = e^{-i/\hbar\, H_{int}\, t_{w_2}} \qquad \text{(II.9)}$$

$$L_3 = e^{-i/\hbar\, H_o (t-\tau-t_{w_2})}$$

L_1 describes the developing of an after pulse I, L_2 the interaction during the short pulse II of duration t_{w_2} and L_3 the time development after Pulse II.

Using (II.3)[112]

$$L_1^{-1}\, a\, L_1 = a(o) e^{-i\omega\tau}$$

$$L_1^{-1}\, a^+\, L_1 = a^+(o) e^{+i\omega\tau} \qquad \text{(II.10)}$$

Therefore, any interaction described by H_{int} which transforms a into a^+ and vice versa will form terms $a_i(o)^{i\omega_i(2\tau - t)}$ and hence give an echo at $t = 2\tau$.

A suitable form of H_{int} is

$$H_{int} = K_1(a^2 + a^{+2}) \qquad \text{(a)}$$

$$H_{int} = K_2(a + a^+)^2 \qquad \text{(b)} \qquad \text{(II.11)}$$

For example, (II.11b) transform[112] a as

$$e^{iK_2/\hbar\,(a+a^+)^2}\; e^{-iK_2/\hbar\,(a+a^+)^2} = (1-2iK_2/\hbar)\, a - 2iK_2/\hbar\, a^+$$

Eq. (II.11a) was discussed by U.K. Kopvillem in detail in[114] assuming

that the observable is $P = (a+a^+)\ P_o$. The echo amplitude is

$$N\ P_o\ A_o\ \sinh\ (\frac{t_{w_2}}{h}\ K_1) \qquad \text{(II.12)}$$

where A_o is an initial amplitude, which was excited by pulse I and N is the number of oscillators. The same author applied this kind of analysis of the response of many different multioscillator systems to a pulse excitation[10, 113, 115].

A similar case for travelling waves is discussed in[12]. The observable (deformation) is

$$\varepsilon(t) = (\varepsilon_q(t) = \varepsilon_{-q}(t))$$

where

$$\varepsilon_q(t) = a_q(t)\ -a_q^+(t)$$

and a suitable hamiltonian, giving one echo after two pulse excitation is of the form

$$H_{int}\ (a_q a_{-q} + a_q^+ a^+_{-q}) \qquad \text{(II.13)}$$

which can be derived from the coupling between the external field h and deformation of the form $\varepsilon^2 h$, and leads to an $h_1 h_2^2$ dependence of the echo amplitude.

The above choices of H_{int} (II.11), (II.13) lead to only one echo after two pulses. The excitation of more echoes requires higher order terms of a, a^+ in the hamiltonian.

In complete analogy with the classical case, the mode a^2 after

pulse I rotates with frequency 2ω. At the time of the second pulse, suitable interaction containing a^{+3} terms will transform a^2 into a^+ and at $t = 3\tau$ (2τ after pulse II) this process will give rise to an echo.

This boson echo, in contrast to the spin echo, does not have an upper limit in amplitude. The spin echo amplitude varies periodically with the turning angle of spins, and the maximum contribution of one spin is limited.

This variation is a consequence of the finite number of spin energy levels. In the boson case there is no restriction on the maximum energy. This can be seen in Eq. II.12, which is similar to the spin echo case except for the fact that the trigonometric function is replaced by a hyperbolic function.not known; therefore this direct approach has little value. However, the terms of H_{int} in II.8 are the lowest order processes leading to an echo and are independent of the actual hamiltonian.

APPENDIX III

Permanently Stored Echoes in Powdered Materials

S. Kupca, I. Maartense, H.P. Kunkel and C.W. Searle

Department of Physics
University of Manitoba
Winnipeg, Canada

Abstract

The permanent echo recently reported by G.A. Sawatzky and S. Huizinga from piezoelectric powders was observed from other types of powders. It is shown that a simple model in which the echo originates from the mechanical alignment of particles is consistent with all known echo properties.

Echoes, following an RF multi-pulse sequence have been observed from many types of powdered materials[1,2]. The echoes are produced by a non-linear parametric interaction between the pulsed-RF field and the elastic vibrations of the particles. RF pulses applied at times $t = 0,\tau$ and T lead to echoes $\varepsilon_1,\varepsilon_2,\ldots\varepsilon_n$ and $\varepsilon_{11},\varepsilon_{12},\ldots\varepsilon_{n\pm m}$ which appear at $t = 2\tau,3\tau\ldots,n\tau$ and $T + \tau$, $T + 2\tau,\ldots mT \pm n\tau$ respectively. These echoes in general decrease with different relaxation times $T_1,T_2,\ldots T_n$ and $T_{11},T_{12},\ldots,T_{m\pm n}$ which depend on the mechanical quality factor, Q, of the particles and decrease inversely with the frequency. At 10 MHz Q is typically 10^3 - 10^5 which leads to relaxation times of the order of 10 - 1000 μsec.

Recently Kuindersma et al[3], and Sawatzky and Huizenga[4] have reported that, in addition to these normal echoes, a two pulse excitation can lead to a permanently stored echo, ε_p, in piezoelectric materials, which can be recalled nondestructively. Read out requires the application of a third pulse at $t = t_i$ ($t_i >> T_1$) which leads to the appearance of ε_p at $t = t_i + \tau$. In contrast to ε_{11}, which requires that $T \approx T_1$, t_i can be on the order of days or weeks. Provided that the spacing between read out pulses satisfies the condition $t_{i+1} - t_i >> T_1$, each read out pulse forms an echo, ε_p, at $t = t_i + \tau$. The above authors[3,4] suggested that some process with an extremely long relaxation time is responsible for ε_p. We have observed this stored echo from a

ferroelectric powder (Rochelle Salt) at 300°K as well as from a normal metal (Al) at 77°K in a biasing magnetic field of 10 KOe.

The observed echo, ε_p, has the following properties:

a) It remains stored in the sample as long as the sample is not disturbed by mechanical vibrations or the application of RF fields of excessive intensity during the read out pulses.

b) After storage by the initial two pulse sequence (pulse separation τ) ε_p decreases rapidly (on the order of minutes) to approximately one half of the initial value. After this ε_p is only weakly dependent on time as shown in Fig. 1.

c) If the initial two pulse write in sequence is made in the presence of a DC electric field, E_w (Rochelle Salt), ε_p depends on the intensity of the electric field, E, applied during the read out pulse. ε_p goes through a maximum when $E = E_w$ as shown in Fig. 2. The actual shape of ε_p vs. E depends on the pulse separation τ and is narrower for larger τ.

A relatively long relaxation time T_{11} for ε_{11} can be expected if energy, after the initial two pulse excitation, is stored in some static form[5]. This mechanism, however, can not explain the non destructive recall of ε_p by the application of a recall pulse at $t = t_i$.

All the observed properties of ε_p can be understood on the basis of Gould's model for echo formation from a multi-oscillator system[6] if one includes the possibility of a varia-

tion of the effective coupling constant between the RF field and the vibrating particles during the second pulse. Gould's model considers sets of particles with vibrational modes which are in phase, with a phase angle $\theta(\tau)$ at a time $t = \tau$ after the first pulse. This particular set of particles, which can be called a θ_{class}, have a $\theta(\tau)$ related to the individual angular vibrational frequencies, ω_k, of the particles in the set by

$$\theta(\tau) = \omega_k\tau - k2\pi \quad \text{or} \quad \omega_k = \frac{\theta(\tau) + k2\pi}{\tau} \tag{1}$$

where $k = 0,1,3,\ldots$. The individual phases of this particular class, $\theta(\tau)$, are given by (for $t > \tau$)

$$\theta_k = \omega_k t = \frac{\theta(\tau) + k2\pi}{\tau}\, t \tag{2}$$

Equation 2 shows that the members of this θ_{class} are generally out of phase except at times $t = n\tau$, where n is an integer, when all members of $\theta(\tau)$ refocus. This is a necessary but not sufficient condition for the formation of an echo, since the linear response to a two pulse sequence can not lead to an echo. A consideration of nonlinear terms leads to the normal echo phenomenon mentioned earlier, but it can not describe ε_p.

Consider a θ_{class}, $\theta_o(\tau)$, which happens to be in phase with the RF field at the time of the second pulse τ (shorter than T_1). Although $\theta_o(\tau)$ is in phase with the RF field, the directions

of vibrations of the individual modes are randomly distributed in the multiparticle sample. The duration of the second pulse, t_{ω_2}, is assumed to be short enough so that $\theta_o(\tau)$ remains in phase during t_{ω_2}. The second RF pulse exerts torques on the vibrating particles of all θ classes but obviously the maximum torques are exerted on $\theta_o(\tau)$ whose particles are preferentially lined up by the RF field. The information about the pulse separation, τ, is now stored in the sample because of the preferential orientation of $\theta_o(\tau)$. Because the amplitude of the particle vibration is related to their phase during the second pulse, different θ classes will experience different effects on their environment which also can lead to permanently stored information about the pulse separation.

The application of a single pulse at a time much longer than the particle's relaxation times will again excite all θ classes. The amplitude of $\theta_o(\tau)$ will be the largest, however, because of its preferential alignment during the original two pulse sequence. Equation 2 shows that $\theta_o(\tau)$ will refocus at time $t = n\tau$ after the application of this single pulse. The oscillating dipole moment due to $\theta_o(\tau)$ at $t = n\tau$ will not be cancelled out by the random distribution of the other θ classes because of the preferential excitation of $\theta_o(\tau)$. This leads to a linear echo, ε_p, at $t = t_i + n\tau$ after any single pulse, which has been read out non-destructively. The effective relaxation time is infinite. Any reduction in ε_p arises because of external

vibrations, which tend to destroy the preferential alignment of $\theta_o(\tau)$.

The model presented above is consistent with all our available data. The fast initial decrease of ε_p, shown in Fig. 1, is due to the relaxing of the initial alignment to some quasi-equilibrium alignment which is then only weakly dependent on time. The dependence of ε_p on the biasing field can be explained as follows. The elastic constants of this ferroelectric material are strongly field dependent and the resonant frequencies ω_k for the individual particles, to first order in E, can be written as

$$\omega_k(E) = \omega_k|_o + \frac{d\omega_k}{dE}\Big|_o E \qquad (3)$$

where $\frac{d\omega_k}{dE}$ is different from particle to particle. Consider a θ_{class} $\theta_o(\tau,E_w)$ whose particles are in phase at the time of the second pulse and are also in phase with the RF field of the second pulse. A combination of equations 1, 2 and 3 leads to the following expression for the individual phases of the particles in $\theta_o(\tau,E_w)$ as a function of E at any time, t, after the application of a read out pulse.

$$\theta_k = \frac{\theta_o(\tau,E_w) + k2\pi}{\tau} t + \frac{d\omega_k}{dE}\Big|_o (E-E_w)t \qquad (4)$$

Ideally the θ_k's are in phase at a time τ after the read out pulse only when E (the biasing field during the read out pulse) is equal to E_w. This occurs because of the continuous distribu-

tion of $\frac{d\omega_k}{dE}\Big|_o$ among the particles in $\theta_o(\tau, E_w)$ and accounts for the peak in ε_p at $E = E_w$. The finite width of $\varepsilon_p(E)$ is due to the fact that the pulse widths are finite which results in a finite band width associated with the ω_k's.

References

1. M. Rubinstein and G.H. Stauss, J. Appl. Phys. 39, 81 (1968).

2. S. Kupca and C.W. Searle, Can. J. Phys. 53, 2622 (1975)

3. P.I. Kuindersma, S. Huizenga, J. Kommandeur and G.A. Sawatzky, Phys. Rev. B. 13, 496 (1976)

4. G.A. Sawatzky and S. Huizenga, J. Appl Phys (1976)

5. R.L. Melcher and N.S. Shiren, Phys. Rev. Lett. 34, 731 (1975).

6. R.W. Gould, Physics Letters 19, 477 (1965).

tion of $\frac{d\omega_k}{dE}\Big|_o$ among the particles in $\theta_o(\tau, E_w)$ and accounts for the peak in ε_p at $E = E_w$. The finite width of $\varepsilon_p(E)$ is due to the fact that the pulse widths are finite which results in a finite band width associated with the ω_k's.

Figure Captions

Figure 1: Amplitude of the echo, ε_p, as a function of the time, t_i, when the reading pulse is applied. The first point (t=0) results from both ε_1 and ε_p.

Figure 2: Amplitude of the echo, ε_p, when a DC electric field, E, is applied during the read out pulse. The initial two pulse write in sequence is made in the presence of a DC electric field, E_w, of 0, 6, 9, 12 KV/cm. The pulse separation, τ, used was 20 μsec.

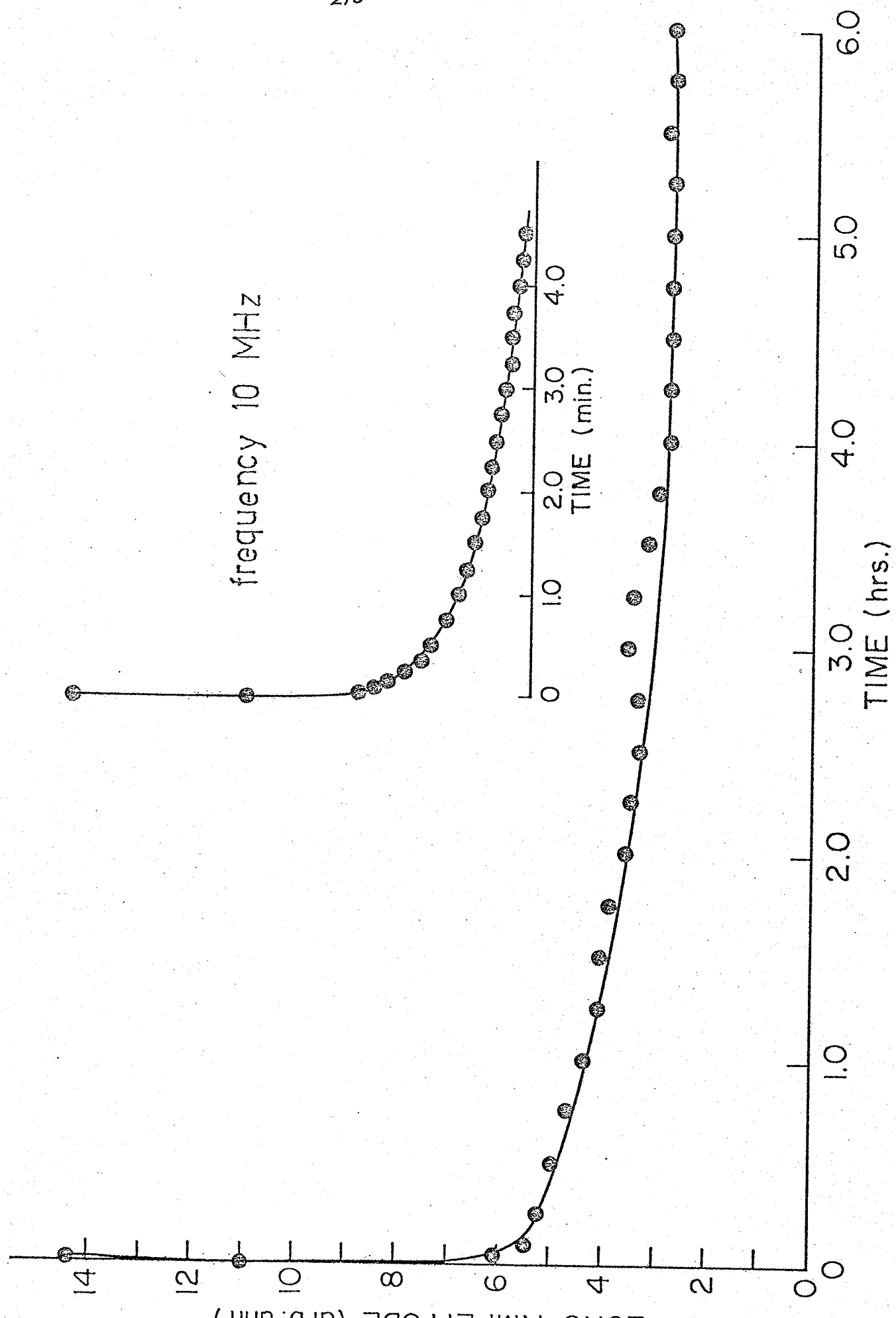
frequency 10 MHz
ECHO AMPLITUDE (arb. unit)
0
2
4
6
8
10
12
14
0
1.0
2.0
3.0
4.0
5.0
6.0
TIME (hrs.)
0
1.0
2.0
3.0
4.0
TIME (min.)

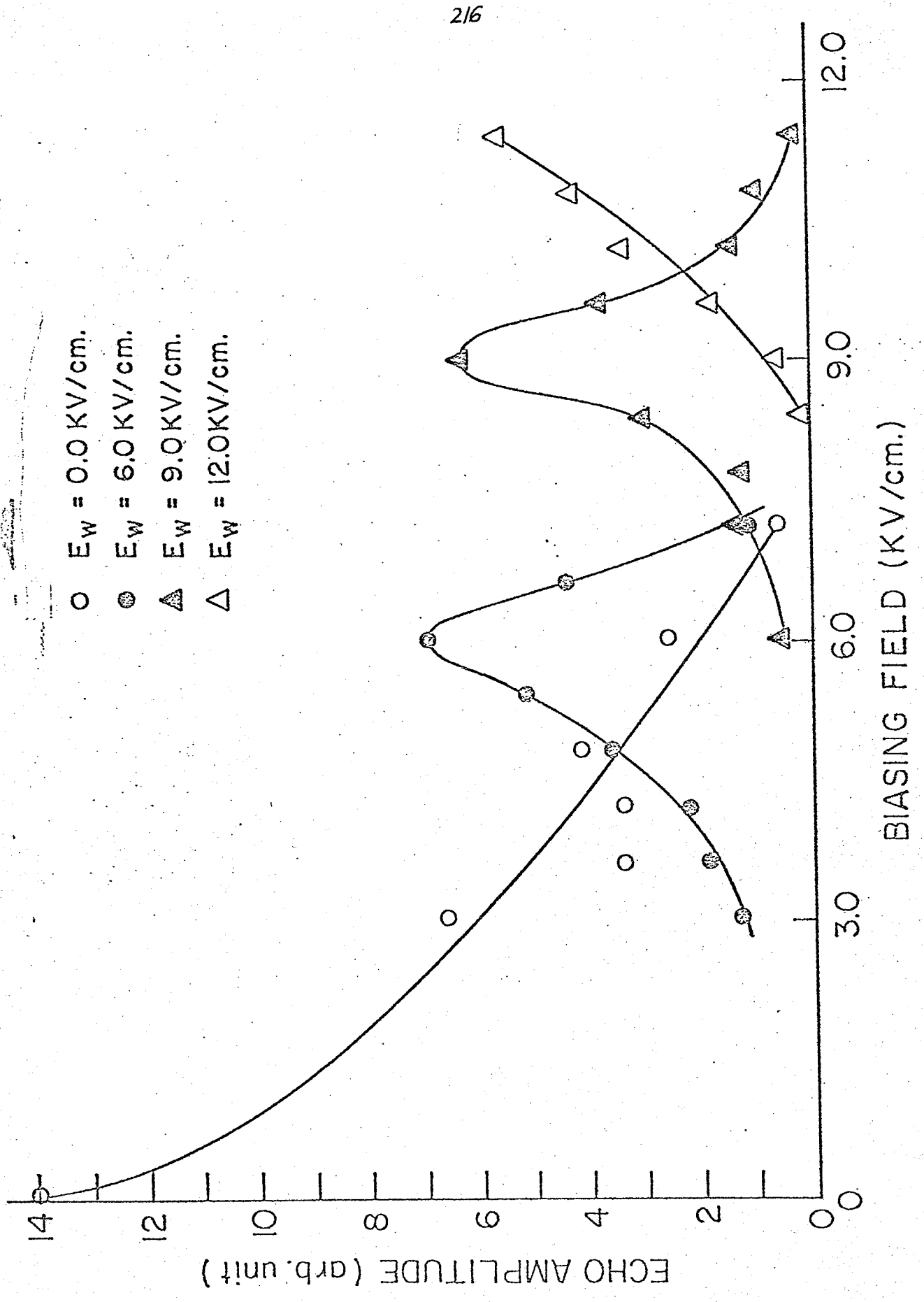
ECHO AMPLITUDE (arb. unit)
0
2
4
6
8
10
12
14
0
3.0
6.0
9.0
12.0
BIASING FIELD (KV/cm.)
O E_w = 0.0 KV/cm.
● E_w = 6.0 KV/cm.
▲ E_w = 9.0 KV/cm.
△ E_w = 12.0 KV/cm.

REFERENCES

(1) E.L. Hahn, Phys. Rev. 80, 580 (1950).

(2) I.D. Abella, N.A. Kurnit, S.R. Hartmann. Phys. Rev. Lett. 13, 567 (1964).

(3) R.P. Feynman, F.L. Vernon, R.W. Hellwarth. J. Appl. Phys. 28, 49 (1957).

(4) R.M. Hill, D.E. Kaplan. Phys. Rev. Lett. 14, 1062 (1965).

(5) R.S. Harp, R.L. Bruce, F.W. Crawford. J. Appl. Phys. 38, 3385 (1967).

(6) G.F. Herrmann, R.M. Hill, D.E. Kaplan, Phys. Rev. 156, 556 (1967).

(7) F.A. Blum, L.O. Bauer, Phys. of Fluids 13. 2162, 2174 (1970).

(8) D.E. Kaplan. Phys. Rev. Lett. 14, 254 (1964).

(9) I.B. Goldberg, E. Ehrenfreund, M. Wagner. Phys. Rev. Lett. 20, 539 (1968).

(10) Y.Y. Asadullin, U.K. Kopvillem, V.N. Osipov, B.P. Smolyakov, R.F. Shapirov. Sov. Phys.-Solid State 13, 2230 (1972).

(11) N.N. Krainik, S.N. Popov. Sov. Phys.-Solid State 12, 2440 (1971).

(12) A. Billmann, Ch. Frenois, J. Joffrin, A. Levelut, S. Ziolkiewicz. J. Phys. (France) 34, 453 (1973).

(13) S. Kupca, C.W. Searle. Can. J. Phys. (1975) In Press.

(14) H. Alloul, C. Froidevaux. Comp. Rendus 265, 881 (1967).

(15) M. Rubinstein, G.H. Stauss. J. Appl. Phys. 39, 81 (1968).

(16) Z.A. Pacult, P.C. Reidi, D.P. Tunstall. J. Phys. (F) Metal Phys. 3, 1843 (1973).

(17) S. Kupca, C.W. Searle, J. Appl. Phys. 45, 5460 (1974).

(18) R. Livingston, Methods of Experimental Physics, Vol. III D. Williams Ed. Academic Press Inc. N.Y. (1962).

(19) G.F. Herrmann, R.F. Whitmer. Phys. Rev. 143, 122 (1966).

(20) R.J. Snodgrass. Phys. Rev. Lett. 24, 864 (1970).

(21) Z.A. Pacult, P.C. Reidi, D.P. Tunstall. J. Phys. F4, L184 (1974).

(22) G.F. Herrmann, D.E. Kaplan, R.M. Hill. Phys. Rev. 181, 829 (1969).

(23) F.W. Crawford, R.S. Harp. Phys. Lett. 21, 292 (1965).

(24) W.H. Kegel, R.W. Gould. Phys. Letters 19, 531 (1965).

(25) J.L. Hushfield, J.M. Wachtel. Bul. Am. Phys. Soc. 11, 538 (1966).

(26) F.W. Crawford, R.S. Harp. J. Appl. Phys. 37, 4405 (1966).

(27) J.W. Strutt (Lord. Rayleigh) Phil. Mag.16, 50 (1883).

(28) A. Yariv, J.E. Pearson Parametric processes, Pergamon Press 1969.

(29) P.W. Gould. 7-th Annual Meeting of APS Plasma Dynamics Division. San Francisco (Nov. 1965).

(30) R.W. Gould. Phys. Lett. 19, 477 (1965).

(31) A.S. Nowick, B.S. Berry, Anelastic Relaxation in Crystaline Solids. Appendix A. Academic Press (1972).

(32) I.C. Chang. Proceeding of the IEEE V54, 1608 (1966).

(33) P.A. Fedders, E. Y. C. Lu. Appl. Phys. Lett. 23, 502 (1973).

(34) A.E.H. Love. Mathematical Theory of Elasticity Ch. 12. Dower (1944).

(35) A.A. Shpunt. Sov. Phys - Solid State V9, 878 (1970).

(36) H.F. Eden, P. Felsenthal. J. Acoust. Soc. Am. 53, 464 (1973).

(37) F. Grossman. Geophysics 16, 673 (1951a).

(38) J.J. Stoker. Nonlinear Vibrations, Chap. II, Interscience Pub., (1950).

(39) J.R. Houck, H.V. Bohm, B.W. Maxfield, J.W. Wilkens. Phys. Rev. Lett. 19, 224 (1967).

(40) J.J. Quinn, Phys. Lett. 25A, 522 (1967).

(41) D.J. Meredith, R.J. Watts-Tobin, E.R. Dobbs. J. Acoust. Soc. Am. 45, 1393 (1968).

(42) J.J. Quinn, J. Phys. Chem. Sol. 31, 1701 (1970).

(43) M.Y. Kravchenko. Sov. Phys. JETP 27, 801 (1968).

(44) R. Casanova. Alig. Phys. Rev. 178, 1050 (1969).

(45) E.R. Dobbs. J. Phys. Chem. Sol. 31, 1657 (1970).

(46) R. Turner, K.R. Lyall, J.F. Cochran. Can. J. Phys. 47, 2293 (1969).

(47) M.R. Gaerttner, W.D. Wallace, B.W. Maxfield. Phys. Rev. 184, 702.

(48) M.R. Gaerttner, B.W. Maxfield, Phys. Rev. Lett. 26, 119 (1971).

(49) K.R. Lyall, J.F. Cochran. Can. J. Phys. 49, 1075 (1971).

(50) R. Turner, E.D. Crozier, J.F. Cochran. Can. J. Phys. 50, 2736, (1972).

(51) R.A. Gordon, G. Seidel. J. Phys. Chem. Sol. 34, 1587 (1973).

(52) C. Zener, R.H. Randal. Metals Tech. 7, 1 (1940).

(53) J.N. Lange Phys. Rev. 179, 631 (1969).

(54) W.P. Mason. Crystal Physics of Interaction Processes. Ch. 6. Academic Press, N.Y. (1966).

(55) R.M. Bozorth. Ferromagnetism, D. Van Nostrand Co., (1951).

(56) E. Kneller. Ferromagnetismus, Springer Verlag (1962).

(57) S. Chikazumi, Physics of Magnetism, Chap. 19. Willey and Sans, N.Y. (1964).

(58) W.P. Mason. Phys. Rev. 83, 683 (1951).

(59) W.P. Mason Rev. Mod. Phys. 25, 136 (1953).

(60) R.M. Bozorth, W.P. Mason, H.J. McSkimin. Bell System Tech. J. 970 (1951).

(61) A.E.H. Levy, R. Truell. Rev. Mod. Physics 25, 140 (1953).

(62) G. Dietz, P. Rudow. IEEE Mag. 6, 394 (1970).

(63) H. Sieger, G. Dietz, Int. J. Mag. V3, 207 (1972).

(64) J.A. Eaton, A.H. Morrish, Can. J. Phys. 49. 2768 (1971).

(65) J.E. Gould. Co balt Alloy Permanent Magnets. Centre D'information du Colbat Brussels (1971).

(66) E.A. Nesbitt, J.H. Warnick. Rare Earth Permanent Magnets, Academic Press (1973).

(67) F. Morin. Phys. Rev. 78, 819 (1956).

(68) W.C. Cady. Piezoelectricity, McGraw-Hill, London (1946).

(69) S. Kupca, C.W. Searle. J. Appl. Phys. In Press (1975).

(70) M. Hanabusa, T. Kushida, J.C. Murphy. J. Appl. Phys. V44, 5106 (1973).

(71) R.W. Makkay, G.H. Geiger, M.F. Fine. J. Appl. Phys. 33, 014 (1963).

(72) Y. Shapira. Phys. Rev. 184, 189 (1969).

(73) S. Kupca, C.W. Searle. J. Appl. Phys. 47.376 (1976).

(74) J.M. Ziman. Electrons and phonons, Oxford 1960.

(75) G. Kittel. Introduction to Solid State Physics, 4-th Ed. p. 219, Wiley, N.Y. (1971).

(76) G.K. White, S.B. Woods. Prc. Roy Soc. 2J1 35 (1959).

(77) C. Rizutto. Reports on Progress in Physics, 37, 146 (1974).

(78) C.M. Hurd. J. Phys. Chem. Sol. 30, 539 (1969).

(79) D. Jha, M.H. Jericho. Phys. Rev. B3, 147 (1971).

(80) H.L. Malm, S.B. Woods, Can. J. Phys. 44, 2293 (1966).

(81) M.S.R. Cheri, J. De Nobel. Physica 25, 60, 84, (1959).

(82) J.S. Kouvel. J. Phys. Chem. Sol. 21, 57 (1961).

(83) R.J. Snodgrass. Phys. Rev. B3, 3738 (1971).

(84) A.D. Caplin, C. Rizzuto. Phys. Rev. Lett. 21, 746 (1968).

(85) W.R. Smythe. Static and Dynamic Electricity, 2-nd Ed., McGraw, New York, (1950).

(86) A.N. Garitsen. Encyclopedia of Physics, Ed. S. Flugge V19, 137 (1956).

(87) B. Abeles. Phys. Rev. Lett. 19, 1181 (1967).

(88) P.D. Southgate. J. Appl. Phys. 40, 22 (1969).

(89) G. Gorodetsky, B. Luthy, T.J. Moran, M.E. Mullen. J. Appl. Phys. V43, 1234 (1972).

(90) R.R. Whymark, J. Acoust. Soc. A., 33, 725 (1961).

(91) Shoji Kajima, Kineo Tsukada, Shizuko Ogawa, Akira Shimauchi. Norio Matsumiya. J. Phys. Soc. Japan 10, 265 (1955).

(92) G. Simon. Z. Naturforschung 3A, 84 (1958).

(93) J. Sakuray. J. Phys. Soc. Japan V19, 311 (1964).

(94) B.A. Lilley, Phil. Mag. 41, 792 (1950).

(95) H.V. Ganganna, N.F. Fiore, B.D. Cullity. J. Appl. Phys. 42, 5792 (1971).

(96) A. Hirai, J.A. Eaton, C.W. Searle, Phys. Rev. B368 (1971).

(97) J. Eisner, Ferroelectrics 4. 213 (1923).

(98) F. Jona, G. Shirane. Ferroelectric Crystals Ch. 7, Pergamon Press (1962).

(99) W. Känzig. Solid State Physcis V9.1. Academic Press, N.Y. (1957).

(100) W.J. Price. Phys. Rev. 75. 946 (1949).

(101) H. Mueller. Phys. Rev. J8, 565 (1940).

(102) S.F. Gibbons. J. Appl. Phys. 28, 810 (1957).

(103) R.L. Melcher, N.S. Shiren. Phys. Rev. Lett. 34, 731 (1975).

(104) B.P. Smolyakov, N.B. Augert. U. Kch. Kapvillem Sov. Phys. Solid State 15, 387 (1973).

(105) J. Joffrin, A. Levelut. Phys. Rev. Lett. 29, 1325 (1972).

(106) E.Y.C. Lu. Ultrasonic Symposium, Montrey, California (1973).

(107) D.K. Garrad, M.S. Shiren, R.L. Melcher, T.G. Koyaka. Ultrasonics Symposium, Montrey, California (1973).

(108) I. Maartense, C.W. Searle. Technical Report AFML-TR-72-234. Air Force Materials Laboratory Air Force Systems Command. Wright - Patterson Air Force Base, Ohio (1972).

(109) C.W. Searle, Private Communications.

(110) W.H. Louisell. Coupled Mode and Parametric Electronics. Wiley and Sons Inc., New York (1960).

(111) A.E. Siegman. Prac. IEEE 54, 756 (1966).

(112) Ch. Frenois, J. Joffrin, A. Lavelut, S. Ziolkiewicz, Solid State Comm. V11, 327 (1972).

(113) U. Kch. Kopvillem. Sov. Phys. - Solid State V9, 813 (1967), V11, 93 (1969).

(114) Ya Ya Asadullin. U. Kch. Kopvillem. Sov. Phys. - Solid State V9, 2150 (1968).

(115) Y.Y. Asadullin, U. Kch. Kopvillem, Fiz. Metal-Metalovedenie (Sov.) V23, 568 (1967).